CRREL
REPORT 87-16

US Army Corps
of Engineers
Cold Regions Research &
Engineering Laboratory

Physical properties of summer sea ice in the Fram Strait, June–July 1984

UNCLASSIFIED
SECURITY CLASSIFICATION OF THIS PAGE

REPORT DOCUMENTATION PAGE

Form Approved
OMB No. 0704-0188
Exp. Date: Jun 30, 1986

1a. REPORT SECURITY CLASSIFICATION
Unclassified

1b. RESTRICTIVE MARKINGS

2a. SECURITY CLASSIFICATION AUTHORITY

2b. DECLASSIFICATION / DOWNGRADING SCHEDULE

3. DISTRIBUTION / AVAILABILITY OF REPORT
Approved for public release; distribution is unlimited.

4. PERFORMING ORGANIZATION REPORT NUMBER(S)
CRREL Report 87-16

5. MONITORING ORGANIZATION REPORT NUMBER(S)

6a. NAME OF PERFORMING ORGANIZATION
U.S. Army Cold Regions Research and Engineering Laboratory

6b. OFFICE SYMBOL (If applicable)

7a. NAME OF MONITORING ORGANIZATION
Office of Naval Research

6c. ADDRESS (City, State, and ZIP Code)
72 Lyme Road
Hanover, New Hampshire 03755-1290

7b. ADDRESS (City, State, and ZIP Code)
800 N. Quincy Street
Arlington, Virginia 22217

8a. NAME OF FUNDING / SPONSORING ORGANIZATION

8b. OFFICE SYMBOL (If applicable)

9. PROCUREMENT INSTRUMENT IDENTIFICATION NUMBER
Grant N0001484 WRM 2406

8c. ADDRESS (City, State, and ZIP Code)

10. SOURCE OF FUNDING NUMBERS

PROGRAM ELEMENT NO.	PROJECT NO.	TASK NO	WORK UNIT ACCESSION NO.

11. TITLE (Include Security Classification)
Physical Properties of Summer Sea Ice in the Fram Strait, June-July 1984

12. PERSONAL AUTHOR(S)
Gow, Anthony J., Tucker, Walter B. III and Weeks, Wilford F.

13a. TYPE OF REPORT	13b. TIME COVERED FROM ____ TO ____	14. DATE OF REPORT (Year, Month, Day)	15. PAGE COUNT
		September 1987	87

16. SUPPLEMENTARY NOTATION

17. COSATI CODES		
FIELD	GROUP	SUB-GROUP

18. SUBJECT TERMS (Continue on reverse if necessary and identify by block number)
Arctic Ocean; Greenland Sea; Sea ice; Crystal structure; Ice floes; First-year ice; Salinity

19. ABSTRACT (Continue on reverse if necessary and identify by block number)

The physical properties of sea ice in the Fram Strait region of the Greenland Sea were examined during June and July 1984 in conjunction with the MIZEX field program. Most of the ice sampled within Fram Strait during this period was multi-year; it is estimated to represent at least 84% by volume of the total ice discharged from Fram Strait during June and July. Thicknesses and other properties indicated that none of the multi-year ice was older than 4 to 5 years. Snow cover on the multi-year ice averaged 29 cm deep while that on first-year averaged only 8 cm. Much of this difference appears to be the result of enhanced sublimation of the snow on the thinner first-year ice. The salinity profiles of first-year ice clearly show the effects of ongoing brine drainage in that profiles from cores drilled later in the experiment were substantially less saline than earlier cores. Bulk salinities of multi-year ice are generally much lower than those of first-year ice. This difference furnished a very reliable means of distinguishing between the two ice types. Thin section examinations of crystal structure indicate that about 75% of the ice consisted of congelation ice with typically columnar type crystal structure. The remaining 25% consisted of granular ice with only a few

20. DISTRIBUTION / AVAILABILITY OF ABSTRACT
☒ UNCLASSIFIED/UNLIMITED ☐ SAME AS RPT. ☐ DTIC USERS

21. ABSTRACT SECURITY CLASSIFICATION
Unclassified

22a. NAME OF RESPONSIBLE INDIVIDUAL
Anthony J. Gow

22b. TELEPHONE (Include Area Code)
603-646-4100

22c. OFFICE SYMBOL
CECRL-RS

DD FORM 1473, 84 MAR

83 APR edition may be used until exhausted.
All other editions are obsolete.

SECURITY CLASSIFICATION OF THIS PAGE
UNCLASSIFIED

19. Abstract (cont'd)

occurrences of snow ice. The granular ice consisted primarily of frazil, found in small amounts at the top of floes, but mainly observed in multi-year ridges where it occurred as the major component of ice in interblock voids. The horizontally oriented crystal c-axes showed varying degrees of alignment, ranging from negligible to strong, in which the alignment direction changed with depth, implying a change in floe orientation with respect to the ocean current at the ice/water interface during ice growth. Evidence of crystal retexturing was observed in the upper meter of nearly every multi-year core. This retexturing, involving grain boundary smoothing and nearly complete obliteration of the original ice platelet/brine layer substructure, is attributed to summer warming; ice exhibiting such substructure can immediately be identified as multi-year ice.

PREFACE

This report was prepared by Dr. Anthony J. Gow and Walter B. Tucker, III, Geologists, and Dr. Wilford F. Weeks, Glaciologist, of the Snow and Ice Branch, Research Division, U.S. Army Cold Regions Research and Engineering Laboratory. Funding for this research was provided by the U.S. Office of Naval Research through Grant No. N0001484 WRM2406.

Dr. G. Maykut of the University of Washington technically reviewed the manuscript of this report.

CONTENTS

ILLUSTRATIONS

Physical Properties of Summer Sea Ice in the Fram Strait, June–July 1984

ANTHONY J. GOW, WALTER B. TUCKER III AND WILFORD F. WEEKS

INTRODUCTION

During June and July 1984, CRREL investigators conducted physical property studies of sea ice in the Fram Strait region of the Greenland Sea. These studies were performed in conjunction with the 1984 Marginal Ice Zone Experiment (MIZEX-84), a multinational research program to study the physical processes by which sea ice, the ocean and atmosphere interact in the outermost parts of a polar ice field (Johannessen et al. 1982). Preliminary results of the ice property investigations have been reported by Tucker et al. (1985).

Fram Strait, located between the East Greenland coast and Spitsbergen, is the major outflow region for ice from the Arctic Basin. The volume of ice outflow is highly variable both seasonally and annually (Vinje 1977); however, estimates generally agree on an average transport of about 0.1 Sv* (Timofeyev 1958, Aagaard and Greisman 1975). Maykut (1985) estimates that approximately 10% of the ice in the Arctic Basin drifts out through the Fram Strait each year. Ice discharge through other passages from the Arctic Basin (e.g. Bering Strait, Canadian Archipelago) is considered negligible by comparison (Aagard and Greisman 1975).

Modeling studies (Hibler 1979) and analyses of ice drift trajectories (Colony and Thorndike 1985) have indicated that ice discharging through Fram Strait can originate in essentially any part of the Arctic Basin. Floes that formed in the western Arctic arrive at Fram Strait via the Transpolar Drift Stream and should include substantial amounts of multi-year ice, while ice from the Lincoln, Barents and Kara Seas can take a more direct approach to the strait and should include a larger percentage of younger ice. Thus, the ice transiting Fram Strait or the Greenland Sea could have originated in any number of different areas within the Arctic Basin. This suggests that, if ice properties are strongly influenced by area of origin, then a large variation in properties might be observed in the region of the ice margin. Of course, the exact areas of origin of individual floes would be unknown unless some diagnostic feature within the ice itself could be identified with a particular source region.

Both Weeks (1986) and Wadhams (1981) point out the lack of published information concerning the physical properties of sea ice in the Greenland Sea. The only significant analysis of sea ice properties in the Greenland Sea conducted prior to MIZEX-84 was that carried out aboard the Swedish icebreaker *Ymer* as part of the Ymer-80 expedition (Overgaard et al. 1983). However, this study did not include systematic examination of the crystal structure, an important property of the ice that is closely related to its growth history. In fact, very few studies of arctic pack ice have included examination of its crystal structure; mainly for logistics reasons most investigators have examined only the structure of the fast ice adjacent to the coast (Weeks and Gow 1978 and 1980). As well as revealing much about the ice growth regime, crystal type and orientation have recently been shown to have a significant effect on ice strength (Cox et al. 1985 and Richter-Menge and Cox 1985). Crystal characteristics are therefore of importance when attempting to infer ice mechanical properties and the forces that an engineering structure must withstand when encroached upon by sea ice.

PROJECT OBJECTIVE

The overall objective of our project was to assess the physical and structural characteristics of the pack ice found in Fram Strait during summer. Goals we hoped to achieve within this objective included the following:

* Sverdrup (1 Sv = 10^6 m^3/s).

1. Acquisition of data in support of remote sensing studies carried out simultaneously with physical property measurements of the sea ice.

2. Assessment of the growth history of first- and multi-year ice, using structural and salinity characteristics to distinguish between the two major ice types and between multi-year ice of different ages.

3. Evaluation of the relative amounts of frazil and congelation crystalline textures contained within the ice.

4. Determination of property differences that may be attributable to ice having originated in different source areas.

5. Subjective estimation of the relative amounts of first- and multi-year ice in this area.

FIELD SAMPLING PROGRAM

Studies were conducted aboard FS *Polarstern*, a modern German icebreaker operated by the Alfred Wegener Institute for Polar and Marine Research, Bremerhaven, F.R.G. This unique research vessel is equipped with excellent coldroom and laboratory facilities that are especially suited to sea ice sampling and analysis. Because *Polarstern* visited many different locations within the Fram Strait during MIZEX-84, it provided an ideal platform for collecting ice core samples over a relatively large area.

The locations of our ice core sampling sites are shown in Figure 1. Sampling was conducted between 15 June and 13 July 1984 and covered a geographical area that extended from 78°20'N to 80°42'N latitude and from 7°16'E to 7°10'W longitude. Individual floes were reached either directly from the side of the ship or by helicopter. Use of helicopters (see Fig. 2) enabled us to extend our range of sampling as well as choose representative floes for our investigation. Examples of the types of floes encountered are shown in Figure 3. Forty individual floes with diameters ranging from 100 m to several kilometers were core sampled, occasionally at more than one location on the same floe. Core drilling was performed at 54 separate sites, and a total of 243 m of core obtained, all but

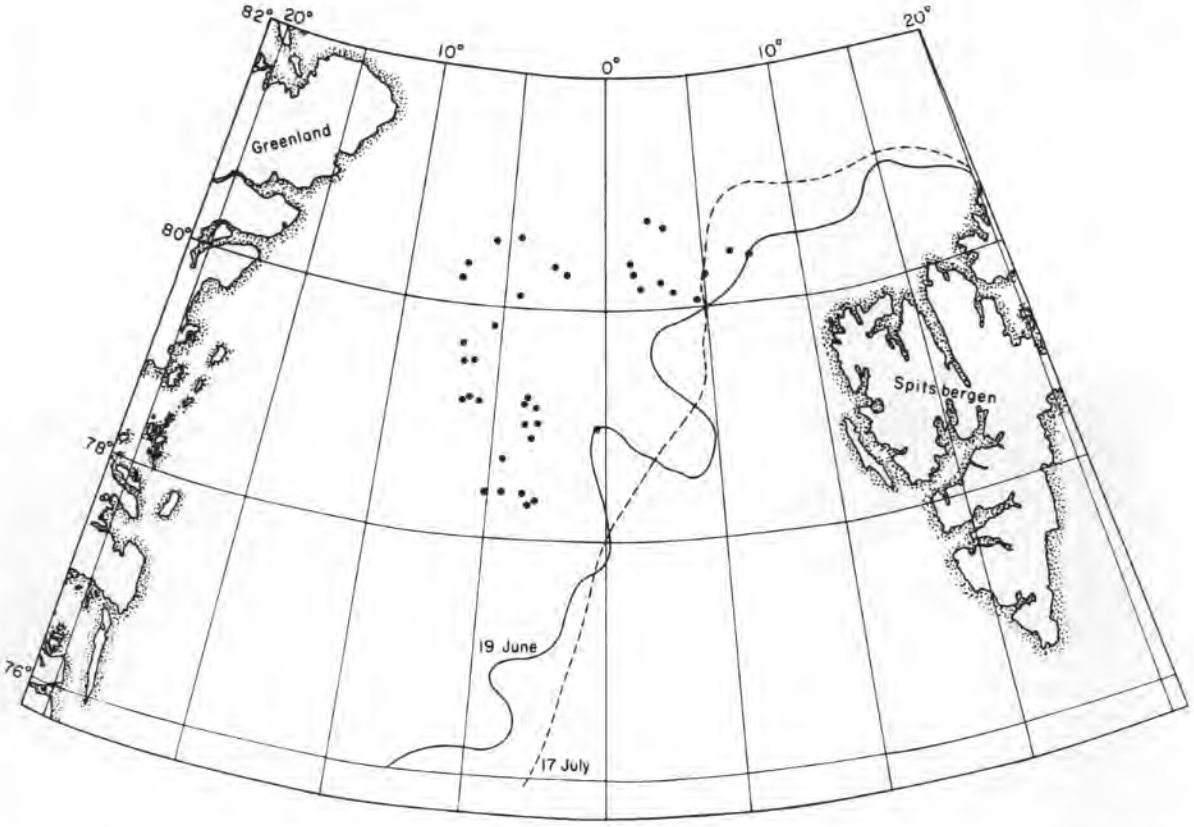

Figure 1. Ice core sampling locations in Fram Strait. Approximate positions of ice edge at the beginning and end of the MIZEX-84 experiment are also shown.

Figure 2. Setting up coring site on multi-year floe with aid of helicopter.

a. First-year floes up to 1 km long.

b. Multi-year floes with thick snow cover.

Figure 3. Characteristics of floes in the Fram Strait.

c. Floes similar to those in (b) with dark water sky on the horizon.

d. Multi-year floes with rubbled surfaces.

e. Multi-year floe with puddled surface.

Figure 3 (cont'd). Characteristics of floes in the Fram Strait.

5 m of which was used for salinity and structural analysis.

Two cores through the thickness of the ice were obtained at each sampling site with coring augers powered by a lightweight gasoline engine. A 7.5-cm-diam core provided samples for salinity analysis while a larger 10-cm core was obtained for structural analysis and for measuring ice temperatures. The salinity samples were prepared by cutting the core on site into 10-cm-long segments and placing them in sealed plastic containers. Ice temperatures were measured (to an accuracy of ± 0.5°C) on the structural cores immediately after drilling, following which the cores were placed in 1-m-long tubes and stored in the ship's -25°C coldroom until further processing. The purpose of the temperature measurements, aside from yielding a generalized profile, was mainly to assess the probable thickness of the ice as drilling progressed. Additional measurements made at each of the sampling sites included size estimates of the floe and a general evaluation of its surface characteristics, inluding snow thickness, roughness, proximity to ridging and refrozen leads, evidence of melt, and melt pond distribution (see Fig. 3). On board *Polarstern* the salinity samples were melted and allowed to warm to room temperature ($\approx$ 20°C). Salinity values were then obtained from conductivity measurements of the melted sample. These measurements were made with a temperature-compensating Beckman Solubridge that was periodically recalibrated against standard solutions prepared from Copenhagen standard seawater (chlorinity, 19.373‰). All salinities were corrected to a reference temperature of 25°C. Measurement precision is estimated at ± 0.2‰. Many of these samples were subsequently used for chemical and biological investigations by other scientists aboard *Polarstern*. Fifty-one cores totaling 116 m in length were drilled for salinity analysis.

The processing of cores for structural analysis began with the documenting of significant stratigraphic features. These included banding, the location of sediment or algae layers, presence of bubbles and observable variations in the translucence (or opacity) of the ice. Then a 0.5-cm-thick vertical slice was cut along the entire length of the core with a bandsaw. We examined this thick section between crossed Polaroids on a large light table to evaluate the overall nature of the texture and structure of the crystals through the total thickness of each floe. Textures and structures were then described in terms of crystal type (columnar or granular), grain size, and c-axis orientation, and their relationship to visible stratigraphy. This thick-section examination also determined where vertical and horizontal thin sections were to be selected in each core. Fifty-four structure cores were drilled and the total length of core obtained was 122 m.

Thin sections were prepared according to the technique described by Weeks and Gow (1978 and 1980). In this technique, a 0.5-m-thick slice is sawed from the core, frozen to a glass plate and thinned further to about 1 mm on the bandsaw. A microtome is then used to reduce the final thickness to between 0.2 and 0.5 mm. At this thickness, grain boundaries, brine drainage channels and the brine pocket/ice platelet structure of individual crystals are clearly revealed when the section is viewed between crossed Polaroids. A total of approximately 300 thin sections were prepared and photographed. A 10- × 12.5-cm press camera was used to photograph thin sections at 1:1 magnification. This camera produces very high quality negatives that can then be contact printed at natural scale or enlarged to yield details of crystal substructure not normally observable at lower magnifications.

A schematic depiction of crystalline texture (based on vertical thick-section studies) together with selected horizontal thin-section crystal structure photographs and temperature and salinity profiles was then prepared for cores from each of the floes sampled. Representative examples of this kind of ice floe characterization for first- and multi-year ice are shown in Figures 4 and 5 (and later in Fig. 17, 19 and 21). Schematic descriptions of all cores from the remaining floes are given in Appendix A. A full listing of pertinent data for all cores is given in Table 1.

SEA ICE STRUCTURE: GENERAL CONSIDERATIONS

Structurally, at least at the crystal size level, sea ice consists of two major crystal types: 1) columnar ice formed by direct freezing of seawater to the underside of the ice sheet, also called congelation ice,* and 2) granular ice occurring mainly as

* The terms congelation ice and columnar ice are often used synonymously, columnar being used to express the *textural characteristics* of the ice and the term congelation being used to describe the process by which columnar-textured crystals are formed.

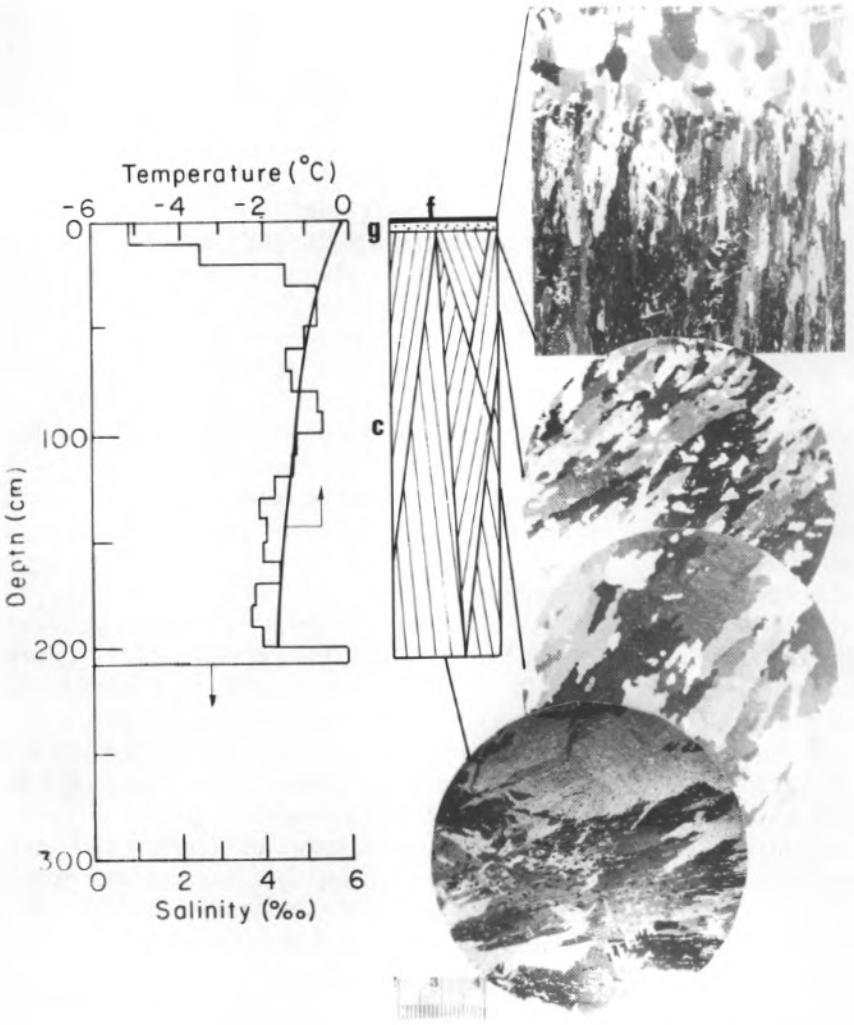

Figure 4. Salinity–temperature–structure profiles of an undeformed first-year floe composed of 97% congelation ice. The top 3 cm consists of low-salinity, transparent ice formed most probably from freezing of fresh water on the surface of the floe. Scale subdivisions beside bottom thin section measure 1 mm. In the structure diagram, the symbols g, f and c are used to designate granular, fresh-water and columnar sea ice respectively.

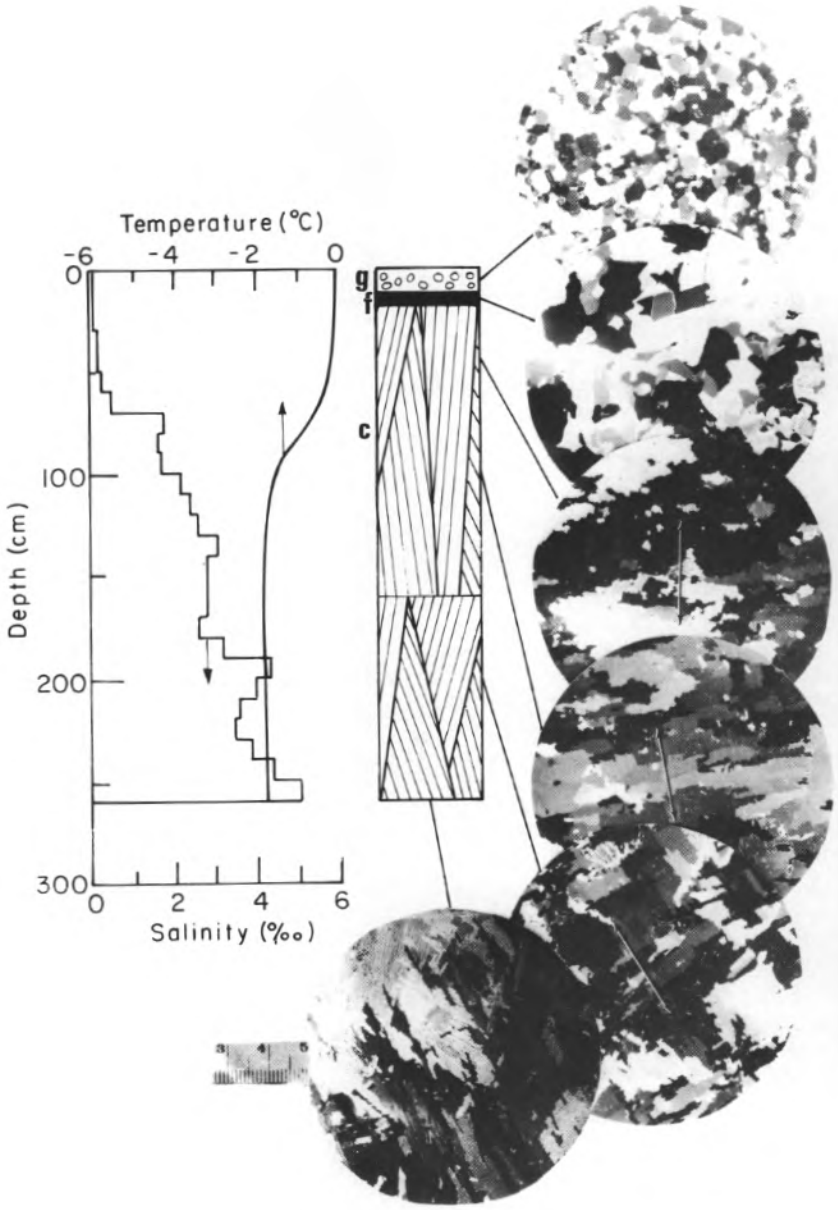

Figure 5. Salinity–temperature–structure profiles of undeformed multi-year ice. This floe consists of 92% congelation ice overlain by 3% pond ice and 5% snow-ice. Arrows on horizontal thin section photographs indicate direction of c-axis alignment. Diagram and symbol designations are the same as for Figure 4.

Table 1. Ice core data from floes in Fram Strait, MIZEX-84.

Core no.	Lat.	Long.	Ice type	Floe size	Thickness (cm)	Snow depth (cm)	Salinity (‰)	Congelation (%)	Granular (%)	Remarks
6-15-1	78°25'N	4°20'W	multi-year	2+ km	205+	45	1.3 ± 1.1	96	4	Undeformed ice; bottom not penetrated
6-15-2	78°42'N	4°30'W	multi-year	sev. km	330	20–40	1.8 ± 1.2	88	12	Undeformed ice
6-16-1	78°54'N	3°20'W	multi-year	200 m	285	20–44	1.9 ± 1.2	97	3	Undeformed ice
6-17-1	79°26'N	3°32'W	multi-year	1–2 km	314	20–40	2.5 ± 1.2	94	6	Undeformed ice
6-18-1	80°06'N	4°27'W	multi-year	100–150 m	290	40	—	55	45	Deformed with tilted blocks
6-18-2	80°03'N	4°33'E	multi-year	200 m	209	30	1.7 ± 1.5	100	0	Undeformed ice
6-19-1	80°08'N	3°13'E	multi-year	2 km	241	10–50	1.7 ± 0.8	66	34	Ridged ice
6-19-2	80°15'N	2°51'E	multi-year	> 7 km	218	40	2.1 ± 1.1	94	6	Undeformed ice
6-20-1	80°17'N	5°01'E	multi-year	150 m	287	48	1.4 ± 0.9	46	54	Deformed with tilted blocks
6-21-1	80°25'N	7°16'E	multi-year	600 m	219	40	1.9 ± 1.5	90	10	Undeformed ice
6-22-1	80°28'N	6°20'E	first-year	sev. km	32	0	3.6 ± 0.8	81	19	Lead ice
6-22-2	80°28'N	6°20'E	first-year	sev. km	76	5	4.3 ± 1.2	76	24	Lead ice
6-22-3	80°28'N	6°20'E	first-year	sev. km	110	10	5.0 ± 1.3	88	12	Thin first-year ice
6-22-4	80°28'N	6°20'E	first-year	sev. km	197	2–3	5.0 ± 1.4	89	11	Undeformed ice
6-22-5	80°28'N	6°20'E	first-year	sev. km	158	14	4.8 ± 0.6	97	3	Undeformed ice
6-24-1	80°11'N	1°52'E	first-year	100 m	67	2–3	5.3 ± 0.8	85	15	Undeformed ice
6-24-2	80°11'N	1°52'E	multi-year	100 m	197	30	1.3 ± 1.4	74	26	Ridge remnant
6-24-3	80°11'N	1°52'E	first-year	100 mkm	83	10	4.8 ± 0.9	76	24	Undeformed ice
6-26-1	80°42'N	3°03'E	multi-year	1 km	234	25	1.2 ± 1.1	71	29	Undeformed ice
6-26-2	80°42'N	3°03'E	first-year	1 km	257	35	4.2 ± 2.3	—	—	Located near rubbly ice
6-26-3	80°42'N	3°03'E	multi-year	sev. km	328	3–4	1.5 ± 1.2	24	75	Undeformed ice
6-27-1	80°20'N	1°34'W	multi-year	sev. km	355	14	3.2 ± 2.1	62	38	Ridged ice
6-27-2	80°23'N	2°30'W	multi-year	sev. km	374+	14	1.6 ± 0.9	47	53	Ridge ice; bottom not penetrated
6-28-1	80°35'N	4°33'W	first-year	sev. km	215	19	4.7 ± 1.1	100	0	Undeformed ice
6-28-2	80°35'N	4°33'W	first-year	sev. km	236	18	—	92	8	Undeformed ice
6-28-3	80°33'N	5°37'W	multi-year	sev. km	261	25	2.3 ± 1.5	92	8	Undeformed ice
6-29-1	80°21'N	7°05'W	multi-year	1 km	382	12–14	2.8 ± 1.4	61	39	Contains rafted pieces
6-29-2	80°15'N	7°10'W	multi-year	100 m	283	25	2.6 ± 1.4	96	4	Undeformed ice
7-01-1	79°14'N	6°15'W	multi-year	500 m	279	65	2.8 ± 1.2	95	5	Undeformed ice
7-01-2	79°13'N	6°28'W	first-year	1–2 km	206	5	4.4 ± 1.1	97	3	Undeformed ice
7-01-3	79°13'N	6°28'W	multi-year	1–2 km	240	30	—	—	—	Undeformed ice
7-01-4	79°13'N	5°40'W	multi-year	150 km	258	37	1.7 ± 0.9	94	6	Undeformed ice
7-01-5	79°12'N	3°45'W	first-year	200 km	81	10	3.9 ± 0.8	86	14	Thin first-year ice
7-01-6	79°10'N	3°25'W	first-year	500 m	222	15	4.2 ± 1.0	95	5	Undeformed ice
7-03-1	80°23'N	1°17'E	first-year	2 km	159	10	3.5 ± 0.8	87	13	Undeformed ice
7-03-2	80°23'N	1°17'E	first-year	2 km	325	80	3.7 ± 1.3	51	49	Ridged ice
7-03-3	80°23'N	1°17'E	first-year	2 km	44	5	2.7 ± 1.1	16	85	Lead ice
7-04-1	80°19'N	1°29'E	multi-year	sev. km	195	25	2.5 ± 1.2	98	2	Undeformed ice
7-05-1	78°23'N	3°27'W	first-year	500 m	109	8	4.3 ± 0.8	95	5	Undeformed ice
7-05-2	78°20'N	3°17'W	multi-year	500 m	235	11	2.4 ± 1.3	70	30	Undeformed ice
7-05-3	78°21'N	3°10'W	first-year	1 km	75	2	3.4 ± 1.1	95	5	Undeformed ice
7-05-4	78°21'N	3°10'W	multi-year	1 km	287	30	2.2 ± 1.4	98	2	Undeformed ice
7-06-1	78°25'N	5° 6'W	multi-year	100 m	234	19	2.3 ± 1.2	29	71	Ridge remnant
7-07-1	78°59'N	0°32'W	multi-year	sev. km	224	30	1.5 ± 1.0	80	20	Ridge remnant?
7-07-2	78°59'N	0°32'W	first-year	sev. km	97	5	3.9 ± 1.1	92	8	Lead ice
7-07-3	78°59'N	0°32'W	first-year	sev. km	136	5	3.5 ± 0.8	93	7	Undeformed ice
7-07-4	78°59'N	0°32'W	first-year	350 m	92	6	3.0 ± 1.1	100	0	Undeformed ice
7-08-1	79°01'N	3°31'W	multi-year	200 m	293	10–15	2.3 ± 1.2	100	0	Undeformed ice
7-08-2	79°01'N	3°43'W	multi-year	200 m	411	25–30	3.6 ± 1.6	80	20	Rafted blocks at top
7-09-1	79°32'N	6°17'W	multi-year	sev. km	282+	15	—	95	5	Undeformed ice
7-09-2	79°32'N	6°17'W	first-year	sev. km	97	5	3.2 ± 0.6	81	19	Undeformed ice
7-09-3	79°32'N	6°17'W	first-year	sev. km	120	7	3.4 ± 1.0	55	45	Lead ice
7-10-1	79°31'N	6°25'W	multi-year	sev. km	500	40	2.2 ± 1.0	42	58	Ridged ice
7-11-1	79°42'N	6°41'W	multi-year	1 km	411	12–20	2.1 ± 1.3	98	2	Undeformed ice
7-13-1	79°49'N	5°26'W	multi-year	1 km	574	15	2.0 ± 1.3	41	59	Ridged ice

frazil particles resulting from the free growth and aggregation of crystals in the water column.

Natural freezing of seawater in the Arctic generally leads to the growth of vertically elongated columnar crystals in sheets that reach 2 m or more in thickness. The topmost part of this ice sheet may include a mixture of granular and columnar ice crystals generally known as the transition zone, which, depending on the freezing conditions in the water column, can vary in thickness from a few centimeters to as much as a meter. In the Arctic, frazil is thought to be mainly the product of turbulent water conditions and thus confined to ice edge margins, leads and polynyas. According to Martin (1979) frazil ice accounts for less than 10% of arctic sea ice, an estimate in agreement with extensive observations by Weeks and Gow (1978, 1980) of shore-fast ice along the coasts of the Chukchi and Beaufort Seas.

Closer inspection of the ice crystals in the columnar zone reveals a substructure of long, vertical plates interspersed with parallel layers of brine inclusions. This gives rise to a substructure which in horizontal section (Fig. 6) reflects the process by which seawater incorporates residual brine at the ice/water interface as freezing progresses. Since the brine cannot be accommodated within the ice crystal lattice per se, it is incorporated instead between the plates. These plates originate as pure ice dendrites with their tips protruding downward into the sea water, and it is in the grooves between these dendrites that brine is systematically trapped. The spacing of these plates (plate width) can vary from a few tenths of a millimeter to 1 mm and de-

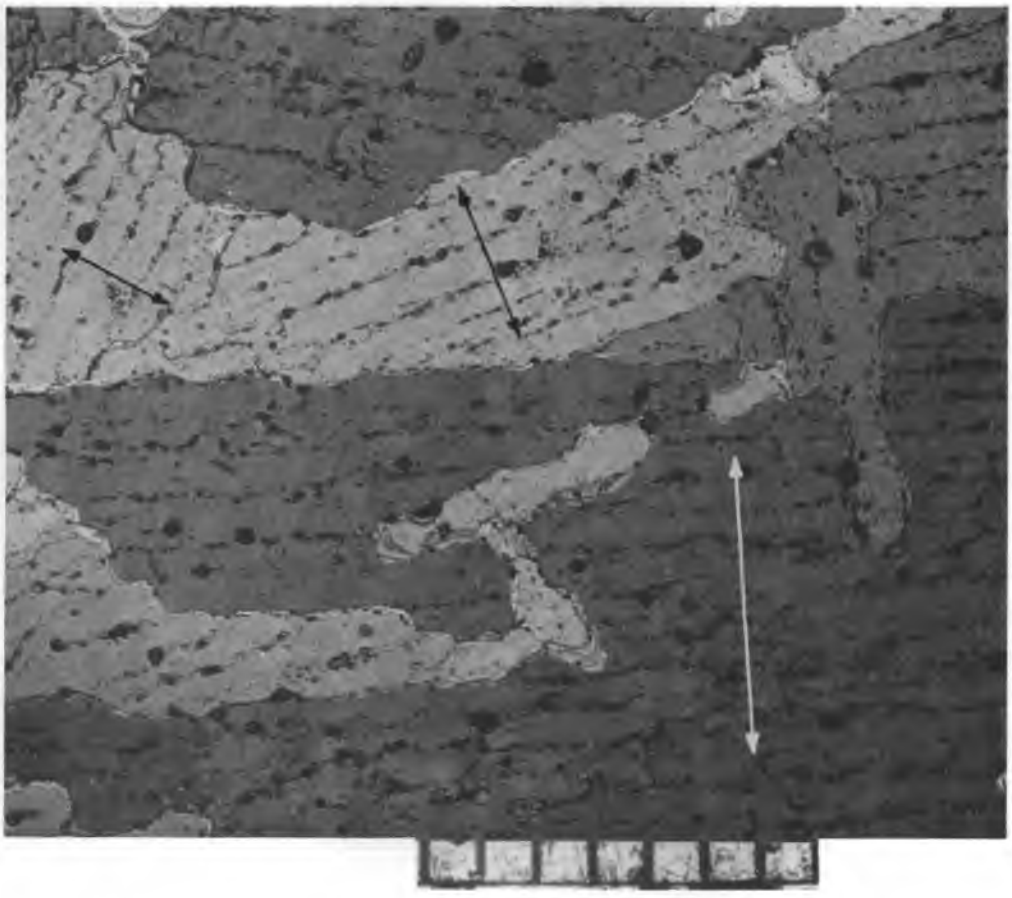

Figure 6. Enlarged horizontal thin-section photograph of congelation sea ice showing brine layer/ice plate crystal substructure composed of parallel strings of brine inclusions sandwiched between plates of pure ice. Arrows indicate crystal c-axis directions, normal to ice platelet/brine layer substructure of individual crystals. Scale subdivisions measure 1 mm.

pends mainly on the rate of growth; the faster the freezing, the narrower the plate spacing and the greater the salinity.

Subsequent changes in this substructure occur mainly in response to temperature changes in the ice. Brine inclusions are particularly sensitive in this regard; even small changes in thermal regime resulting from day-to-day variation in surface air temperature can cause significant changes in the geometry of the inclusions and the concentration of the entrapped brine. In the case of sea ice subjected to protracted warming, originally disconnected brine inclusions will tend to coalesce into vertical channels that promote migration of the brine. Such a process can lead to substantial redistribution of the brine and eventual drainage and desalination of the ice. Furthermore, changes in the distribution of the brine are often accompanied by changes in the mechanical properties of the ice. Since these effects are maximized in the case of multi-year ice, measurements of the above properties were also used in the current study to differentiate between the two principal ice types—multi- and first-year. Physical property changes, particularly those affecting the salinity profile of the ice and the free water content of snow on top of the ice, are also responsible for major changes in the electrical properties of the ice, insofar as they influence remote sensing signatures.

Congelation ice growth invariably leads to the formation of vertically elongated crystals with their c-axes oriented in the horizontal plane. This planar distribution of c-axes often is transformed into one in which the c-axes become aligned in a given direction. Such alignments of c-axes are commonplace in shorefast sea ice (often extending over areas of many square kilometers) and the direction of the alignment can usually be correlated with the measured or implied direction of current motion at the ice/water inteface. Weeks and Gow (1978) theorized that the action of the seawater flowing across the dendritic interface of the sea ice actually controls the ultimate c-axis alignments observed. Recent laboratory work by Langhorne (1983) and Langhorne and Robinson (1986) tends to confirm this relationship between c-axis alignment and the direction of the prevailing current. As such, c-axis alignments can be used to infer the principal current direction at a given location in shore-fast ice and, in the case of a multi-year floe, can be correlated with periods of ice growth when the floe was immobilized in the tight winter pack. However, any loosening of the pack and subsequent rotation of the floe during active ice growth would tend to inhibit such aligning of the crystals.

Granular ice also includes snow ice formed from the freezing of interstitial water in snow that had been soaked by either rain, snow meltwater or seawater. Naturally, such ice would be restricted to the top of the ice sheet. However, it is necessary to be able to differentiate snow ice from frazil ice, and occasionally, frazil ice from fine-grained congelation ice (Fig. 7). The formation of sea ice often begins with the growth of frazil crystals at the surface, but frazil can also form at some depth in the water column beneath the ice. By floating upward either as crystals or clumps of crystals, frazil is able to adhere directly to the bottom of an existing ice sheet. Such a process occurs on a widespread scale in the Weddell Sea, Antarctica (Gow et al. 1982, Gow et al. in press). One of the objectives of the study described in this report was to determine if a similar scale of frazil production also occurs in the Arctic Basin.

Generally, the various forms of granular ice can all be distinguished from fine-grained columnar ice on the basis of the ice plate/brine layer substructure that characterizes the latter, and differences in texture usually suffice to allow the various granular types to be differentiated. Snow ice, for example, is generally much coarser-grained and more bubbly than frazil ice.

A standard taxonomy for the classification of sea ice based on its stage of growth has been developed by the World Meteorological Organization (WMO 1956). Most of this terminology deals with very young ice, however. It is more common to refer to thicker ice (> 50 cm) as simply first- or multi-year. The WMO definition of multi-year ice requires that it have survived two summers. The distinction between multi-year ice and second-year ice is subtle, however, since one melt season gives the ice a characteristic surface relief appearance of alternating hummocks and melt ponds. In this report we will make only the large distinction between first-year ice and other ice that has survived at least one summer, which we will call multi-year ice.

RESULTS AND DISCUSSION

Our coring program attempted to sample both multi-year and first-year ice floes. We sought to take cores from flat areas of the floes in order to ensure sampling of undeformed ice. However,

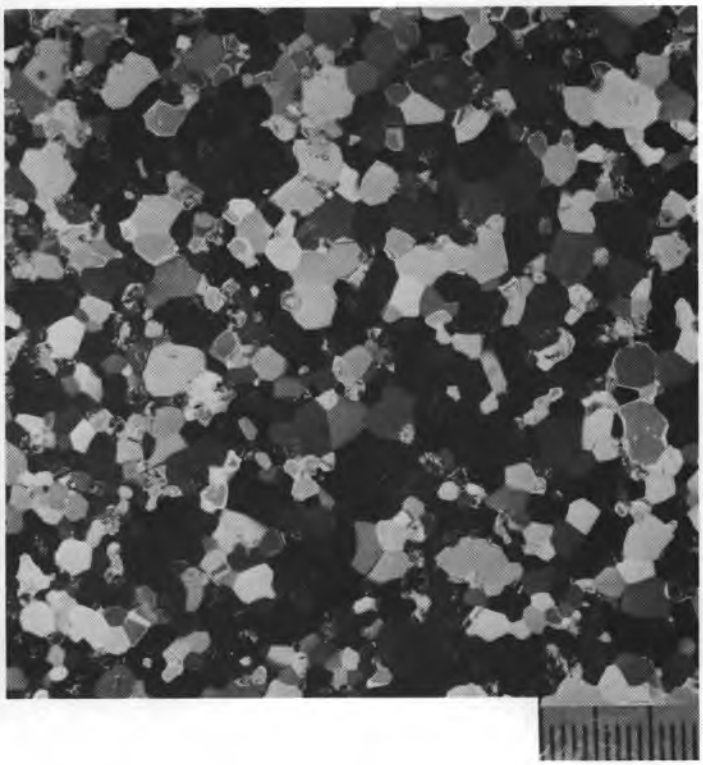

a. Snow ice.

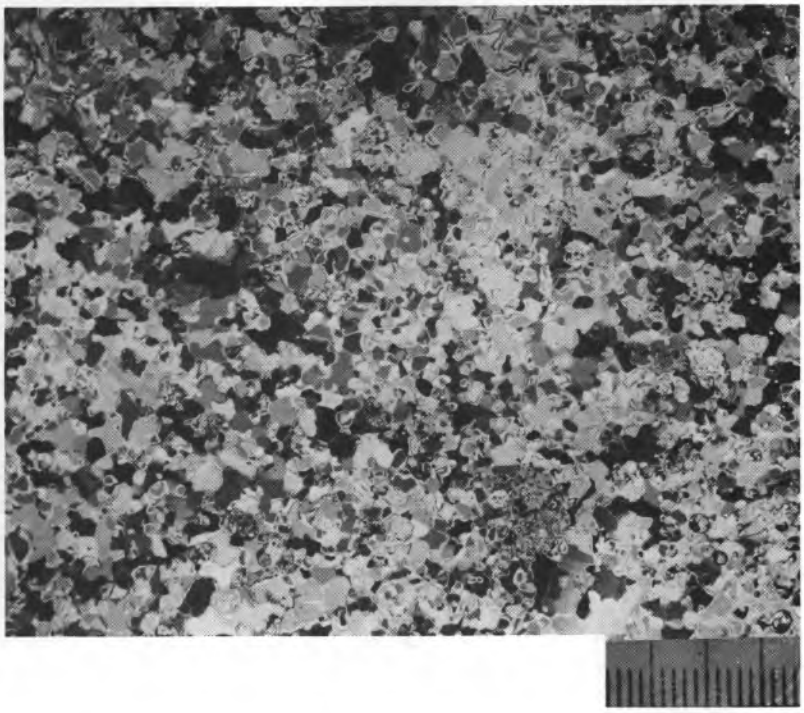

b. Frazil ice.

Figure 7. Horizontal thin-section photographs of snow ice, frazil ice and fine-grained congelation sea ice. Scale subdivisions are 1 mm.

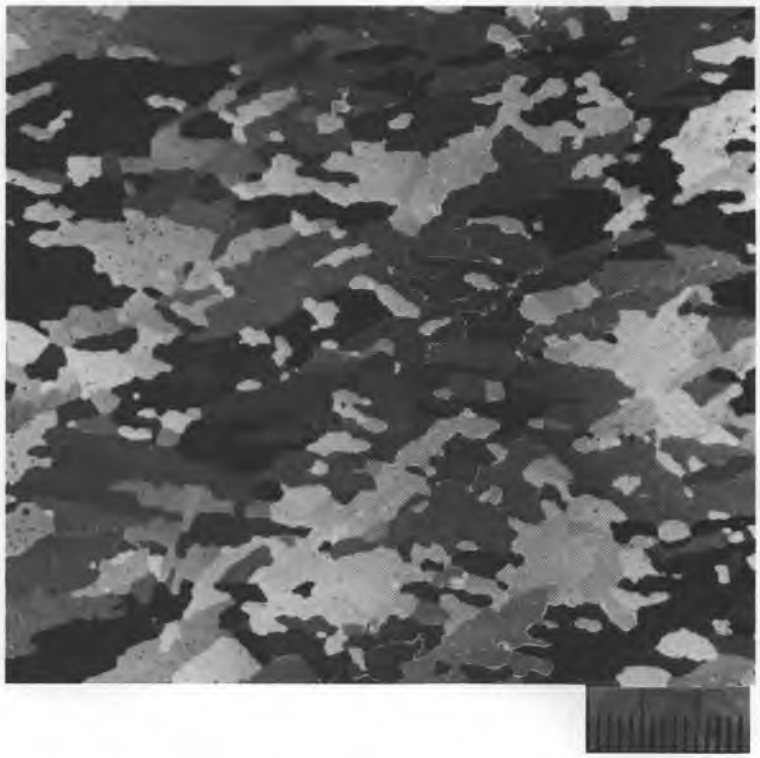

c. Fine-grained congelation sea ice.

Figure 7 (cont'd). Horizontal thin-section photographs of snow ice, frazil ice and fine-grained congelation sea ice. Scale subdivisions are 1 mm.

heavy snow cover made it difficult to detect small surface undulations, and later structural analysis revealed that we occasionally had drilled in previously deformed ice. In addition, we sometimes unintentionally sampled refrozen melt ponds.

First- and multi-year sea ice abundance

Of the 40 individual floes sampled, 27 were identified as multi-year, nine as first-year and four as composite floes made up of a combination of first-year and multi-year ice. These composite floes usually consisted of undeformed first-year ice attached to multi-year floes. Because we sampled first-year ice whenever the opportunity arose, the percentage of first-year ice we examined was biased toward higher values than actually existed in the region. High concentrations of multi-year ice were reported by the ice observer on board *Polarstern** and were also observed in the analysis of scanning multi-channel microwave radiometer (SMMR) data.† For a selected grid in the Fram Strait the SMMR data show large daily oscillations in the relative concentration of multi-year ice that may not be realistic, but multi-year fractions as high as 72% are observed. On the basis of the number fraction of multi-year/first-year ice floes examined, we estimate that the fraction of multi-year ice would exceed 75% in most areas transited by the *Polarstern*. On a volume basis, if we assume that multi-year floes average 70% thicker

* K. Strübing, German Hydrographic Institute, personal communication, 1984.

† P. Gloersen, Goddard Space Flight Center, NASA, unpublished data, 1984.

than first-year floes, multi-year ice would constitute more than 85% of the volume of ice discharged from Fram Strait during this period. This contrasts significantly with earlier estimates, for example, those based on visual observations on U.S. Navy Birdseye flights (Wittmann and Schule 1966) which indicated that multi-year ice represented less than 40% of the spring (June and July) ice cover in the Greenland Sea. Only early during the experiment, on 22 June, did we observe a high concentration of large to vast first-year floes near the ice edge at about 80°30′N, 6°30′E.

Two possibilities can explain the low percentage of first-year ice. The first is that first-year ice does not exist in large quantities in the source regions responsible for generating the ice that was transiting the Fram Strait during the MIZEX-84 period. The second possibility is that much of the first-year ice is deformed and crushed prior to entering the Fram Strait. Although we observed rubbled first-year ice heaped onto the edges of many multi-year floes, probably no significant areal fraction of first-year ice was consumed in this manner.

Snow depths

The depth of the snow cover on the ice was measured at each coring site. Because we chose sites located on level ice, generally a reasonable distance (> 50 m) from ridges or hummocks, our measured snow depths would seemingly be representative of level floes. We were surprised at the large depths of snow found here as compared to those observed during our previous studies in the Beaufort Sea. The snow masked surface features and depressed freeboards of the Fram Strait ice, making ice type identification very difficult, in contrast to the Beaufort Sea where multi-year ice can be easily identified from aircraft. Maykut (1984), however, reported large snow depths on a multi-year floe measured during the 1983 MIZEX pilot experiment, and we discovered that deep snow is always associated with multi-year ice in the Fram Strait.

Figure 8 shows the snow depths measured vs the calendar date with first-year and multi-year ice identified separately. The data plot clearly shows the greater thicknesses of snow observed on the thicker multi-year ice floes. Snow depths on multi-year ice ranged from 3 to 65 cm and averaged 28.5 cm. On first-year ice the snow cover was much thinner, averaging only 8 cm and never exceeding 20 cm. Figure 8 also shows a significant decrease in snow layer thickness for the period of the experiment. This decrease is much larger on the thicker multi-year floes than on first-year ice, and is mainly the result of densification of the snowpack coincident with progressively increasing surface air temperatures.

We have considered a variety of reasons for the very significant differences in snow depths on the first-year and multi-year ice floes. The most obvious explanation is that the first-year ice had formed after storms in the early fall had deposited significant snowfall on the existing multi-year floes. However, much of the first-year ice, including some attached to multi-year floes, was 2 m or more thick, implying that it had probably started growing in the early fall. It seems unlikely, then, that the large amounts of snow observed on multi-year floes could have been deposited prior to the onset of growth of the thick first-year ice.

Although we have no way of knowing the dates or amounts of snowfall events, we have plotted (in Fig. 9) the August 1983 through May 1984 monthly precipitation amounts at Alert and Nord, the two coastal stations believed to be in the closest proximity to the drifting ice that passed through Fram Strait during MIZEX-84. Precipitation is reported in water equivalent amounts, but most of the precipitation would have occurred as snow since the mean temperatures for both stations were well below freezing for every month except August. Although these water equivalent amounts cannot be accurately converted to snowfall thicknesses, a nominal snowfall/water equivalent ratio is 10:1. For the period August through December 1983, Alert received a total of 61 mm of precipitation while Nord received 79 mm. From January until May 1984, Alert received 31 mm and Nord received 109 mm. The latter amounts indicate that both stations received significant amounts of their annual cumulative snowfalls during winter and spring. If similar conditions prevailed over the nearby pack ice, we would have expected the earliest formed and thicker first-year ice to have snow depths comparable to those on multi-year ice. This was not the case.

An alternative and seemingly more plausible explanation of differences in snow cover thickness is that the snow on the first-year ice is more susceptible to loss by sublimation than that on the multi-year ice. Because the first-year ice is relatively thin, more heat is conducted from the ocean to the ice surface, and sensible and latent heat losses to the atmosphere are correspondingly larger than those for thick ice. Maykut (1978) presents modeling results for snow-free ice which show that 3.0-m-thick ice experiences negligible latent heat

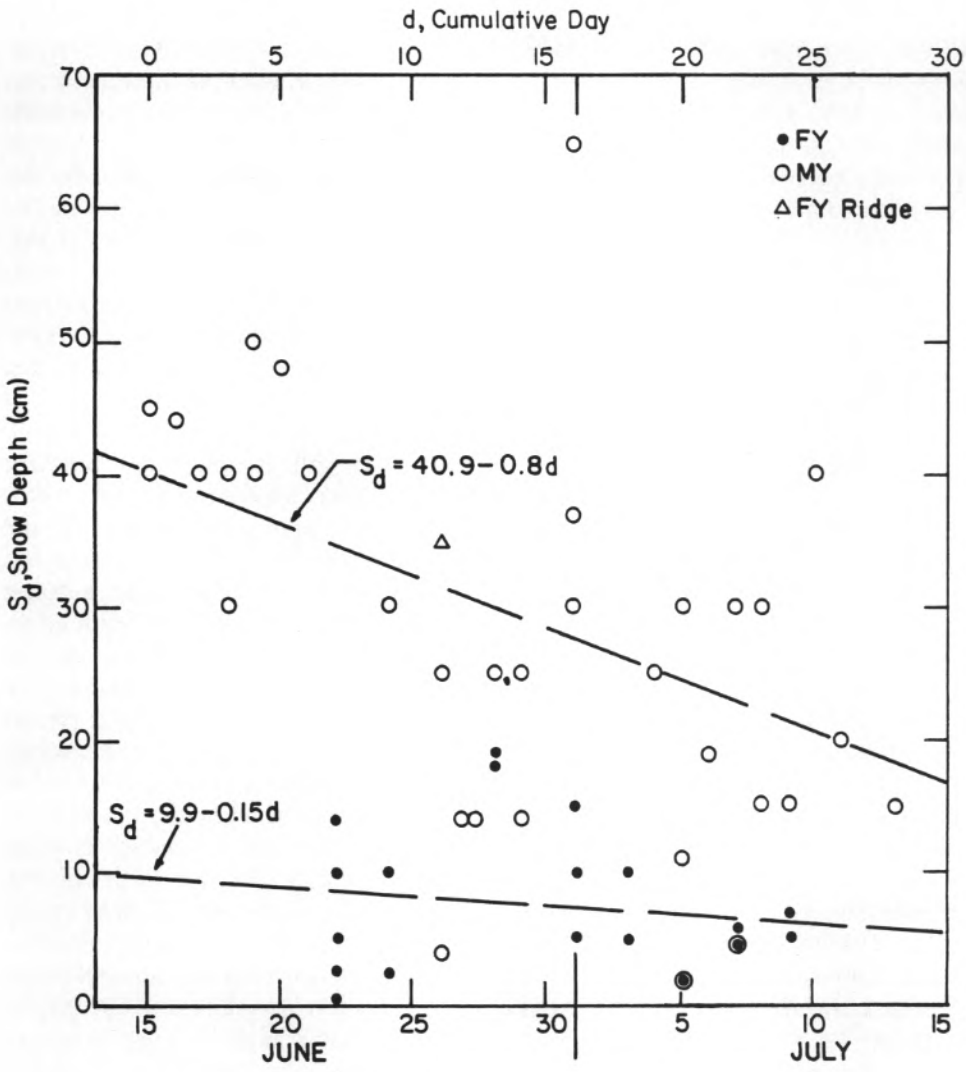

Figure 8. Snow depth measured at coring sites vs calendar date.

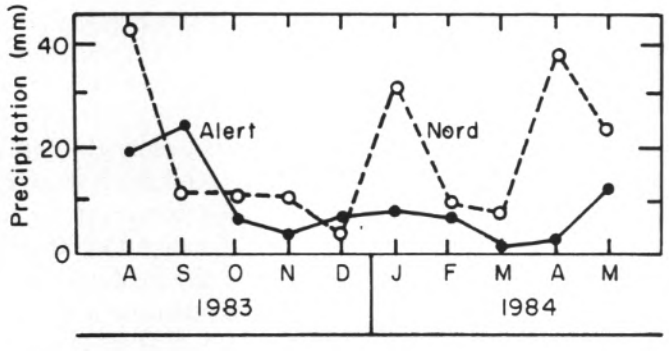

Figure 9. Monthly precipitation amounts at Alert, N.W.T., and Nord, Greenland, during fall 1983 and winter and spring 1984.

loss from November through May, while thinner ice experiences substantial heat loss. Thus, the transfer of oceanic heat through young, thinner sea ice may be sufficient to sublimate substantial quantities of snow cover, and according to calculations by Maykut (1978) of the latent heat flux for a 40-cm-thick ice sheet, sufficient energy is available to sublimate 7 cm of snow from mid-November until 1 March. From 1 March to the end of May approximately 23 cm of snow can be sublimated. We are currently investigating this effect with a full thermodynamic ice growth model that includes a snow cover.

Ice thickness and freeboard

First-year ice thicknesses ranged from 38 cm in a newly refrozen lead to a maximum of 236 cm in a flow that measured several kilometers in diameter. Multi-year ice thicknesses ranged from 174 to 536 cm but the thicker of these came from old ridge fragments. The greatest thickness observed that showed no evidence of previous deformation was 411 cm, but only in one floe exceeding 3.5 m in thickness was the ice undeformed. Ten of the 31 multi-year cores retrieved were identified as having been drilled in ridged ice. As stated earlier, we intentionally attempted to avoid ridged ice, but the fact that one-third of our multi-year ice cores contained ridged ice indicates that the snow effectively obscured surface features and also that multi-year floes may be composed of a significant amount of deformed ice that has no intrinsic surface expression. Indeed, the reason that multi-year floes survive for several years may inherently result from their being composed of a large percentage of stronger and thicker multi-year ridges. The thicknesses of the undeformed multi-year floes that we cored are shown in the histogram presented in Figure 10. As shown, the majority of the floes measured between 2 and 3 m thick. These thicknesses are less than the 3- to 4-m equilibrium thickness for undeformed arctic sea ice as predicted from thermodynamic modeling (Maykut and Untersteiner 1971). If these thicknesses are representative of the floes on which the coring sites were located, then the thicknesses indicate that most of these floes are relatively young, having not yet grown to equilibrium thickness. Other ice properties (described later) verify that this is in fact the case.

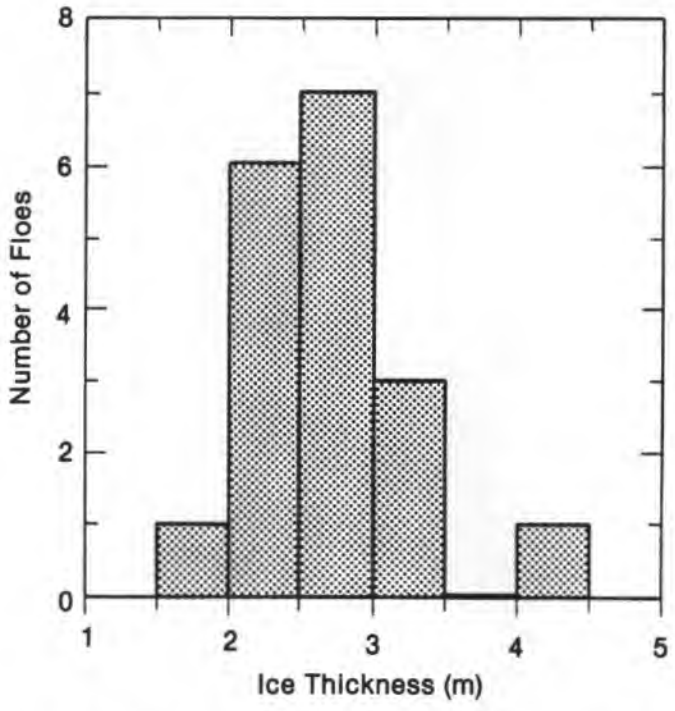

Figure 10. Frequency of undeformed multi-year ice thickness.

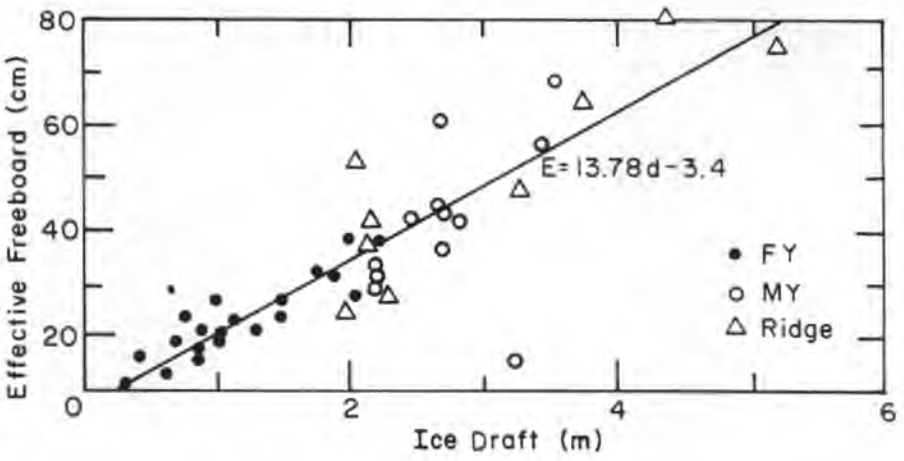

Figure 11. Effective freeboard E *vs ice draft,* d. *Effective freeboard increases the measured freeboard by an amount equal to the product of the ratio of snow to ice density and snow depth.*

The height of the ice surface above water level in the coring hole was also measured at each drilling site. The freeboards varied from zero (in the case of flooded surfaces) to 55 cm on very thick ice. Snow cover depresses the ice; therefore, examining freeboard and thickness has little value unless the snow cover is accounted for. We have calculated an effective freeboard by converting the snow depth to an equivalent ice thickness and then adding this value to the measured freeboard.

Figure 11 shows the effective freeboard plotted vs ice draft for our data. In the calculation of effective freeboard we assumed an ice density of 0.92 Mg m^{-3} and a snow density of 0.45 Mg m^{-3}. The snow density was a reasonable average of measured densities made at many of our coring sites by Burns and Larson (1985). The effective freeboard correlates with ice thickness with a coefficient of 0.87. As shown, the largest errors are associated with multi-year ice or ridge fragments. In general, however, the figure indicates that our drilling sites were located in areas of reasonable isostatic equilibrium. Although our investigations were not intended to obtain freeboard-draft relationships, this sparse data set yields a draft/effective freeboard ratio of 7.25:1.

Salinity

The salinity profiles (a total of 51 from 40 individual floes) usually allowed for positive identification of the ice as first-year or multi-year, especially in cases where the thickness may have indicated otherwise. That the salinity in upper layers of multi-year ice is very low is apparent in Figure 12, which contains the mean salinity profiles for all of the multi-year and first-year ice cores. Separate profiles have been calculated for the first-year ice cores obtained in June (15–28 June) and for those obtained in July (1–9 July) in order to examine the possible effects of ongoing brine drainage.

That the first-year ice was losing brine for the duration of the field program is clearly shown by the June and July mean profiles in Figure 12. The July profile is much less saline (by nearly 2.0‰ at some levels) than the June profile to a depth of 1.5 m where the profiles begin to converge. All first-year cores had relatively low near-surface salinities in contrast to normal winter first-year ice which typically exhibits a c-shaped salinity profile with higher salinities at the top and bottom of the growing ice sheet (Nakawo and Sinha 1981). The low upper level salinities that we observed are indicative of drainage resulting from warming of the ice prior to our sampling, which began in mid-June.

The multi-year ice salinities showed no such temporal dependence when individual mean profiles were calculated for June and July. Extensive desalination during previous summers left the ice nearly free of brine and solid salts, especially in the upper 1.0 m, making further changes difficult to detect. We also calculated mean salinity profiles for deformed and undeformed multi-year ice. In this case, the mean profiles showed little difference but the standard deviations at individual levels of the deformed ice profile were larger than those for undeformed ice. This higher variability

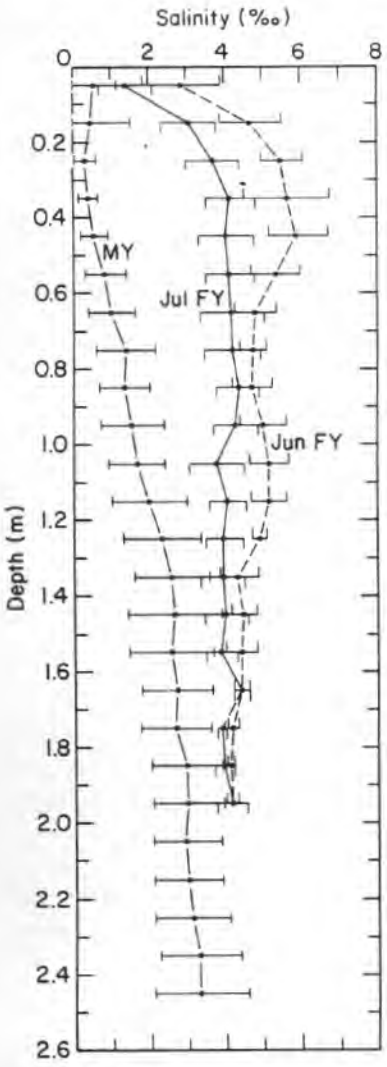

Figure 12. Mean salinity profiles for all multi-year ice cores and for first-year ice cores for June and July.

is probably attributable to the modification of drainage processes when ice blocks are left in tilted positions after ridging and also to differences in initial brine entrapment and drainage in granular ice which apparently forms in the voids between the ice blocks.

The variation of the bulk salinity with thickness for both ice types is shown in Figure 13. Both first-year and multi-year ice show a slight salinity increase with thickness. The sharp distinction between the bulk salinities of first- and multi-year ice is clearly seen in Figure 13. For multi-year ice, the best fit linear regression line of salinity S_i to thickness h is

$$S_i = 1.58 + 0.18h.$$

This least-squares fit is in excellent agreement with that found by Cox and Weeks (1974) for warm multi-year ice in the Beaufort Sea. On the Ymer-80 expedition, however, where samples were collected in the Greenland and Barents Seas by Overgaard et al. (1983) the dependence of salinity on thickness was found to be

$$S_i = 1.59 + 0.37h.$$

The slope is twice that found by us or Cox and Weeks (1974) and indicates that thicker ice sampled during the Ymer-80 cruise was more saline ($\approx 0.8‰$ for 3.0-m-thick ice). However, the differences may not be significant because, as Figure 13 clearly shows, a large scatter in the bulk salinities exists, particularly in the thicker ice categories.

For first-year ice, we found the relation

$$S_i = 3.75 + 0.22h$$

while that found by Overgaard et al. (1983) was

$$S_i = 2.15 + 0.19h.$$

Here lower salinities for the Ymer-80 data are indicated. The Ymer-80 sampling took place later in the summer than MIZEX, and the observed results are in keeping with the trend of descreasing salinities during summer warming. Again, desalination is explained in terms of the very active brine drainage occurring in the ice as it warms.

In several cases, extremely low salinities were observed in transparent ice in the upper few centimeters of first-year floes. Six cores exhibited salinities of less than $1.0‰$ in the upper 10 cm. Figure 4 is an example of this situation. This ice was composed primarily of columnar crystals typical of ice that forms when fresh water freezes. The indication is that the surfaces of these floes were at some point covered by a layer of fresh water that originated either from melting snow or from rain. In either case, it appears that above-freezing temperatures had influenced the surface properties of the floes at some time prior to our sampling them.

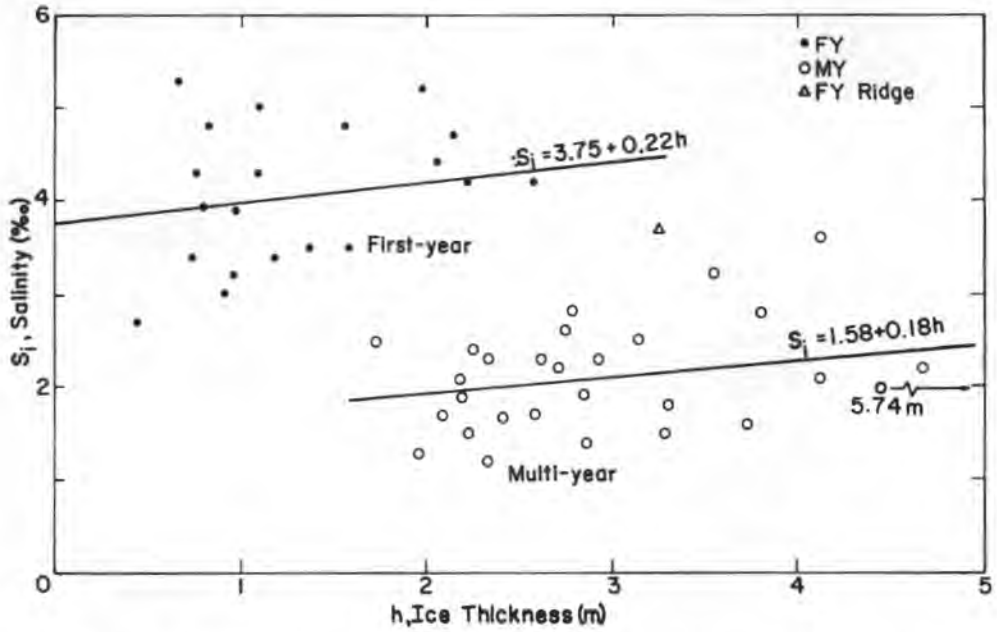

Figure 13. Bulk salinity values of ice cores as a function of floe thickness.

In contrast, surface salinities exceeding 3.5‰ were found on two multi-year floes. In both cases, the weight of the snow cover had been sufficient to depress the floes until their surfaces became flooded with seawater. Some of the seawater was subsequently absorbed into the upper layers of the ice, raising its overall salinity.

A comparison of MIZEX-84 data with Antarctic summer sea ice salinity profiles indicates significant differences in bulk salinities of both first-year and second-year sea ice, especially the latter. For example, in the only comparable studies made in the Antarctic (see Ackley et al. 1981, Gow et al. 1982 and Gow et al. 1987), in the Weddell Sea, an average bulk salinity relationship of $S_i = 3.83 + 0.11h$ was obtained for multi-year ice. This relationship yields substantially higher salinities than those found in Fram Strait ($S_i = 1.58 + 0.18h$). These salinity differences can be immediately attributed to differences in surface air temperatures, which rarely rise above 0°C in the Weddell Sea pack, thereby generally diminishing drainage of brine by flushing, a major cause of desalination of sea ice in the Arctic during summer. Differences between first-year ice were not so great, with average bulk salinities being higher for Weddell Sea ice by only about 0.3 to 0.4‰.

Ice temperature

In general, the temperature profiles trended from near 0°C at the ice surface to the freezing point, around –1.8°C, at the ice/water interface. Rather than being linear, most profiles showed the largest temperature gradient in the upper meter, and then were generally isothermal through the remainder of the thickness. As time progressed, the profiles became more linear, indicating warming of the deeper ice. Temperatures as low as –4.0°C were recorded in some of the very thick floes. Such low temperatures, usually located close to the thickness midpoint, immediately indicated that considerable drilling remained prior to penetrating the floe.

Drift history

The geographical region of origin and the drift path followed by the individual floes that we examined is of obvious interest to us. Unfortunately this information is virtually impossible to ascertain. At least part of the drift track may be estimated, however, by comparison with the tracks of drifting buoys that passed through the region. We are fortunate in that two such buoys passed through the Fram Strait at the time we were conducting our investigations. These buoy tracks and our general sampling area are shown in Figure 14. Although the buoys passed through the western reaches of our sampling area, they provide some evidence as to drift of the ice before it passed through the Fram Strait. We can probably assume that the ice passing through the region we sampled also transited an area to the east of these buoy

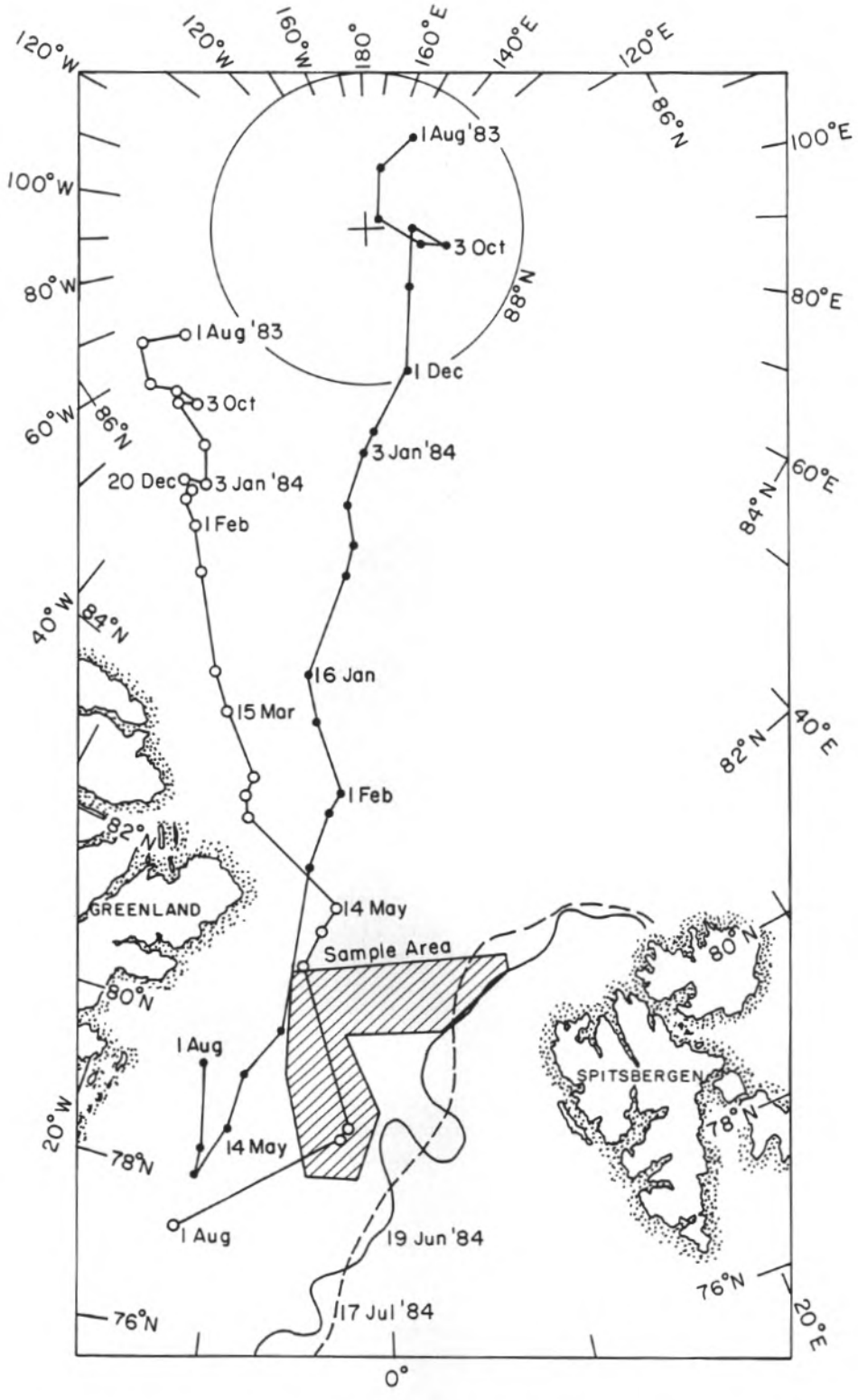

Figure 14. Drift tracks of two buoys that passed through Fram Strait during MIZEX. Shaded area covers Polarstern *sampling area.*

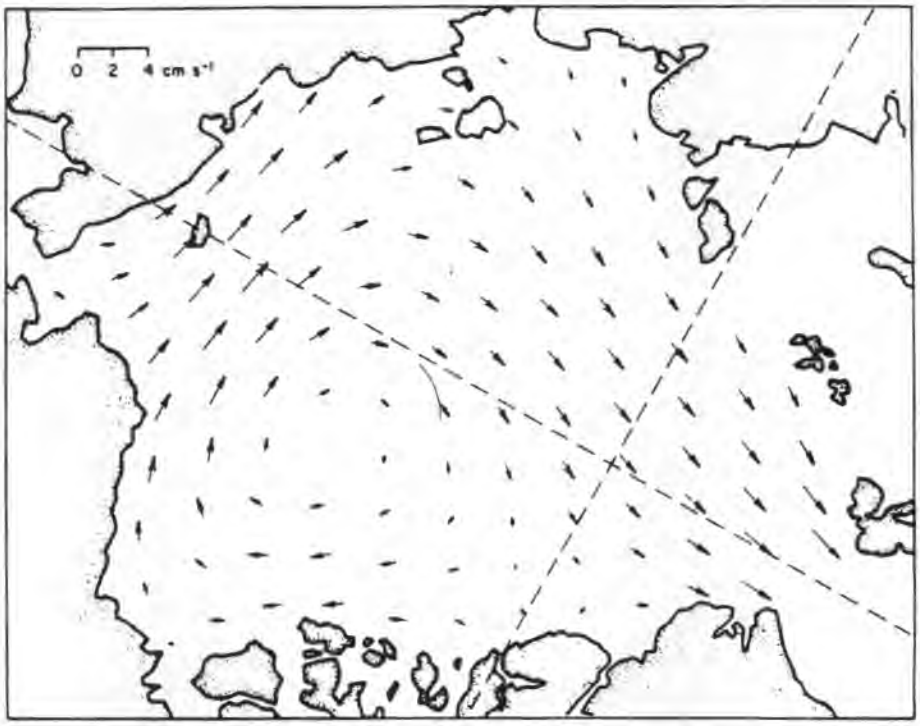

Figure 15. Mean sea ice motion field interpolated from research station positions and automatic data buoys. (After Colony and Thorndike 1984.)

tracks. Analysis of mean sea ice motion fields by Colony and Thorndike (1984, 1985) verifies this assumption. Figure 15 shows the mean field of ice motion derived from drift tracks of buoys and ice stations. This figure indicates that ice in the Fram Strait east of the Greenwich Meridian either originated or spent a considerable amount of time east of that meridian on its voyage south.

Crystalline structure and composition

Analysis of the crystalline structure of Fram Strait ice floes shows that ice textures are predominantly of columnar (congelation) origin in both multi-year and first-year floes. Combining core lengths from all the floes (a total of 122 m of core was examined for structure) we found that 75% of the ice consisted of columnar ice and 25% was composed of granular ice. Data presented in Figure 16 show that small amounts of granular ice, mainly frazil ice but including some snow ice, were found in nearly every core. This is not surprising since the freezing of seawater generally begins with the formation of grease or slush ice. If we exclude ridged ice from our ice composition estimate we find the congelation component increasing to 85% of total ice thickness in undeformed floes. Thus, while the granular ice content of undeformed ice floes is somewhat higher (15%) than the 5–10% that Martin (1979) reports for arctic nearshore conditions, it should be noted that Martin restricted his study to thick first-year ice whereas our investigations spanned a large range of ice thicknesses dominated by multi-year floes. However, the amounts of frazil are very much smaller than those observed in floes in the Weddell Sea, Antarctica, where frazil often occurs in excess of columnar ice and is estimated to represent 50–60% of the total ice in the Weddell Sea pack (Gow et al. 1982, Weeks and Ackley 1982, Gow et al., in press).

Most of the granular ice we observed was associated with frazil crystal formation in old ridges. Such frazil occurred both in the voids between blocks of ice and near the bottoms and on the flanks of ridges. Only limited amounts of granular ice appear to have originated by crushing of coarser-grained ice during the ridging process. However, we speculate that small particles consisting of snow or crushed ice nucleate frazil crystal growth in the voids. On average, the multi-year ridges consisted of 40 to 60% frazil ice. An example of ice structure in an old ridge fragment is shown in Figure 17. The top meter of ice consisted of a mixture of tilted blocks of columnar ice with

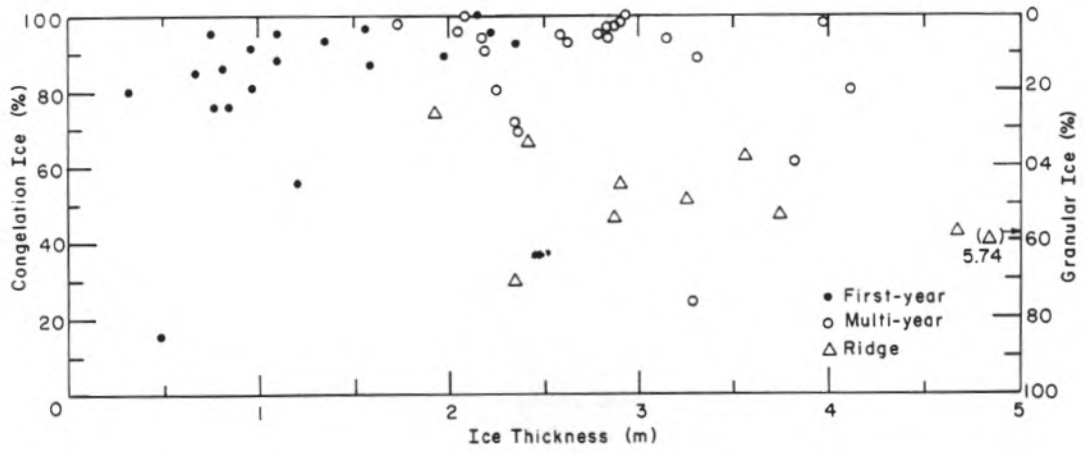

Figure 16. Percentages of congelation and frazil (granular) ice for each core shown as a function of ice thickness.

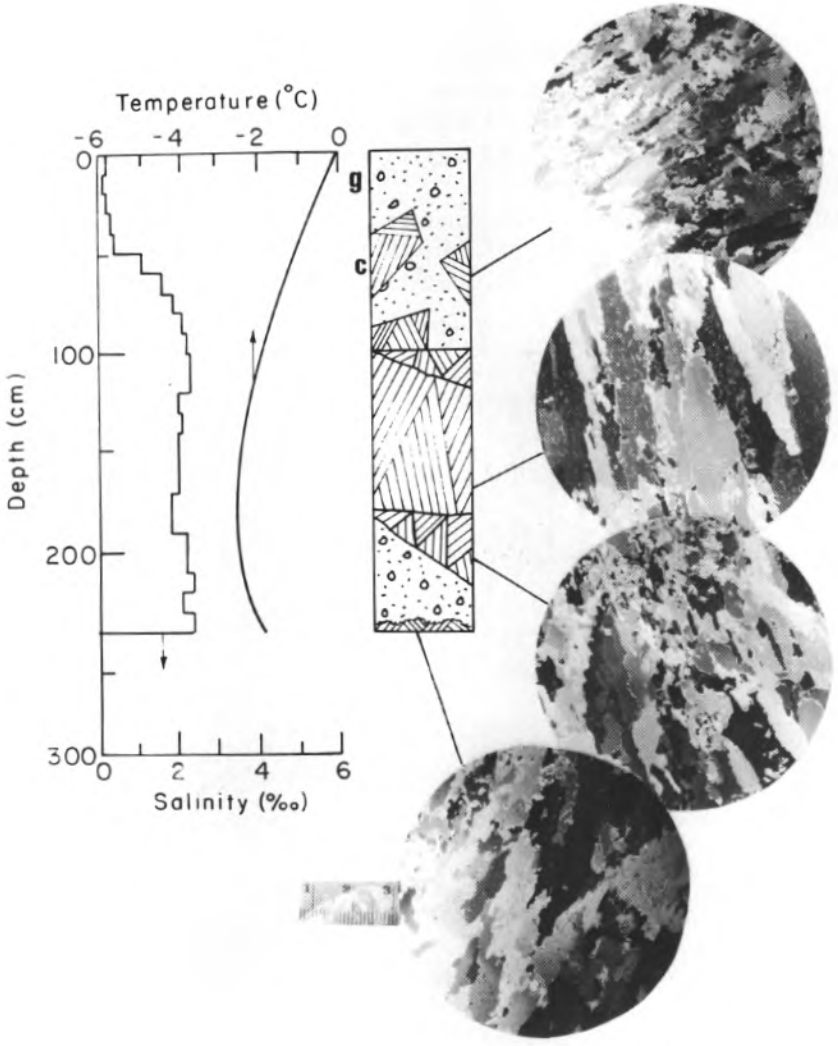

Figure 17. Salinity–temperature–structure profiles of a multi-year ridge fragment. Diagram and symbol designations are the same as for Figure 4.

granular ice between the blocks. The lower part of the ridge contained more granular (principally frazil) ice underlain by columnar ice representing recent growth on the flank of the ridge. In only one multi-year floe lacking evidence of ridging did we find substantial amounts of granular (frazil) ice.

As noted above, columnar ice is the dominant crystal type observed in Fram Strait floes, representing at least 75% of the ice we examined during MIZEX-84 and constituting 85% of the ice in undeformed floes. It occurred in a variety of textures, a representative sampling of which is shown in Figure 18. Figure 18a shows columnar ice in horizontal section in which the c-axes are not only horizontal but also are strongly aligned. The c-axes are normal to the long dimensions of the crystals. This particular section was prepared from ice at a depth of 203 cm. In sharp contrast, Figure 18b shows a section from near the bottom of a 236-cm-thick first-year floe. In addition to exhibiting a variety of crystal sizes and shapes, very little crystal alignment is observed here.

An example of much finer-grained columnar ice than in either of the sections featured in Figure 18 is shown in Figure 7c. Note also in this fine-grained variant of congelation ice the absence of any significant alignment of the crystals. This section of ice was obtained from a depth of 225 cm in a multi-year fragment.

The variation in the degree of alignment of horizontally oriented c-axes ranged from entire floes containing crystals, randomly oriented within the horizontal plane, to floes exhibiting preferred c-axis alignment that remained constant throughout the greater part of the ice thickness. However, among the more interesting examples of orientation texture were those in which the direction of c-axis alignment changed with depth in the floe. One example in which two zones of distinctly different alignment direction are underlain by unaligned bottom ice is shown in Figure 19. Such alignments clearly record growth in stable or stationary environments (either shore-fast or tight pack) with the changes in alignment direction reflecting changes in the orientation of the floe with respect to current motion at the ice/water interface. Lack of preferred orientation at the bottom of the site 7-5-1 core (Fig. 19) indicates that this ice grew under conditions of continual rotation of the floe, most probably during its passage through Fram Strait. Most floes showed evidence of aligned

a. Strongly aligned c-axes (normal to platelet structure) from 203-cm depth.

Figure 18. Horizontal thin sections showing variations of texture in columnar ice.

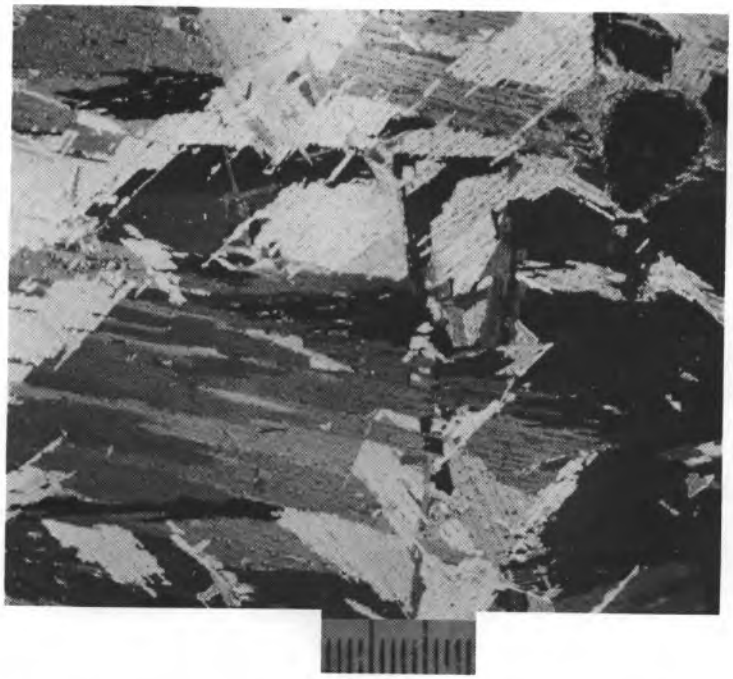

b. Variable c-axis orientations at bottom of 216-cm-thick floe.

Figure 18 (cont'd).

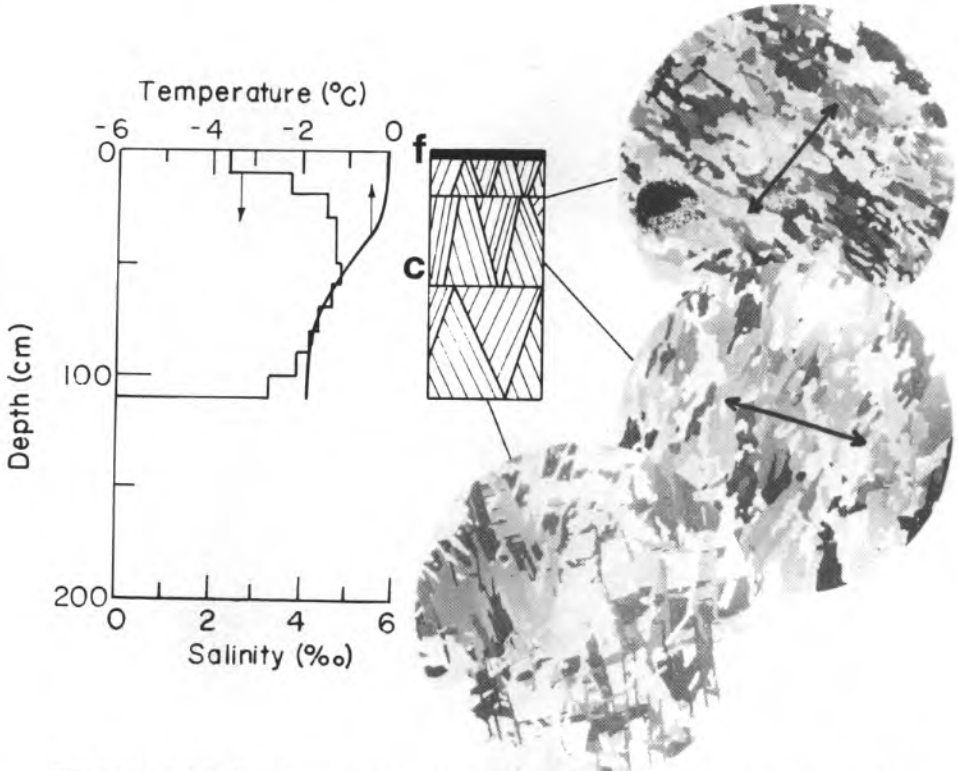

Figure 19. Salinity–temperature–structure profiles of first-year ice core from site 7-05-1. Arrows indicate direction of preferred c-axis alignment. Diagram and symbol designations are the same as for Figure 4.

c-axis growth; in multi-year floes changes in c-axis alignment from one year to the next clearly reflect oriented crystal growth during periods when the floe was immobilized in a tight pack and constrained from rotating with respect to the currents immediately beneath the ice.

Refrozen melt ponds were found to have crystal textures that are very similar to those observed in ice formed on freshwater lakes. Figure 20a shows typical melt pond crystal texture as observed in a horizontal section. Grain cross-sectional diameters up to 1 cm are commonplace and the c-axes are randomly distributed in the horizontal plane. The location of this section was 7 cm below the top of the melt pond on a multi-year floe. The salinity at this depth measured less than 0.2‰. The vertical section of this ice (not shown here) displayed a columnar texture with vertically oriented crystals. A much more dramatic example of melt pond structure is shown in Figure 20b, a vertical section of the top 15 cm of ice from a different multi-year floe. Here a 5-cm-thick layer of snow ice, made up of large, randomly oriented crystals, overlies a melt pond exhibiting vertical c-axis crystals. The individual crystals here are very large, the result of slow unseeded freezing of the water.

Gow (1986) points out that the type of crystal structure, occurring in lake ice covers, is determined by whether or not the lake water is seeded at the onset of freezing. Seeding leads to the growth of columnar, c-axis horizontal crystals, and unseeded (spontaneously nucleated) growth promotes the formation of massive, c-axis vertical crystals. The same is also true of melt ponds freezing on the tops of multi-year sea ice floes. Beneath the melt-pond ice, a sharp transition to columnar sea ice is evident. Refrozen melt-pond layers were typically 10 to 20 cm thick. In one extreme exam-

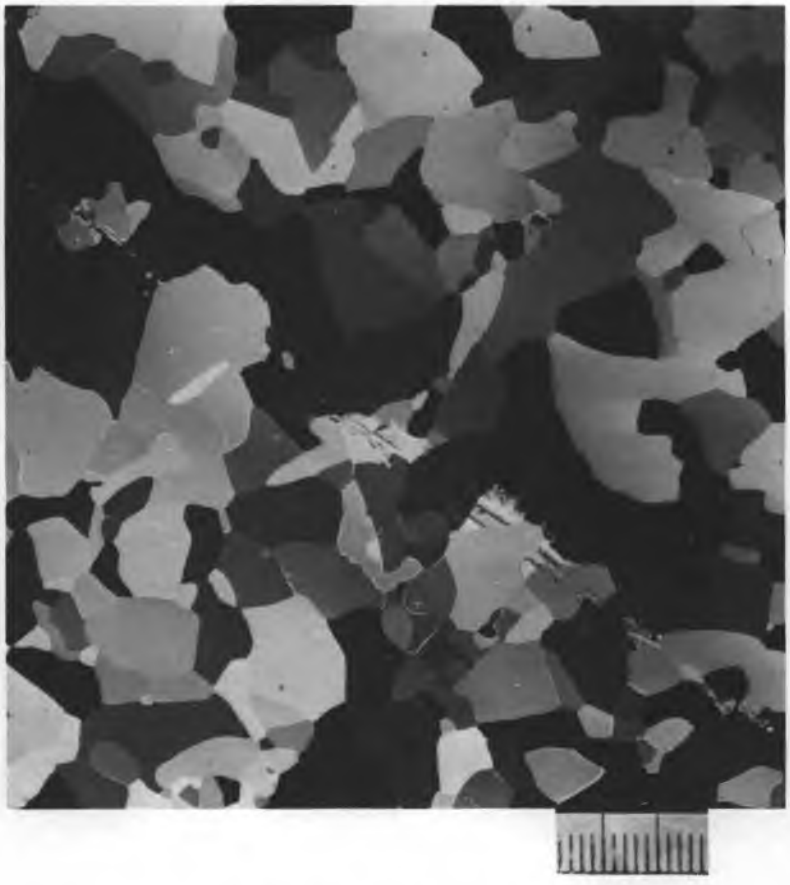

a. Horizontal section from 7-cm depth, site 6-21-1.

Figure 20. Thin-section photographs of refrozen melt pond structure.

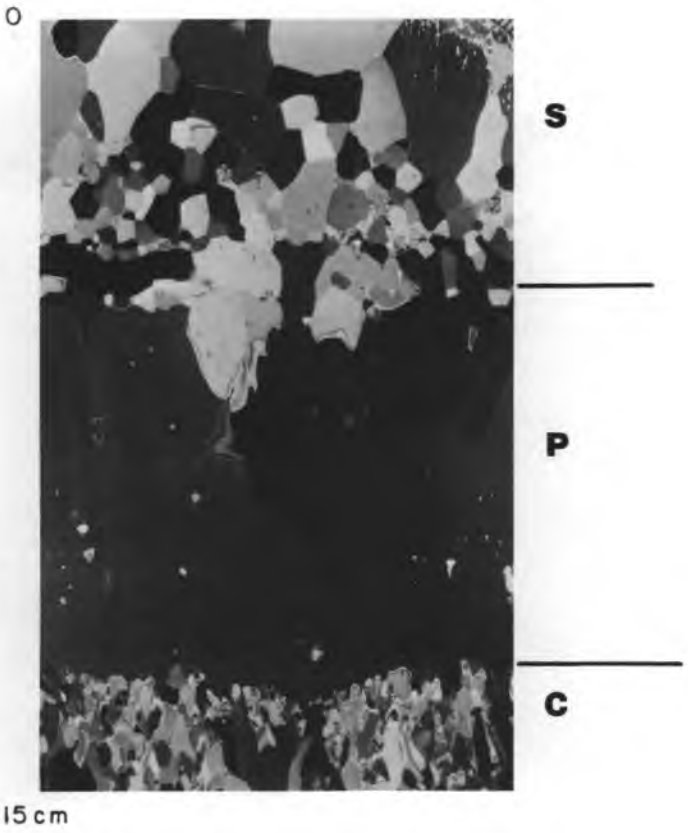

b. Vertical section from 0 to 15 cm from site 7-06-1 showing granular snow ice (s) overlying freshwater pond ice (p) with vertical c-axes, underlain by columnar sea ice (c).

Figure 20 (cont'd).

ple, however, as demonstrated in the ice floe profile shown in Figure 21, the refrozen melt pond extended to a depth of 1 m. In this instance the melt pond froze with a substantially vertical c-axis structure. The freshwater nature of this ice is clearly reflected in the very low values of salinity compared to those in the underlying sea ice, resulting in a very sharp transition between the two ice types.

Cores from many of the floes examined during MIZEX-84 exhibited banding. These bands, generally less than 1 mm thick, are readily observed on account of their semi-transparent appearance. They appear very similar to bands reported elsewhere in the Arctic by Bennington (1963) and in the Antarctic by Gow et al. (in press) where their formation has been attributed to fluctuations in growth velocity. Bands were only found in congelation (columnar) ice and thus constitute *prima facie* evidence of columnar crystal ice growth when observed in freshly drilled cores.

Algae was occasionally observed, usually attached to the bottom of the ice, but frequent observations of the ice upturned by *Polarstern* as she traversed the pack did not indicate widespread occurrence. Dirt bands of unknown origin were observed at two separate levels in one floe. Generally, it could be said that floes discharging through Fram Strait during MIZEX-84 were remarkably free of debris of any kind.

First- and multi-year ice structure distinctions

In the Arctic, undeformed multi-year ice is usually distinguished from first-year ice on the basis of 1) its rolling hummocky surface, the result of differential melt, and 2) its salinity profile showing near-zero values in the ice above sea level, but

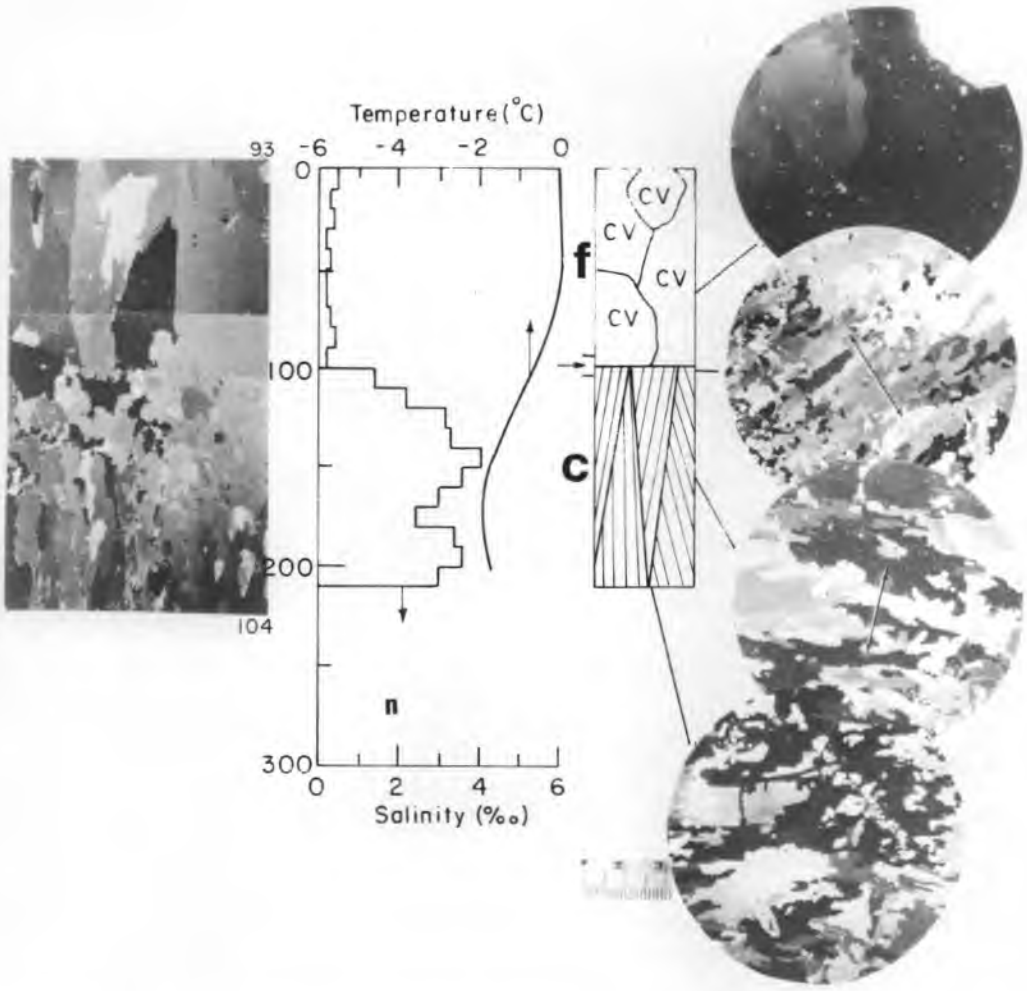

Figure 21. Salinity–temperature–structure profiles of a multi-year floe (site 6-18-2) consisting of congelation ice overlain by a 1-m-deep refrozen melt pond. Vertical section at left shows transition from melt pond ice to sea ice. Diagram and symbol designations are the same as for Figure 4.

then increasing to 3–4‰ in the lower parts of the floe. Identification on the basis of the former proved difficult during MIZEX-84 because of the heavy layer of snow that blanketed the surface of most multi-year floes. However, as described earlier, it was our experience that snow layer thickness, being much thinner on first-year floes, was often sufficient to distinguish between first-year and multi-year floes. This relationship certainly holds for ice we observed in Fram Strait during June and July and, from our preliminary analysis based on snow ablation modeling, a plausible case can probably be made for its application generally to ice entering Fram Strait from the Arctic Basin.

Identification of multi-year ice on the basis of freeboards or drilled thickness was not always reliable, especially in the region of thickness overlap where the thinnest multi-year ice (1.7 to 1.8 m) was appreciably thinner than the thickest first-year ice (2.3 m thick). However, even ignoring snow layer thickness and freeboard considerations, we could usually make identification of multi-year ice from observations of the appearance and mechanical condition of ice cores in the top meter of a floe. First-year ice is characteristically opaque, mainly because of the light scattering effect of the numerous brine pockets located within the substructure of the sea ice crystals. However, our experience in Fram Strait was that the top half-meter to one meter of ice in multi-year floes is 1) much less opaque and often semi-trans-

parent in appearance, and 2) much more resistant to drilling and sawing than first-year ice.

These changes to harder, less opaque ice within the top meter or so of multi-year floes can be attributed to the exposure of the ice to elevated temperature during the previous summer or summers. This results not only in substantial loss of brine, as borne out by salinity measurements, but also in significant changes in the crystalline texture of the ice. These changes include major modification of the ice plate/brine lamella substructure of brine pockets, and substantial smoothing out of the typically angular, interpenetrated outlines of the crystals themselves. We saw no evidence that this textural modification of the crystals resulted in changes in the lattice orientation (original c-axis alignments are usually retained), and for this reason we prefer to describe this process as *retexturing* rather than recrystallization.

Although the sequence of horizontal thin sections in the multi-year profile in Figure 5 clearly indicates some diversity of crystal structure, evidence for retexturing of the ice is best observed in magnified sections, such as those shown in Figure 22. These sections were obtained from depths of 20, 93, and 192 cm, respectively, in a 294-cm-thick floe that was very similar structurally to that shown in Figure 5. Vertical sectioning of the core verified that it consisted entirely of congelation (columnar) ice.

In ice from 192 cm (Fig. 22a), crystals are still interpenetrated structurally and also retain the well-defined platelet/brine lamalla substructure so characteristic of congelation ice. However, the salinity (2.5‰) clearly indicates some loss of the originally entrapped brine even at this level in the floe. Since this floe was 294 cm thick, ice now at 192 cm was probably formed two winters ago but

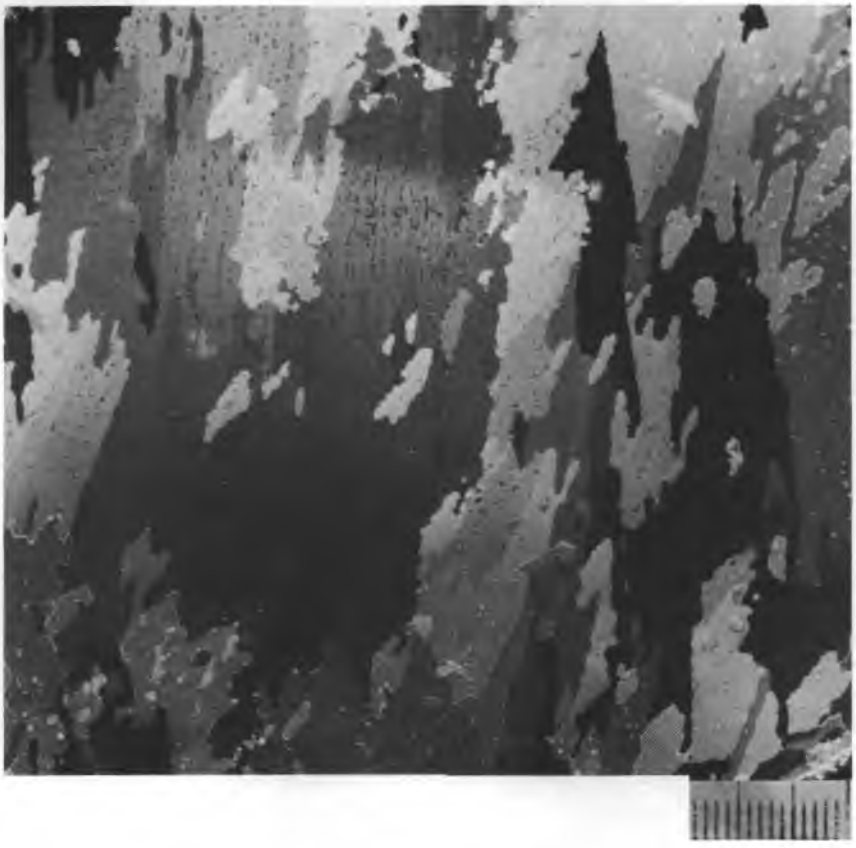

a. 192-cm depth.

Figure 22. Horizontal thin sections demonstrating retexturing in upper levels of a multi-year ice floe, 285 cm thick (site 6-16-1). Scale subdivision measures 1 mm.

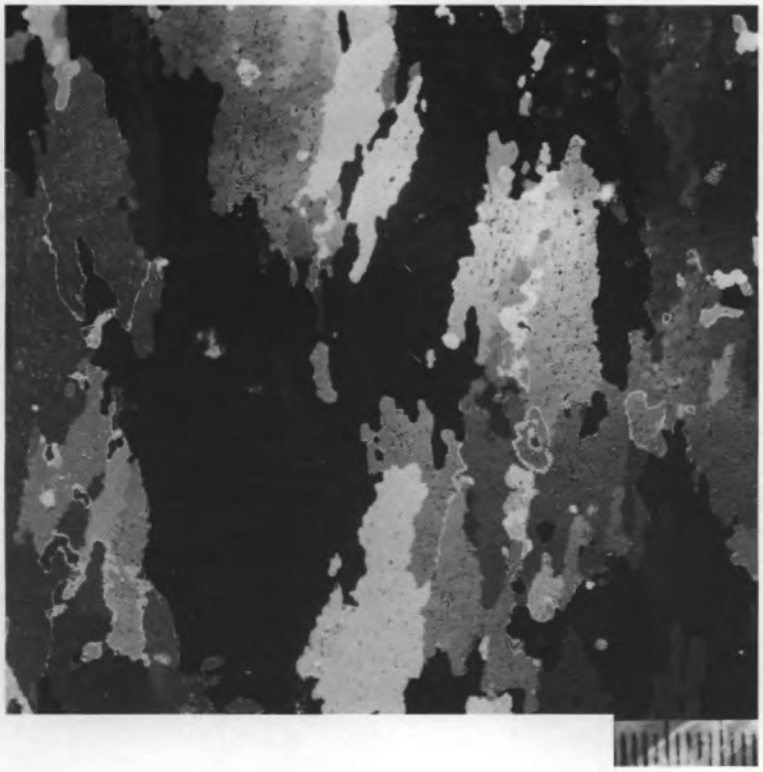

b. 93-cm depth.

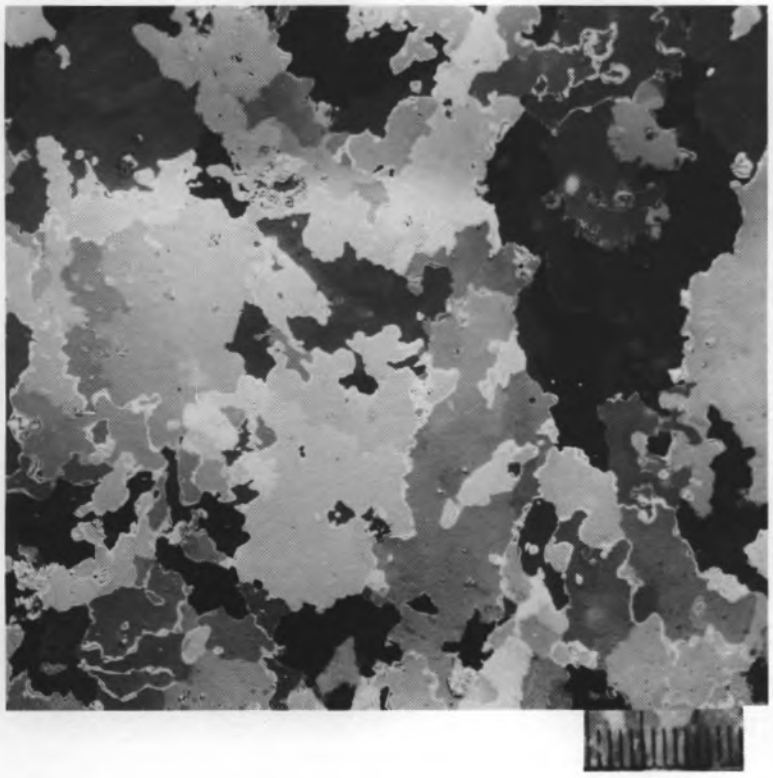

c. 20-cm depth.

Figure 22 (cont'd). Horizontal thin sections demonstrating retexturing in upper levels of a multi-year ice floe, 285 cm thick (site 6-16-1). Scale subdivision measures 1 mm.

was located deep enough in the floe to protect it from the dramatic effects of surface warming during the intervening summer (1983). However, this situation is not true of ice at 93 cm (Fig. 22b) where only vestiges of the original ice platelet/brine layer substructure of crystals are preserved, and the salinity has been reduced to 1.7‰, indicative of substantial desalination. The situation is even more extreme in the case of ice from 20 cm (Fig. 22c), which bears little resemblance whatsoever to congelation sea ice. Crystal boundaries have developed sutured outlines, and all trace of substructure has disappeared. Total loss of brine pocket structure in this is also reflected in the salinity, which measured less than 0.2‰.

This retexturing (additional examples are shown in App. B) is probably equivalent to the so-called recrystallization that Meeks et al. (1974), using microwave measurements, inferred to have occurred in the upper levels of multi-year ice in the Beaufort Sea (AIDJEX-72 Pilot Experiment). Weeks (1986) has also suggested the strong possibility of recrystallization in ice subjected to elevated summer temperatures, mainly on the basis of the recrystallization known to occur where impure hexagonal metals with substructure similar to sea ice are annealed. Knight (1962) observed polygonization in aged sea ice and related it to internal stress, a process different than the thermally induced retexturing that we observed here.

Retexturing of sea ice probably begins with the onset of the arctic melt season, its extent being determined by the duration and intensity of summertime temperatures and solar radiation and the number of years that the floe has been exposed to the retexturing process. The process occurs simultaneously with summer surface meltwater flushing, the principal mechanism by which brine is drained downward from the floe to create ice with multi-year salinity characteristics. By this stage the retextured, glacier-like brine-poor ice at the top of the floe bears little resemblance to the original sea ice, with resultant significant changes in the mechanical, optical and electromagnetic properties of the ice and its response to remote sensing signals.

Structurally, retextured ice can be readily distinguished from ice formed during the freezing of melt ponds on the tops of floes. Crystal structure and patterns of vertically elongated air bubbles produced during freezing of melt ponds are typically those observed in ice covers forming on freshwater lakes (Gow and Langston 1978).

While drilling the top meter or so of floes generally sufficed to distinguish between first-year and multi-year ice types, complete drilling of a multi-year floe was needed to obtain an estimate of its age. Cherepanov (1957) and Schwarzacher (1959) were able to delineate annual layering in sea ice on the basis of textural changes in the ice. However, our estimates of age were usually based on a combination of properties, including ice thickness, surges in the salinity profile and discontinuities in structure related to changes in either the sizes and shapes of crystals or the direction of alignment of crystallographic c-axes. Applying these criteria we did not encounter any ice floes demonstrably older than 4 to 5 years.

Numerical calculations carried out by Maykut and Untersteiner (1971), based on a theoretical thermodynamic model, indicate that the equilibrium thickness of sea ice growing under conditions typical of the central Arctic is between 3 and 4 m. When this thickness is reached, approximately 40 cm of ice grows and ablates on an annual basis. We observed annual growth increments of 60 to 80 cm at the bottom of multi-year floes—consistent with the undeformed thicknesses of between 2 and 3 m for the majority of the multi-year floes examined (Fig. 10). In addition we would expect older and thicker floes with correspondingly slower ice growth rates (40 cm per year) to have had extra-crystalline plate widths of 1 mm or more. In actual fact the plate spacings we measured in the older multi-year floes typically measured 0.6 to 0.7 mm, dimensions consistent with ice growth rates of 60 to 80 cm per year, which in floes 2–4 cm thick would represent 3–5 years of growth.

Although Cherepanov (1957) reported longer lived ice floes at the Soviet ice stations SP-4 (where 10 separate annual increments of ice growth were identified) our experience indicates that, within the restrictions of our sampling array, such floes are relatively rare. Nor did we observe undeformed floes 10 to 12 m thick, of the type on which a different Soviet ice station, NP-6, was located (Cherepanov 1964).

The ability to differentiate between ice types is obviously important when selecting representative floes from a ship or helicopter. This proved difficult in Fram Strait because of the blanketing effect of the snow cover. However, as mentioned earlier, once on the surface we could generally identify ice type on the basis of snow layer thickness. Occasionally, snow-covered, worn-down remnants of ridges were mistaken for undeformed multi-year

floes. The true nature of such ice was generally resolved on the basis of tilted block structures observed in vertically sliced sections of core. Using a combination of analytical techniques, as outlined above, we are confident that all the MIZEX-84 floes we examined were accurately classified according to ice type and approximate age.

Nothing in terms of the surface characteristics or the internal structure of the floes proved sufficiently diagnostic to allow us to assign an area of origin to any of the floes we sampled. This is in accord with the view of Weeks (1986) who, on the basis of satellite observations, concluded that appreciable lateral mixing of ice types could be expected because of the turbulent nature of flow occurring within the pack in the Greenland Sea.

CONCLUSIONS

Our observations regarding the state of the sea ice in Fram Strait during June and July 1984 lead us to the following conclusions:

1. The volume of multi-year ice discharging through Fram Strait greatly exceeded that of first-year ice. Statistical studies of 40 floes we examined in detail, together with observations of overall ice conditions in the marginal ice zone (aerial ice reconnaissance and SMMR satellite data), show that at least 84% of the ice exiting Fram Strait was multi-year.

2. Snow as deep as 65 cm was measured on multi-year floes while relatively little snow (averaging less than 10 cm) was observed on the top of first-year floes. This difference in the amount of accumulated snow proved such a reliable criterion for ice type that provisional identification could generally be made on this basis. Preliminary calculations based on snow ablation modeling suggest that thinner first-year ice can lose most of its snow by sublimation and that this is a general situation applying to most of the first-year ice entering Fram Strait from the Arctic Basin.

3. One-third of our multi-year ice cores contained previously deformed ice, indicating that multi-year floes in general may be composed of substantial amounts of deformed ice. Most of the undeformed multi-year ice floes that we examined had thicknesses ranging between 2 and 3 m, less than the expected equilibrium thickness of 3 to 4 m.

4. Drilling the first meter of core usually sufficed to distinguish between first-year and multi-year ice floes. Because of the nature of its transformation—by thermal modification of first-year ice during the summer—the top half meter or so of multi-year ice is very much harder and appreciably more transparent than that portion of first-year ice. The opaque appearance and relative softness of first-year ice are both closely linked to an abundance of brine pockets that drain and largely disappear to yield ice with the hardness and transparency characteristics observed in the upper levels of multi-year ice.

5. The retexturing of ice crystals, related to the elimination of brine pockets and the rounding of crystal boundaries at elevated air temperatures during the summer, is also a characteristic feature of ice in the uppermost levels of multi-year floes. Though such a process has been suggested by others, observations reported here verify for the first time the extent and nature of such a process in multi-year ice. This retexturing in the upper layers of floes and the attendant decrease in salinity, often to values $< 1‰$, also serve to distinguish multi-year ice from first-year ice.

6. Salinity profiles measured during MIZEX-84 agree well with those observed at comparable times of the year in other parts of the Arctic. The mean salinity of first-year ice averaged $4‰$, decreasing to $2.1‰$ in multi-year floes.

7. Ice structure consisted primarily of columnar crystals, formed by direct freezing (congelation) of seawater to the underside of the ice sheet. Granular ice, mainly frazil but also including snow ice, represented less than 25% of the total ice in the 40 floes we examined. In undeformed floes frazil averaged less than 15% of the total ice thickness. Frazil was found in small amounts in the surface layers of most floes (often in conjunction with snow ice) and in larger amounts in old ridges where it was mainly the material filling voids between ice blocks.

8. Most floes exhibited evidence of c-axis alignments related to growth of ice under the direct influence of oceanic currents. Changes in the direction of alignment at two or more levels in the ice were observed in a number of floes. Such changes are attributed to episodes of movement and immobilization of a floe and thus constitute a record of a floe's orientation relative to the direction of current motion beneath the ice. Assuming that the c-axes align on an annually repeating basis, consistent with wintertime growth, we have used such changes in alignment direction, together with crystal texture changes and surges in the salinity profile (which often coincide with change of crystal alignment), to estimate the ages of multi-year

floes. Floes demonstrably older than 4 to 5 years were not observed. Conversely, the absence of aligned c-axis structure can be correlated most probably with growth during unencumbered drift or rotation of the ice floe. This was a common condition of recently formed or actively growing ice on the bottom of floes in the process of exiting Fram Strait.

LITERATURE CITED

Aagard, K. and P. Greisman (1975) Toward new mass and heat budgets for the Arctic Ocean. *Journal of Geophysical Research,* **80**(27): 3821–3827.

Ackley, S.F., A.J. Gow, K.R. Buck and K.M. Golden (1081) Sea ice studies in the Weddell Sea aboard USCGS *Polar Sea. Antarctic Journal of the United States,* **15**(5): 84–86.

Bennington, K.O. (1963) Some crystal growth features of sea ice. *Journal of Glaciology,* **80**(27): 669–688.

Burns, B.A. and R.W. Larson (1985) Trip report: ERIM activities on *Polarstern* to support MIZEX-84 remote sensing. Environmental Research Institute, Michigan, Informal Information Report.

Cherepanov, N.V. (1957) Using the method of crystal optics for determining the age of drift ice (in Russian). *Problemy Arktiki,* **2**: 179–184.

Cherepanov, N.V. (1964) Structure of sea ice of great thickness (in Russian). *Trudy Arktiki i Antarktiki, Nauchno-Issled. Institute,* **267**: 13–18.

Colony, R. and A.S. Thorndike (1984) An estimate of the mean field of arctic sea ice motion. *Journal of Geophysical Research,* **89**(C6): 10623–10629.

Colony, R. and A.S. Thorndike (1985) Sea ice motion as a drunkard's walk. *Journal of Geophysical Research,* **90**(C1): 965–974.

Cox, F.G.N. and W.F. Weeks (1974) Salinity variations in sea ice. *Journal of Glaciology,* **13**(67): 109–120.

Cox, G.F.N., J.A. Richter, W.F. Weeks, M. Mellor, H. Bosworth, G. Durell and N. Perron (1985) Mechanical properties of multi-year sea ice. Phase II: Test results. USA Cold Regions Research and Engineering Laboratory, CRREL Report 85-16.

Gow, A.J. (1986) Orientation textures in ice sheets of quietly frozen lakes. *Journal of Crystal Growth,* **74**(2): 247–258.

Gow, A.J. and D. Langston (1977) Growth history of lake ice in relation to its stratigraphic, crystalline and mechanical structure. USA Cold Regions Research and Engineering Laboratory, CRREL Report 77-1.

Gow, A.J., S.F. Ackley, W.F. Weeks and J.W. Govoni (1982) Physical and structural characteristics of Antarctic sea ice. *Annals of Glaciology,* **3**: 113–117.

Gow, A.J., S.F. Ackley, K. Buck and K. Golden (1987) Physical and structural characteristics of Weddell Sea pack ice. USA Cold Regions Research and Engineering Laboratory, CRREL Report.

Hibler, W.D. III (1979) A dynamic-thermodynamic sea ice model. *Journal of Physical Oceanography,* **9**(4): 815–846.

Johannessen, O.M., W.D. Hibler III, P. Wadhams, W.J. Campbell, K. Hasselmann, I. Dyer and M. Dunbar (1982) MIZEX, A program for mesoscale air-ice-ocean interaction experiments in the arctic marginal ice zone. II. A science plan for a summer marginal ice zone experiment in the Fram Strait/Greenland Sea, 1984. USA Cold Regions Research and Engineering Laboratory, Special Report 82-12.

Knight, C.A. (1962) Polygonization of aged sea ice. *Journal of Geology,* **70**: 240–246.

Langhorne, P.J. (1983) Laboratory experiments on crystal orientation in NaCl ice. *Annals of Glaciology,* **4**: 163–169.

Langhorne, P.J. and W.H. Robinson (1986) Alignment of crystals in sea ice due to fluid motion. *Cold Regions Science and Technology,* **12**(2): 197–214.

Martin, S. (1979) A field study of brine drainage and oil entrapment in sea ice. *Journal of Glaciology,* **22**(88): 473–502.

Maykut, G.A. (1978) Energy exchange over young sea ice in the central Arctic. *Journal of Geophysical Research,* **83**(C7): 3646–3658.

Maykut, G.S. (1984) Heat and mass balance measurements during the MIZEX-83 drift program. In *MIZEX Bulletin IV: Initial Results and Analysis from MIZEX-83.* USA Cold Regions Research and Engineering Laboratory, Special Report 84-28.

Maykut, G.A. (1985) An introduction to ice in the polar oceans. University of Washington, APL-UW 8510.

Maykut, G.A. and N. Untersteiner (1971) Some results from a time-dependent, thermodynamic model of sea ice. *Journal of Geophysical Research,* **76**(6): 1550–1575.

Meeks, D.C., G.A. Poe and R.O. Ramseier (1974) A study of microwave emission properties of sea ice—AIDJEX-1972. Aerojet Electrosystems Company, Azusa, California, Final Report 1786FR-1.

Nakawo, M. and N.K. Sinha (1981) Growth rate and salinity profile of first-year sea ice in the high Arctic. *Journal of Glaciology,* **27**(96): 315–330.

Overgaard, S., P. Wadhams and M. Lepparänta (1983) Ice properties in the Greenland and Barents Sea during summer. *Journal of Glaciology,* **29** (101): 142–164.

Richter-Menge, J.A. and G.F.N. Cox (1985) The effect of sample orientation on the compressive strength of multi-year pressure ridge ice samples. In *Civil Engineering Arctic Offshore, Proceedings of Conference Arctic '85, San Francisco,* pp. 465–475.

Schwarzacher, W. (1959) Pack-ice studies in the Arctic Ocean. *Journal of Geophysical Research,* **64**: 2357–2367.

Timofeyev, V.T. (1958) On the limits of Atlantic water in the Arctic Basin (in Russian). *Problemy Arktiki,* **5**: 27–31.

Tucker, W.B. III, A.J. Gow and W.F. Weeks (1985) Physical properties of sea ice in the Greenland Sea. In *Proceedings, 8th International Conference on Port and Ocean Engineering Under Arctic Conditions (POAC-85), Narssarssuaq, Greenland,* pp. 177–188.

Vinje, T.E. (1977) Sea ice conditions in the European sector of the marginal seas of the Arctic, 1966–75. *Norsk Pol. Inst. Arbok 1975,* pp. 163–174.

Wadhams, P. (1981) The ice cover in the Greenland and Norwegian Seas. *Reviews of Geophysics and Space Physics,* **19**(3): 345–393.

Weeks, W.F. (1986) The physical properties of the sea ice cover. In *The Nordic Seas* (B.G. Hurdle, Ed.), pp. 87–100.

Weeks, W.F. and S.F. Ackley (1982) The growth, structure and properties of sea ice. USA Cold Regions Research and Engineering Laboratory, Monograph 82-1.

Weeks, W.F. and A.J. Gow (1978) Preferred crystal orientation along the margins of the Arctic Ocean. *Journal of Geophysical Research,* **83**(C10): 5105–5121.

Weeks, W.F. and A.J. Gow (1980) Crystal alignments in the fast ice of arctic Alaska. *Journal of Geophysical Research,* **85**(C2): 1137–1146.

Wittmann, W.I. and J.J. Schule (1966) Comments on the mass budget of arctic pack ice. In *Proceedings, Arctic Heat Budget and Atmospheric Circulation* (J.O. Fletcher, Ed.). The Rand Corporation, Santa Monica, California, Report RM-5223-NSF.

WMO (1956) *Abridged Ice Nomenclature.* World Meteorological Organization, Executive Committee Report, vol. 8, pp. 107–116.

APPENDIX A: SALINITY-TEMPERATURE-STRUCTURE PROFILES OF FRAM STRAIT ICE FLOES

This appendix contains schematic depictions of the crystalline texture of all cores drilled during MIZEX-84 together with their temperature and salinity profiles. Diagnostic criteria for distinguishing multi-year ice from first-year ice include low salinities in the top half meter or so of the core and the concomitant formation of semitransparent ice that is much more resisant to coring and cutting than the normally opaque, softer ice of first-year floes. These changes in the optical and mechanical properties of the ice are also accompanied by significant changes in the texture and intracrystalline makeup of the ice. Details of the nature and causes of this crystal retexturing and associated modification of brine pocket structure are discussed in the main text of this report. For purposes of structural diagramming we have broken down crystalline structure into three basic ice types: granular, columnar and fresh water as already demonstrated in several examples presented in the body of this report (Fig. 4, 5, 17, 19 and 21).

In diagramming the structural profiles we have also indicated relative size changes in the granular and columnar ice layers. The c-axis alignments are also shown, where appropriate, by double-headed arrows on the horizontal thin-section photographs.

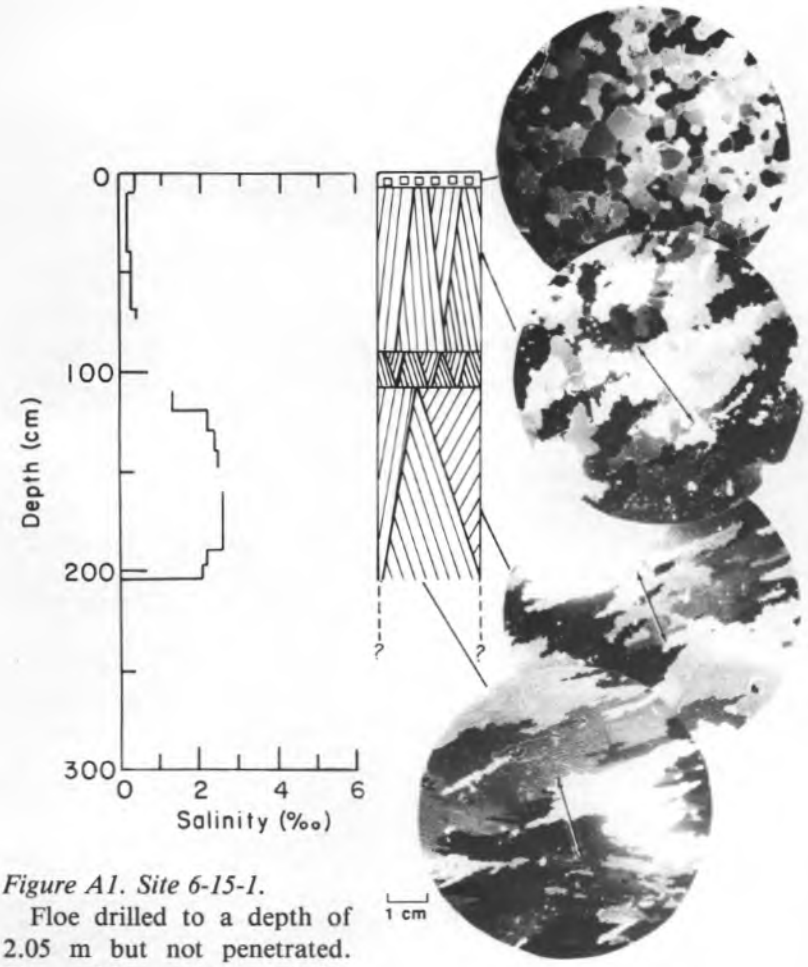

Figure A1. Site 6-15-1.

Floe drilled to a depth of 2.05 m but not penetrated. The multi-year nature of this floe was indicated by very low salinities in the top meter of core and a bulk salinity of only 1.3‰. Structurally, the core was composed of 7 to 8 cm of coarse-grained snow ice overlying transparent, retextured sea ice to 80-cm depth. Below 80 cm the core consisted entirely of opaque congelation sea ice. The thermally modified condition of the sea ice in the top 80 cm of core is clearly revealed in the horizontal thin section photographed at 45 cm showing sutured crystal boundaries and virtual disappearance of original brine pockets from within the crystals themselves. Such retexturing (discussed in detail in the text of this report and in Gow et al., in press) confirms multi-year identification of the floe based on its salinity characteristics. Aligned c-axes in thin sections from 1.57 and 2.05 m are indicative of current-controlled growth of this ice. The fresh-looking, interfingered nature of crystals at 2.05 m together with the strongly developed state of the ice plate/brine pocket substructure, indicates that this ice was formed during the 1983–84 winter. This in turn would indicate that coring was terminated close to the bottom of this floe and that the ice is no older than two years. Congelation ice constituted 96% of the drilled core length.

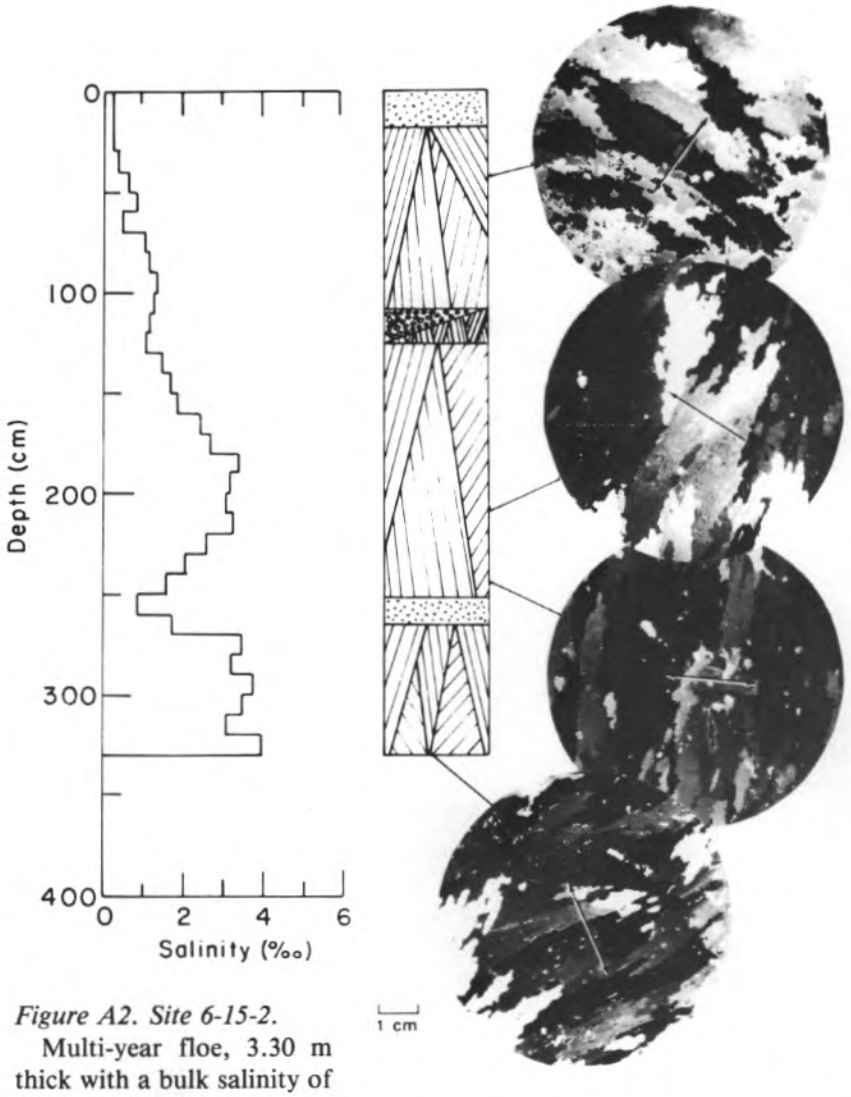

Figure A2. Site 6-15-2.

Multi-year floe, 3.30 m thick with a bulk salinity of 1.8‰ and believed to represent three winters' growth based on surges in the salinity profile. The top meter of core was characterized by the semi-transparent, retextured state of the ice, abundant bubbles and aligned c-axes, underlain by opaque sea ice of the second and third winters' growth that also exhibited aligned c-axes; however, the directions of alignment are different and the changes appear to coincide with the salinity surges. The transition from the second to the third year's growth was characterized by a granular ice layer containing significant amounts of unidentified particulate matter. Ice in this floe consisted of 88% congelation crystals and was undeformed.

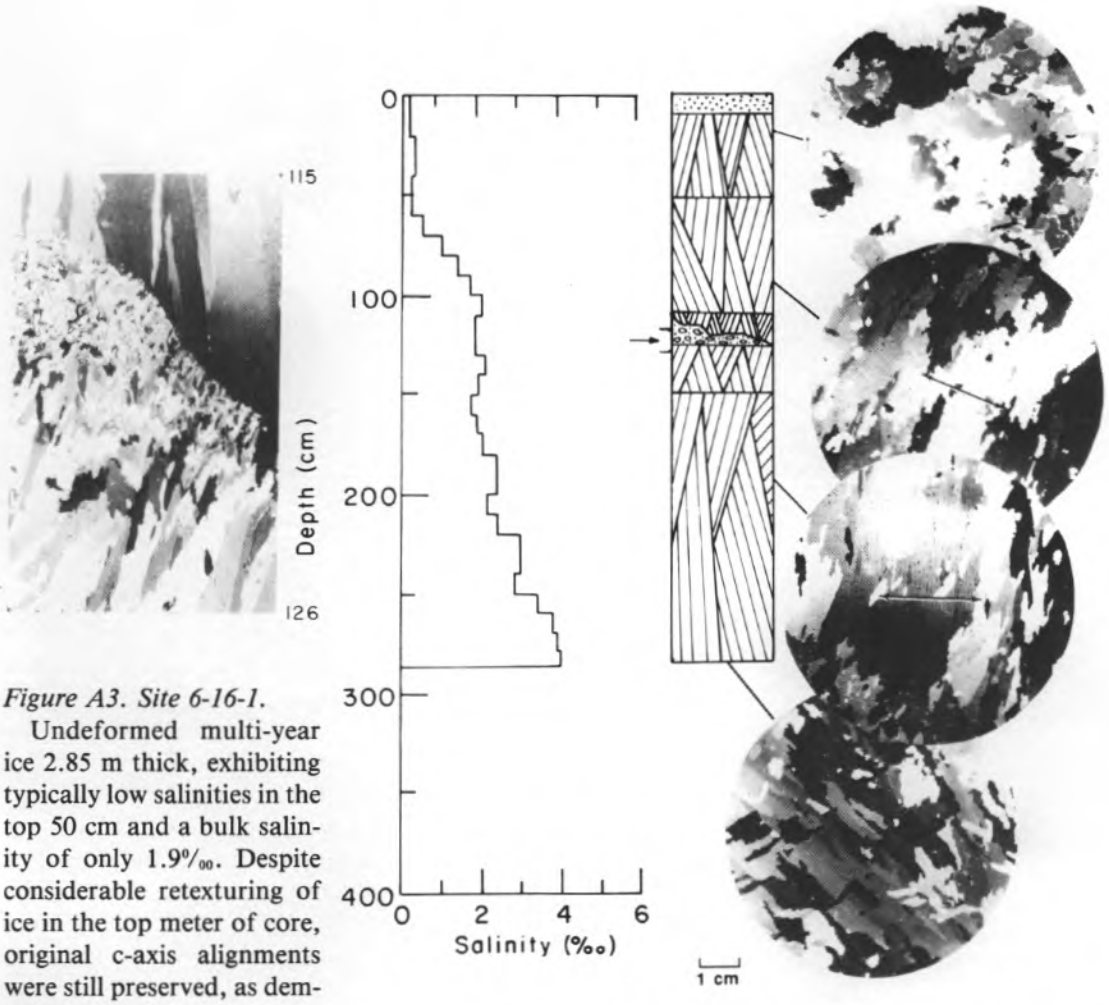

Figure A3. Site 6-16-1.

Undeformed multi-year ice 2.85 m thick, exhibiting typically low salinities in the top 50 cm and a bulk salinity of only 1.9‰. Despite considerable retexturing of ice in the top meter of core, original c-axis alignments were still preserved, as demonstrated in the section from 83 cm. A thin layer of granular ice (frazil) at around 1.20 m is believed related to the onset of growth of second-year ice, and an approximate 80° change in direction of crystal c-axis alignment at 2.84 m compared to that in the section at 1.92 m is interpreted as indicating a third year's growth of ice between 1.92 and 2.85 m. The floe at this location consisted of 97% congelation ice.

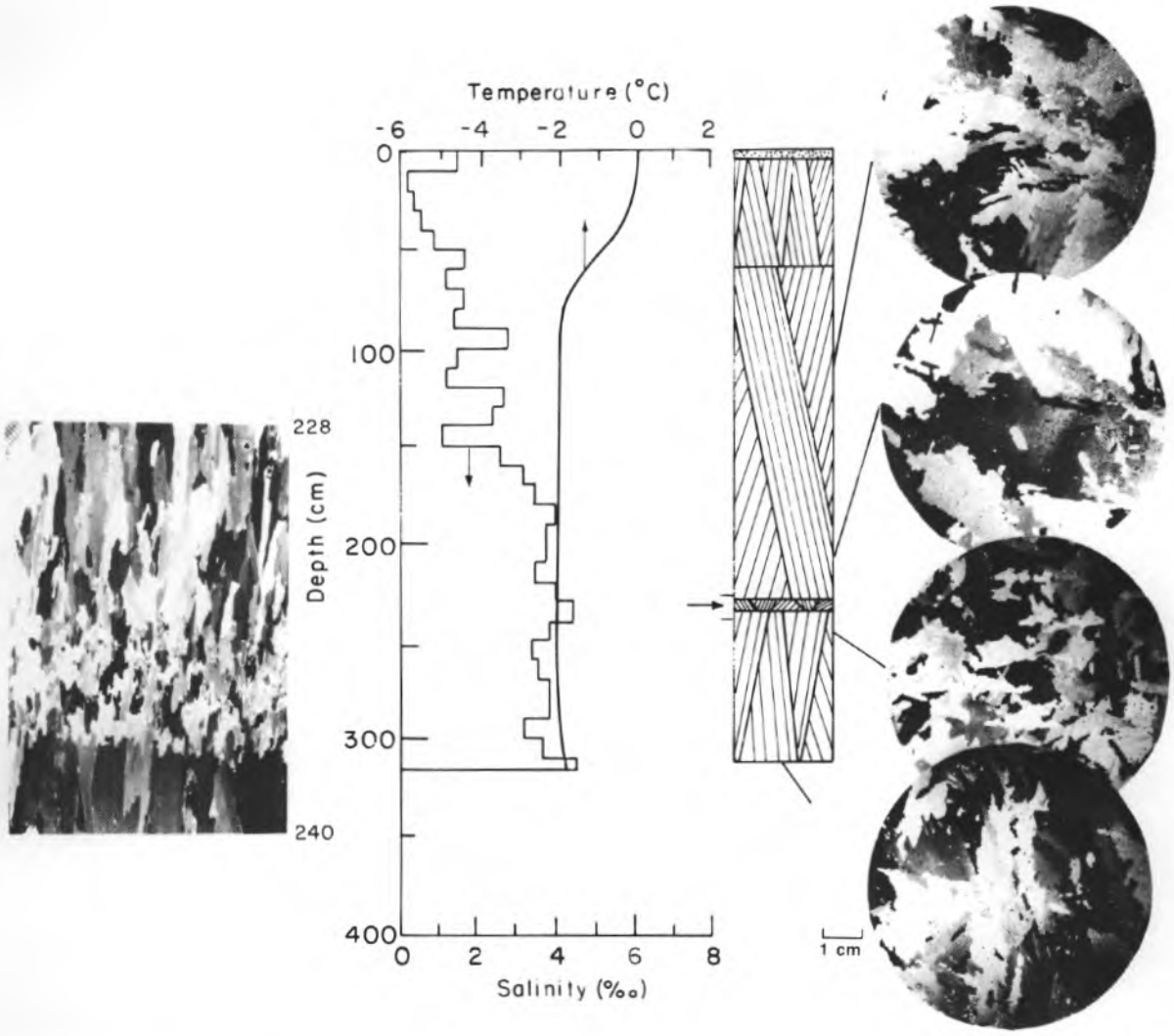

Figure A4. Site 6-17-1.

Undeformed ice in a large multi-year floe composed of 94% congelation ice. The ice at this particular location was 3.14 m thick with a mean salinity of 2.5‰. The top 60 cm of core consisted of low salinity semi-transparent, bubbly, retextured ice that exhibited extensive brine channeling. Structure is interpreted to indicate three years of ice growth, with the 1983–84 winter increment occurring directly beneath a fine-grained layer of congelation ice that separates it from the previous winter's growth (this discontinuity is demonstrated in the vertical section from 2.28 to 2.40 m). The core from this floe was notable for the lack of any significant alignment of c-axes of the crystals in the congelation ice.

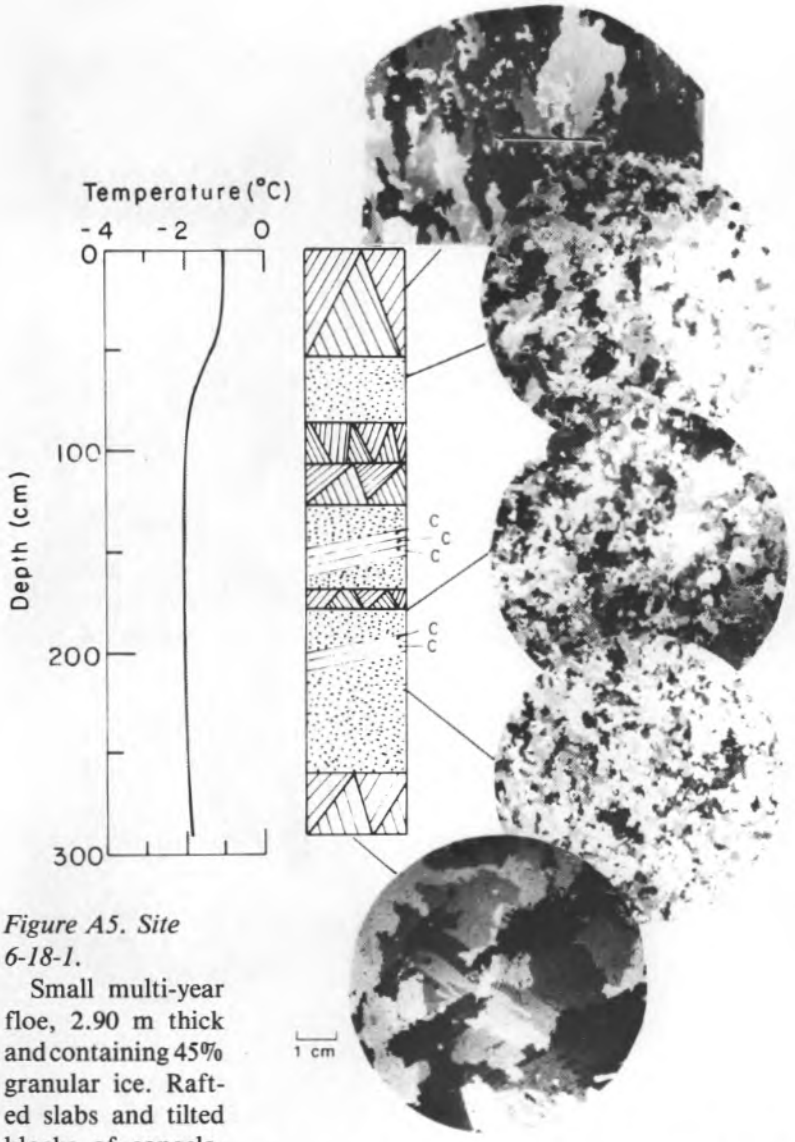

Figure A5. Site 6-18-1.

Small multi-year floe, 2.90 m thick and containing 45% granular ice. Rafted slabs and tilted blocks of congelation ice intermixed with frazil clearly show that this core was drilled through a ridge. Thin, semi-transparent slabs of ice in the middle of the section (marked with the symbol c) gave the core a distinctly banded appearance. The top layer of congelation ice contained numerous cavities and brine drainage tubes. The bottom ice consisted of fresh-looking congelation ice crystals that lacked all trace of c-axis alignment, indicating that this ice had accreted to the bottom of the floe while it was making its way out of the Arctic Basin and into Fram Strait.

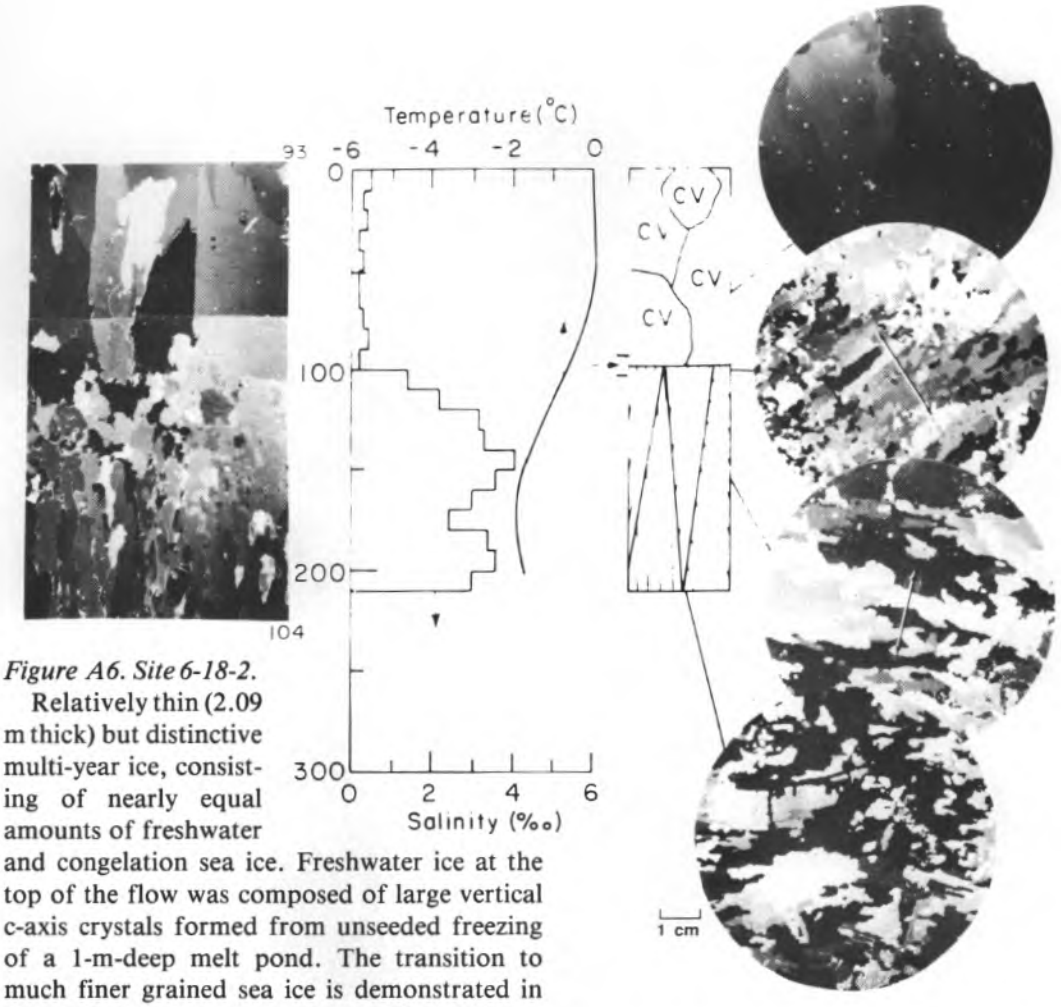

Figure A6. Site 6-18-2.

Relatively thin (2.09 m thick) but distinctive multi-year ice, consisting of nearly equal amounts of freshwater and congelation sea ice. Freshwater ice at the top of the flow was composed of large vertical c-axis crystals formed from unseeded freezing of a 1-m-deep melt pond. The transition to much finer grained sea ice is demonstrated in the vertical section photograph at 93 to 104 cm. This transition also coincided with a very sharp five-fold change in salinity and the occurrence of brine drainage channels in the top 10 to 15 cm of sea ice. The very large (80°) change in c-axis alignment between 1.0 and 1.5 m would imply that the melt pond at the end of the summer was underlain by only a thin layer of sea ice and that the bottom 0.5 to 1.0 m of ice represented growth during the ensuing winter (1983–84). This situation is also supported by salinities of less than 2‰ in the top 10 to 20 cm of sea ice directly beneath the melt pond, followed by salinities of 3–4‰ in the underlying sea ice.

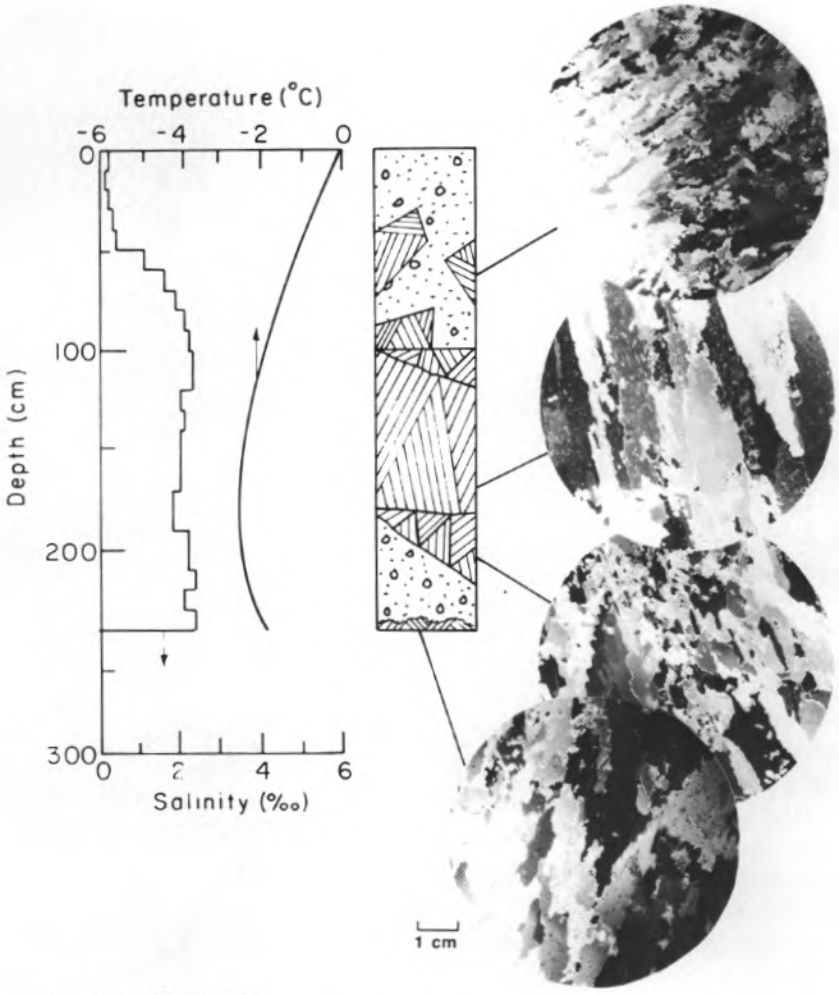

Figure A7. Site 6-19-1.

Salinities averaging less than 0.5‰ in the top 50 cm, confirming multi-year nature of this core. Structure studies clearly show that it was drilled in ridged ice, though the flat surface relief at the drill site gave no indication that such was the case. This is part of a large floe which at this particular location measured 2.41 m thick with a mean salinity of 1.7‰. The core contained tilted blocks of congelation ice mainly derived from sheet ice with strongly aligned c-axes. Frazil ice made up 34% of the total thickness of the core from this worn-down ridge remnant.

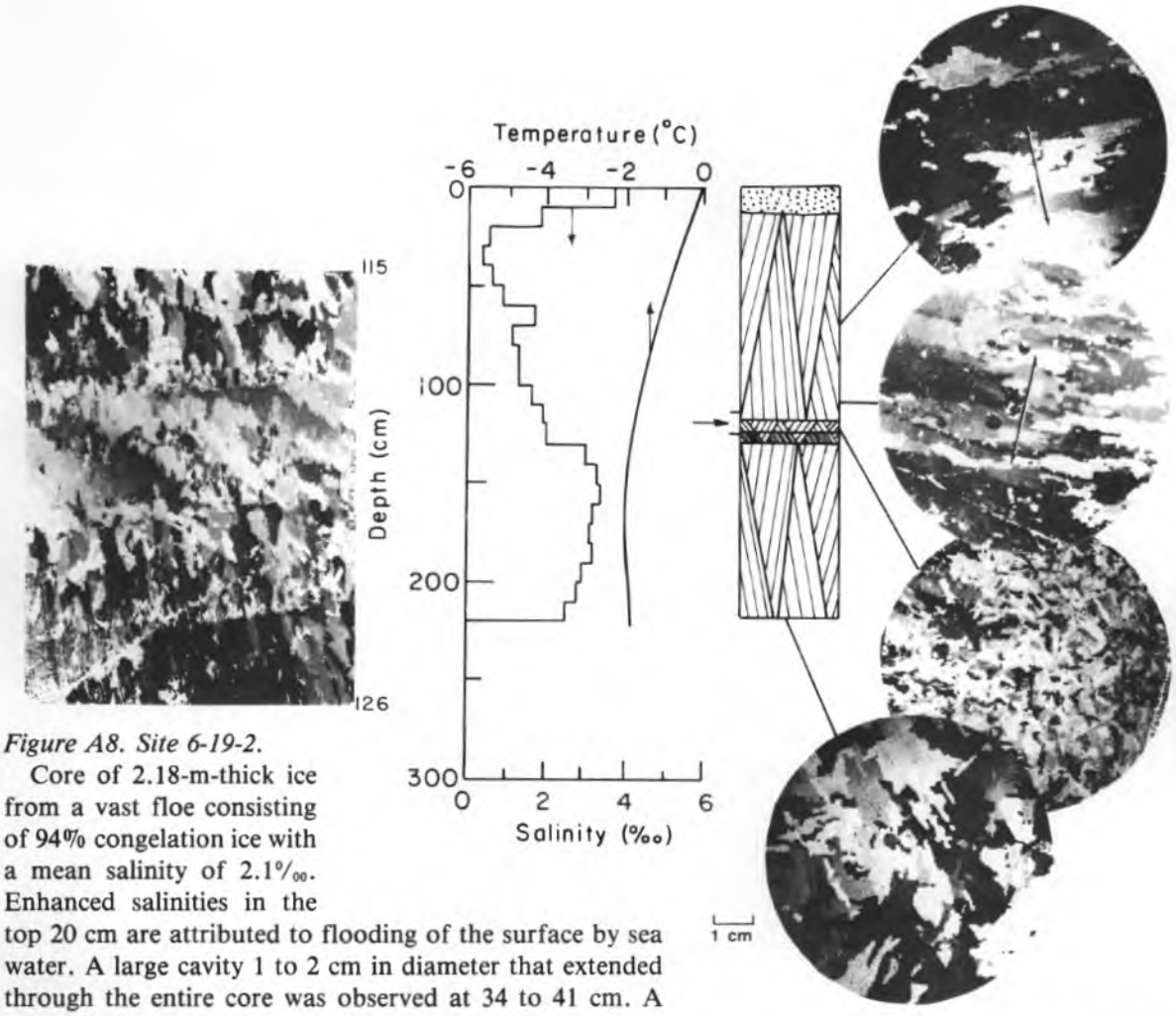

Figure A8. Site 6-19-2.

Core of 2.18-m-thick ice from a vast floe consisting of 94% congelation ice with a mean salinity of 2.1‰. Enhanced salinities in the top 20 cm are attributed to flooding of the surface by sea water. A large cavity 1 to 2 cm in diameter that extended through the entire core was observed at 34 to 41 cm. A strong structure transition involving an 8-cm-thick layer of fine-grained congelation ice separating two zones of coarse-grained congelation ice (the nature of this transition is demonstrated in the vertical section at 1.15 to 1.26 m) was interpreted as marking the change-over from first- to second-year ice. The onset of the second year's growth also coincided with a surge in salinity. Though most of the first year's growth had undergone considerable retexturing, original c-axis alignments were retained as indicated by nearly identical alignment directions in ice at 69 cm and at 1.10 m, near the bottom of the first-year growth. A section of ice from the bottom of the floe, at 2.18 m, showed no significant alignments of c-axes, indicating that the final stages of growth occurred as the floe was drifting freely on its way through Fram Strait.

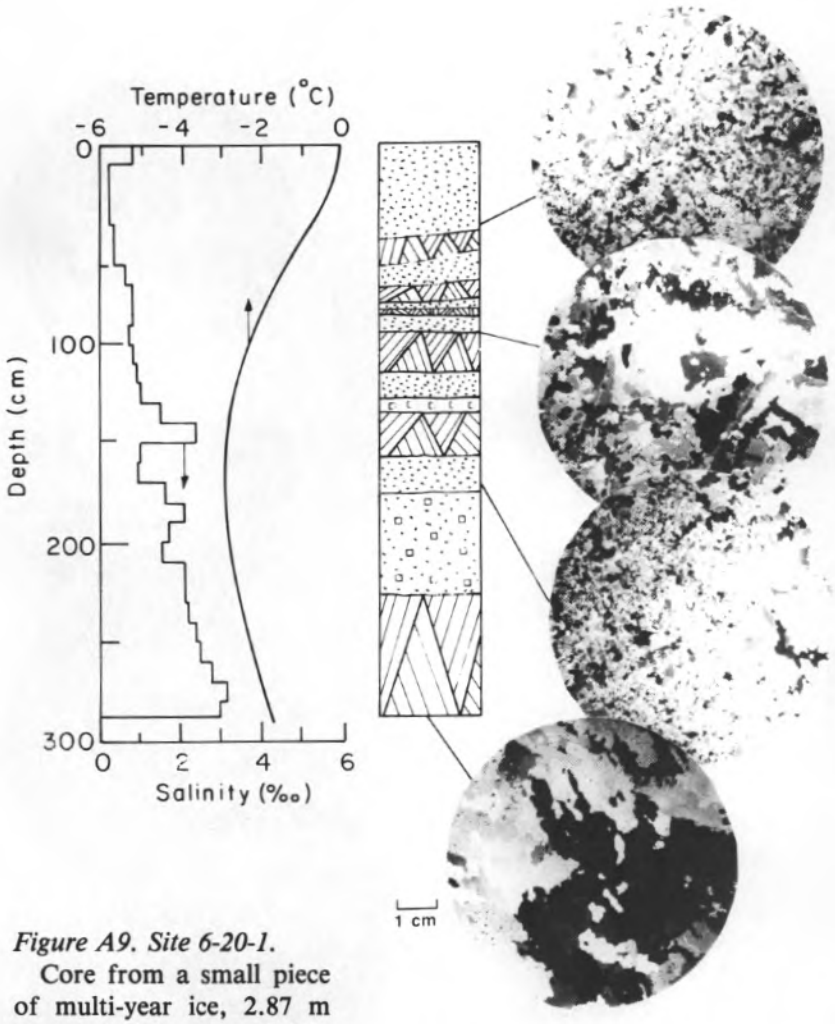

Figure A9. Site 6-20-1.

Core from a small piece of multi-year ice, 2.87 m thick and with a mean salinity of 1.4‰. Salinities did not exceed 1.0‰ in the top 1.2 m. The intermixing of tilted blocks and frazil ice clearly shows that most of the ice was incorporated during ridge building. Layers of algae were observed at several different levels in the floe. Structure and salinity characteristics of the bottom 60 cm are consistent with the growth of congelation ice during the 1983–84 winter.

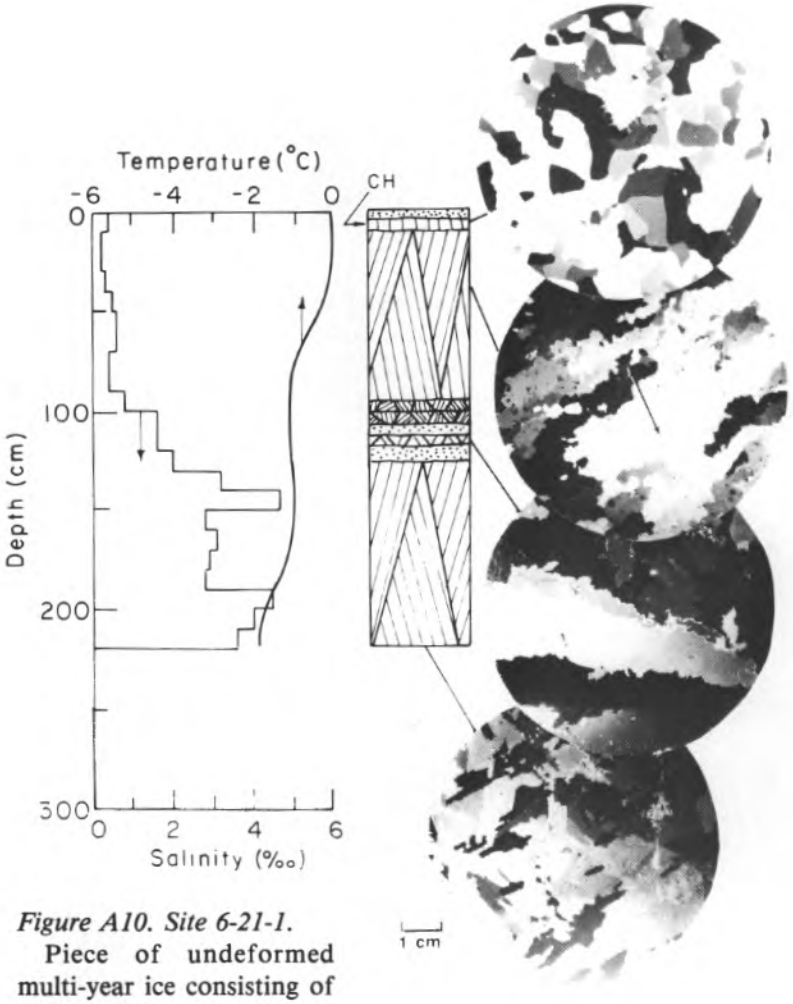

Figure A10. Site 6-21-1.

Piece of undeformed multi-year ice consisting of 90% congelation ice including, near the top of the floe, a 5-cm-thick layer of melt pond ice with columnar, horizontal c-axis crystals. Very low salinities in the top meter of the floe attest to considerable thermal modification that has led also to substantial retexturing and formation of semi-transparent ice. The section at 44 cm showed rounded and sutured grain boundaries and virtually complete loss of brine pocket structure within the crystals. However, original c-axis alignments were still preserved. Intermixing of layers of fine-grained congelation and frazil ice between 1.0 and 1.25 m was followed by growth of coarse-grained congelation ice and a simultaneous surge in salinity to values exceeding 4‰. This ice was interpreted as having originated during the 1983–84 winter, making the ice in the floe at least two years old.

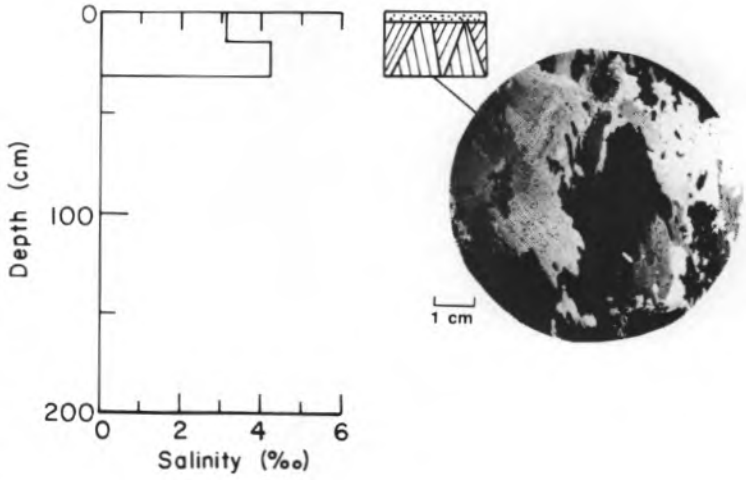

Figure A11. Site 6-22-1.

First of several cores drilled in a vast first-year floe. The core at this particular location was taken from thin (32-cm) ice from a frozen lead; it was composed mainly of congelation ice, the base of which had just begun to develop a preferred orientation (alignment) of its c-axes.

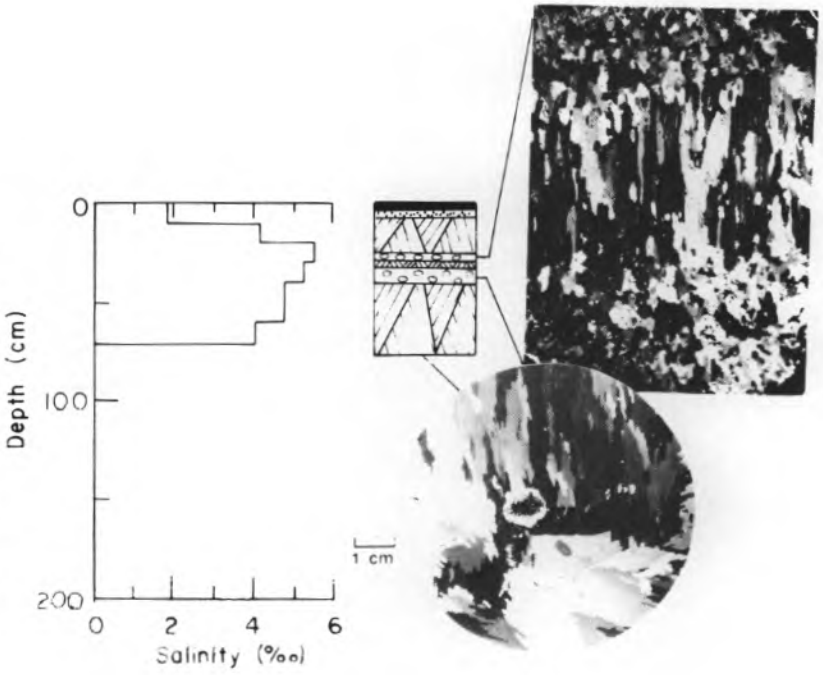

Figure A12. Site 6-22-2.

Thick (76-cm) lead ice with a mean salinity of 4.3‰ and composed of 76% congelation ice. A thin (3-cm) layer of freshwater ice at the top of the floe is attributed to a recent episode of freezing rain. This core was located less than 50 m from that at site 6-22-1 but, unlike the latter, it contained an unusual combination of fine-grained congelation and frazil ice layers in the middle section of the core, as demonstrated in the vertical section photograph at 27 to 39 cm. This core also contained numerous brine drainage vesicles and tubes.

Figure A13. Site 6-22-3.

First-year ice, 1.10 m thick with a bulk salinity of 5.0‰. The core consisted of 88% congelation ice in which c-axes were strongly aligned in the top half but much less so in the bottom half. Whereas the ice in the upper part of the core most likely grew under the influence of a strongly directed current, subsequent weakening of the c-axis alignment is probably linked to continued growth of congelation ice as the floe was moving out of the Arctic Basin into Fram Strait. Some of the fine-grained congelation ice in the middle of the core may reflect the changeover in ice growth regime. The smoothed nature of the bottom surface would imply that melting was now occurring at the ice/water interface. The occurrence of optical banding in the lower half of the core is attributed to fluctuations in ice growth velocity.

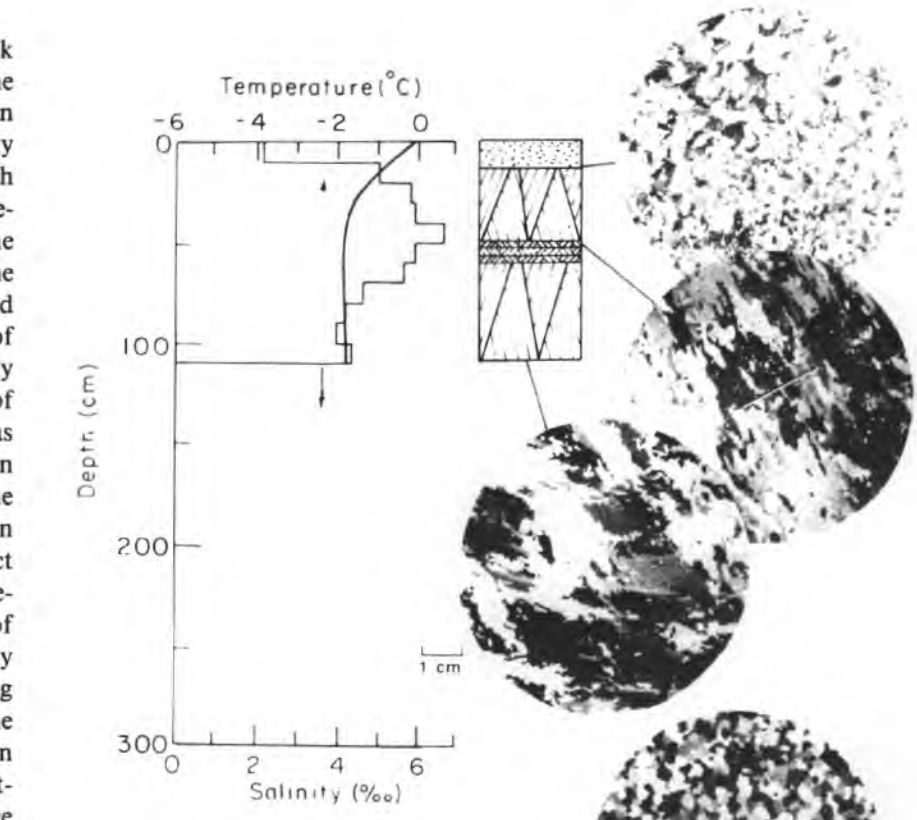

Figure A14. Site 6-22-4.

Core taken from a thicker (1.97 m) and saltier ($\bar{S}$ = 5.0‰) part of the floe, including a maximum salinity of 7.7‰, indicative of mature first-year sea ice. The core consisted predominantly of congelation ice (89% of total ice thickness) in which the c-axes of crystals were moderately to weakly aligned. A thin ice layer, similar to that at site 6-22-1 was found at the top of the core. The bottom half of the core exhibited abundant optical bonding similar to that at site 6-22-3.

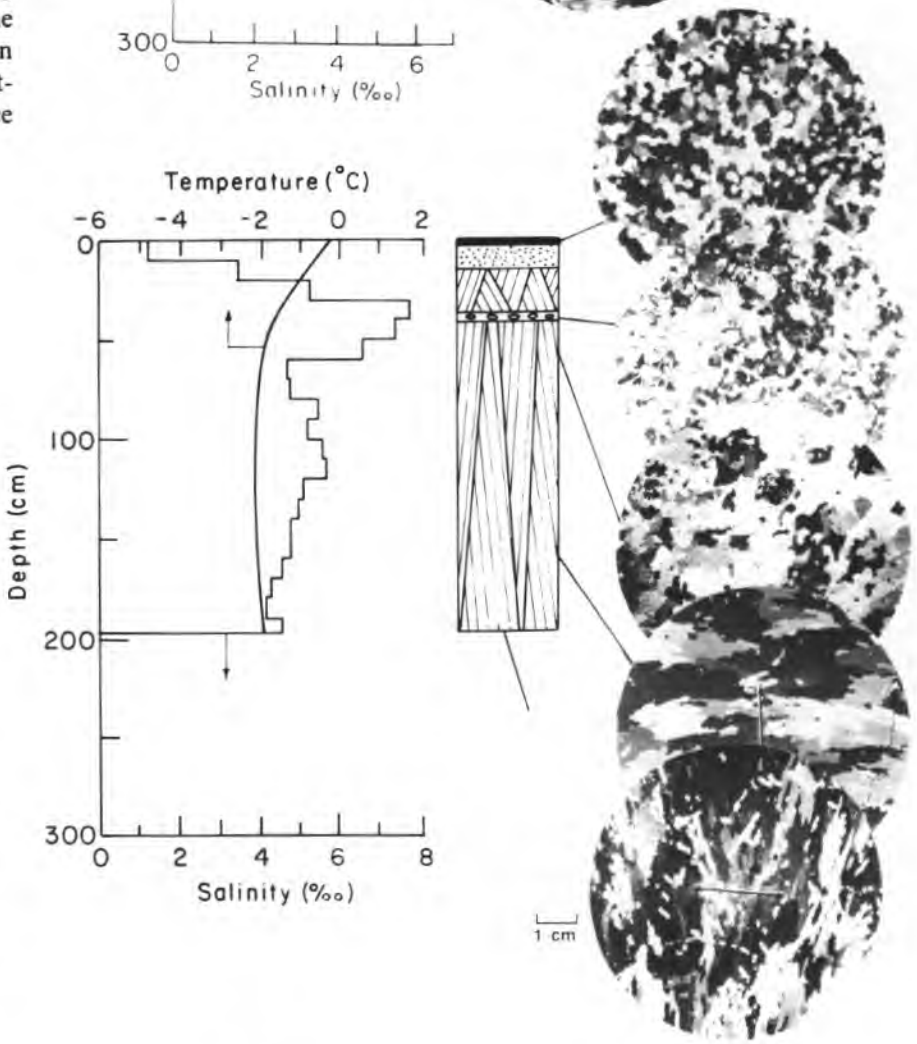

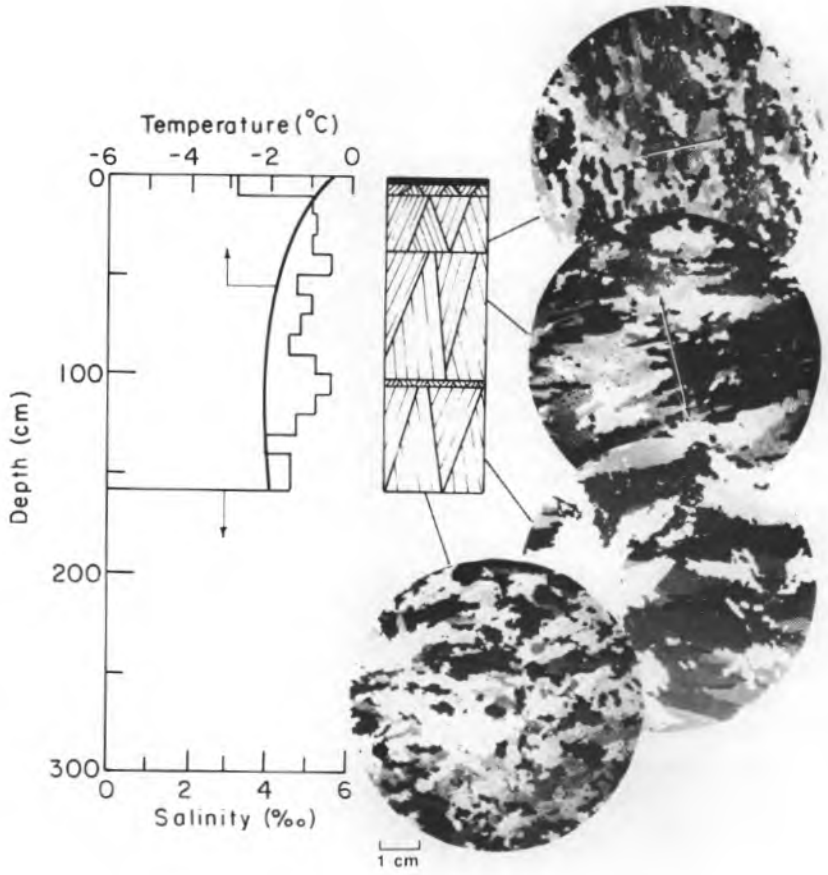

Figure A15. Site 6-22-5.

Ice appreciably thinner (1.58 m) than at site 6-22-4. The top of the core exhibited the same 3- to 4-cm-thick ice layer observed at two other locations on this floe. A mean salinity of 4.8‰ identifies the ice as first-year. The core beneath the surface freshwater ice layer was composed entirely of congelation ice in which crystals exhibited very strong to moderate c-axis alignments in the top half of the core but which in the lower half were weakly oriented to unaligned. These changes are consistent with a changeover from fast ice to freely drifting growth conditions similar to those recorded in the structure of the cores at sites 6-22-3 and 6-22-4.

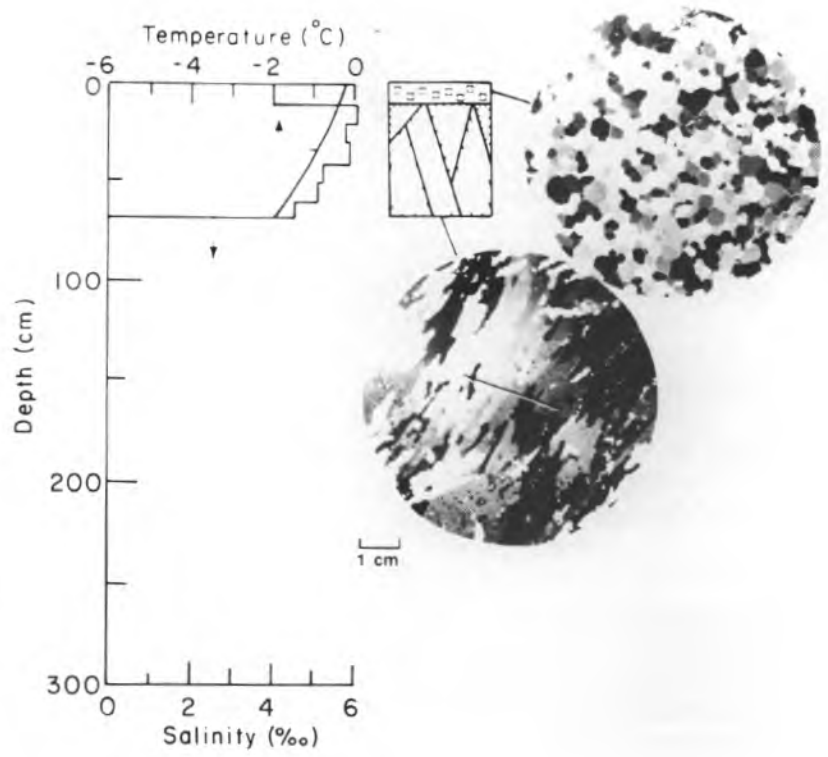

Figure A16. Site 6-24-1.

Small piece of thin (0.67-m) first-year ice with a mean salinity of 5.3‰. Floe was overlain by moderate- to coarse-grained snow ice representing 15% of the total ice thickness. The remaining core was composed of congelation ice crystals exhibiting strongly aligned c-axes.

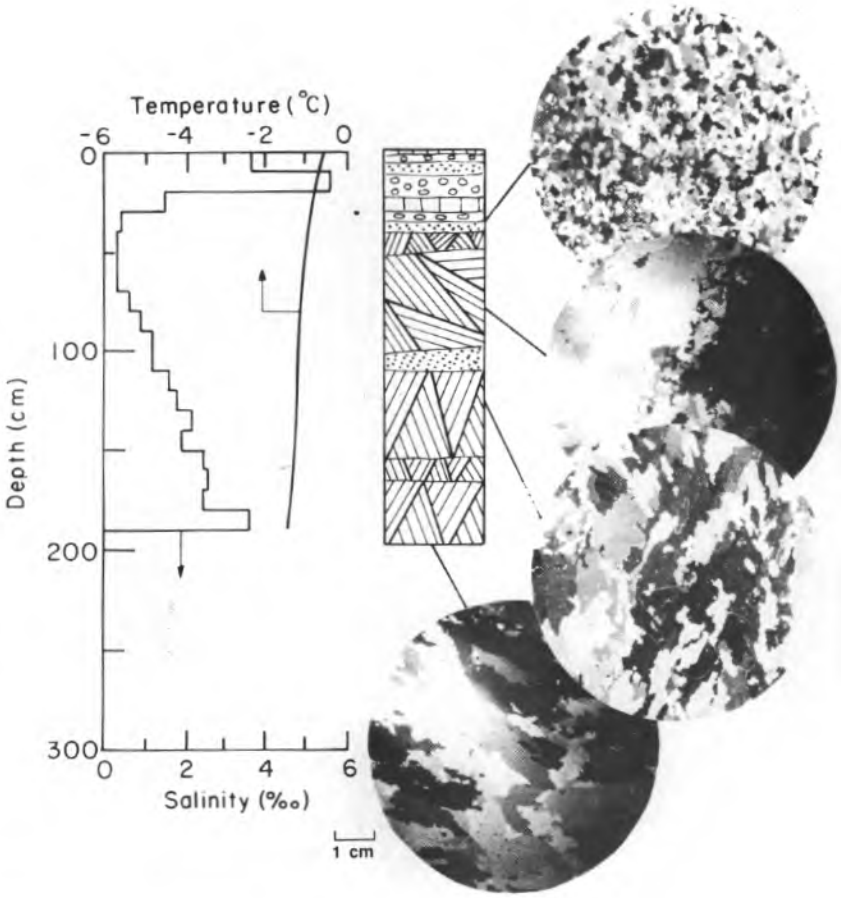

Figure A17. Site 6-24-2.

Worn-down remnant of deformed multi-year ice composed mainly of blocks of retextured congelation ice overlain, in order from the bottom, by snow ice, a thin layer of freshwater ice, and a thick (20- to 25-cm) layer of snow flooded by sea water and subsequently refrozen. This accounts for the relatively high salinities at the top of the floe, below which were observed salinities more typical of multi-year ice.

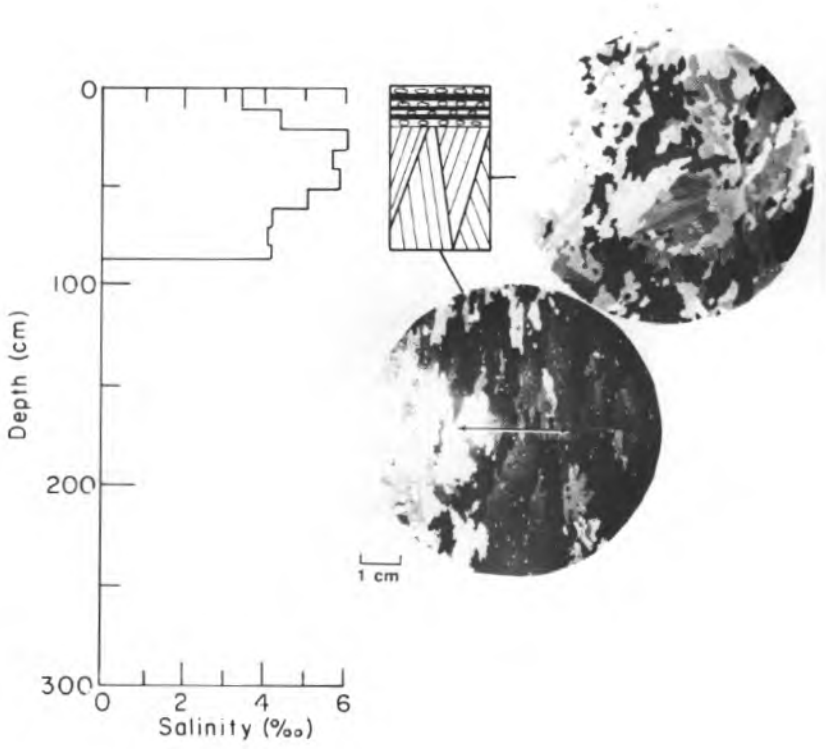

Figure A18. Site 6-24-3.

Small floe, 0.83 cm thick, with a mean salinity of 4.8‰. The top of the floe was unusual in that it contained several thin, semi-transparent ice layers interspersed with granular ice layers, most probably snow ice. The remaining ice, representing 76% of the total thickness, consisted of congelation ice in which the c-axes became increasingly more aligned with depth.

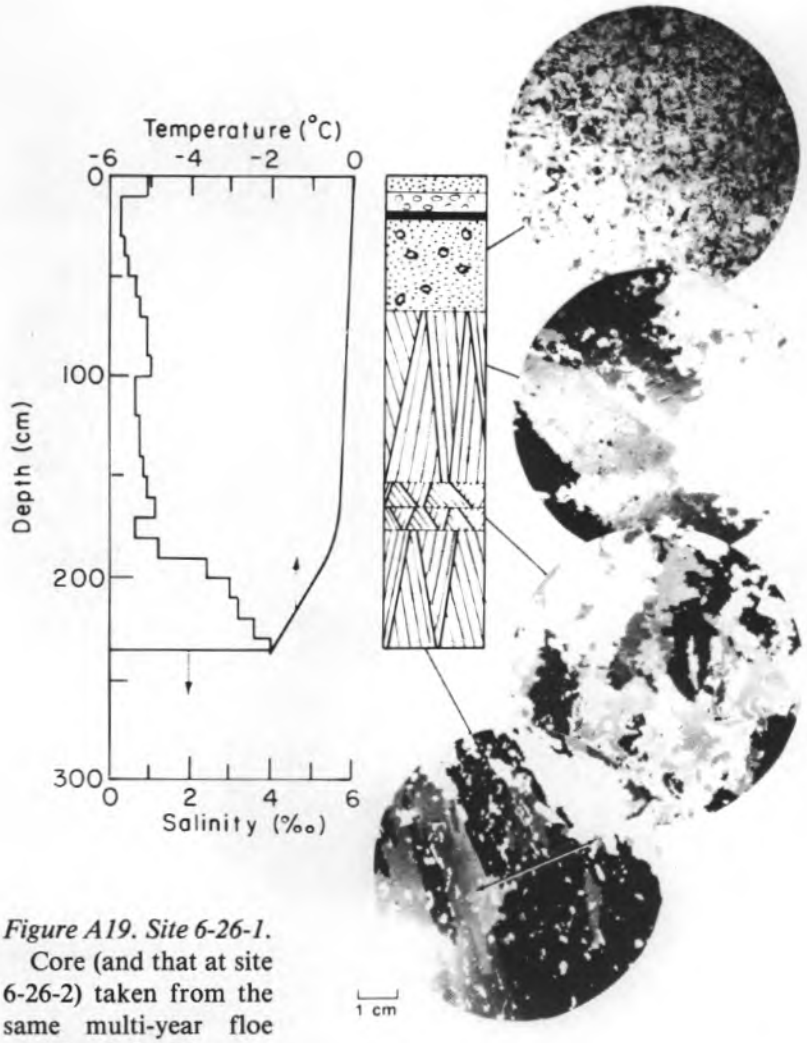

Figure A19. Site 6-26-1.

Core (and that at site 6-26-2) taken from the same multi-year floe used by *Polar Queen* as a freely drifting research platform during June and July 1984. Though this particular core was located close to a ridge, it showed no obvious signs of deformation related to ridge building, e.g. tilted blocks intermixed with frazil-filled voids. However, the top of the core contained granular ice (mainly frazil) that represented 29% of the total ice thickness. It very likely originated under conditions of sustained turbulence at the sea surface in a wide lead or polynya. The floe was clearly multi-year based on its salinity and structural characteristics. The transition from a zone of fine-grained congelation ice at 1.55 to 1.75 m to much coarser-grained ice below also coincided with a sharp increase in salinity, most likely related to the onset of the 1983–84 winter ice growth. However, a mean salinity of only 1.2‰ might indicate that this floe is older than two years.

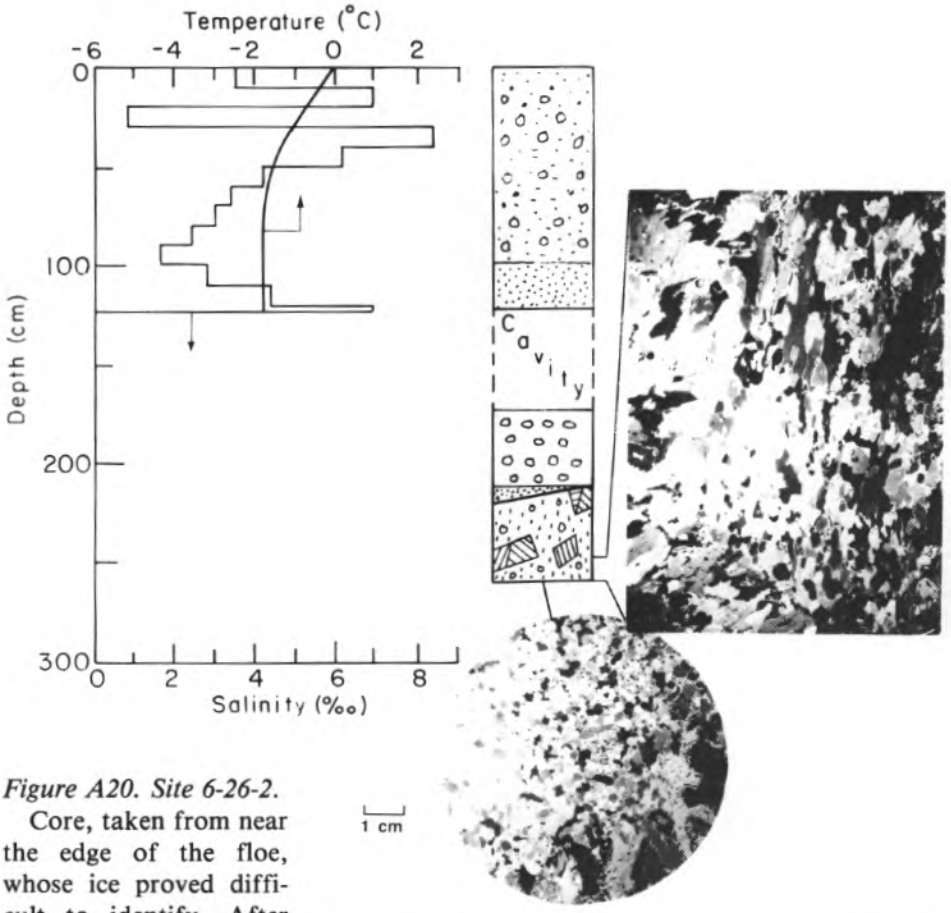

Figure A20. Site 6-26-2.

Core, taken from near the edge of the floe, whose ice proved difficult to identify. After drilling through 1.20 m of granular ice (derived mainly from the freezing of flooded snow) a large cavity was encountered that extended to a 1.70-m depth. This was followed by cavity-ridden ice composed of frazil underlain by pieces of congelation ice intermixed with frazil as demonstrated in the vertical section from 245–257 cm. Considering the somewhat erratic nature of the salinity profile, including salinities in excess of 7‰ above the cavity, together with the structural characteristics of the core, it would appear that this ice was ultimately linked to a recent episode of ridging at the edge of a multi-year floe.

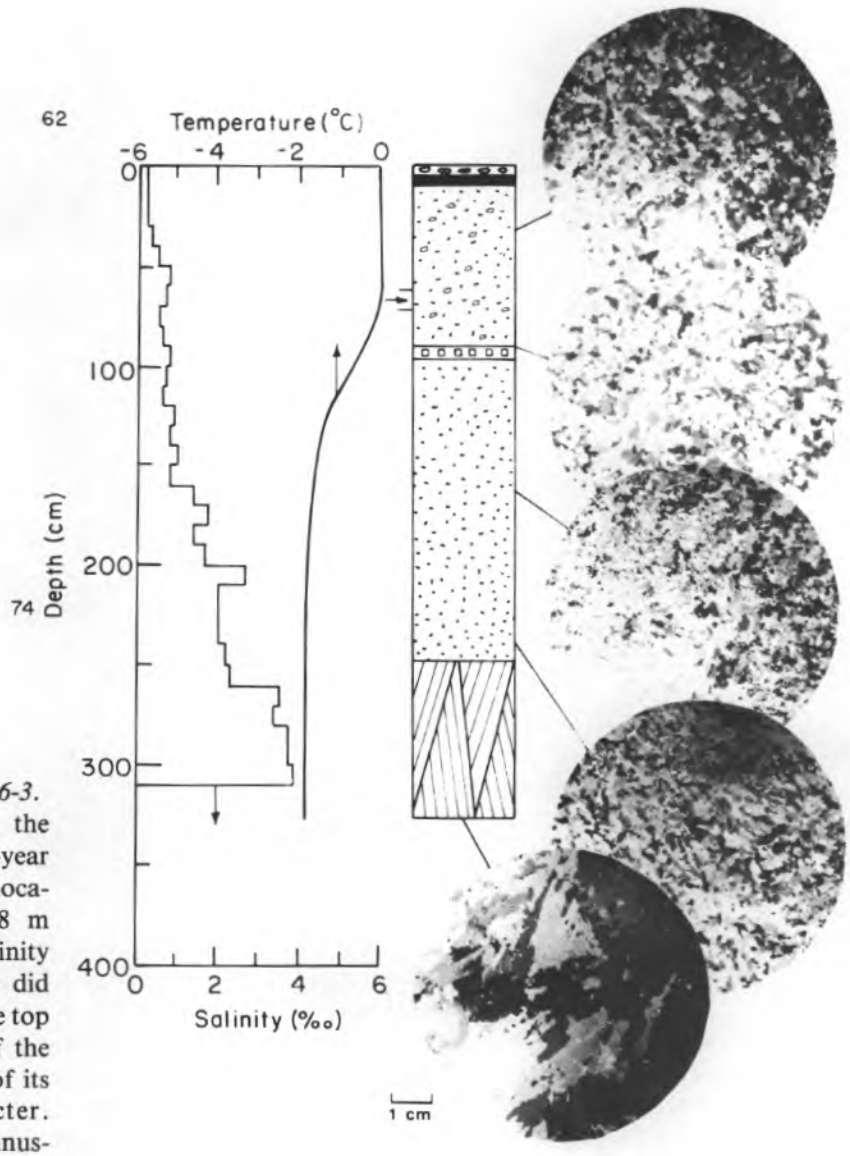

Figure A21. Site 6-26-3.

Core taken near the edge of a vast multi-year floe which, at this location, measured 3.28 m thick with a bulk salinity of 1.5‰. Salinities did not exceed 1‰ in the top meter and a half of the floe, a certain sign of its multi-year character. However, the most unusual feature of this floe was the very thick layer of frazil ice extending from 0.10- to 2.50-m-depth, representing 75% of the total ice thickness. Below 2.50 m the ice consisted entirely of congelation ice that exhibited only weak to random c-axis alignments. There was no evidence in the core that this part of the floe was ever associated with ridging. However, the vertical section of ice from 62- to 74-cm depth displayed a granular texture very similar to that observed in frazil ice in river ice covers, which might indicate that this floe was formed close to where a river was discharging into the sea along the coast of the Arctic Ocean. At least a mixing of fresh water with sea water is indicated.

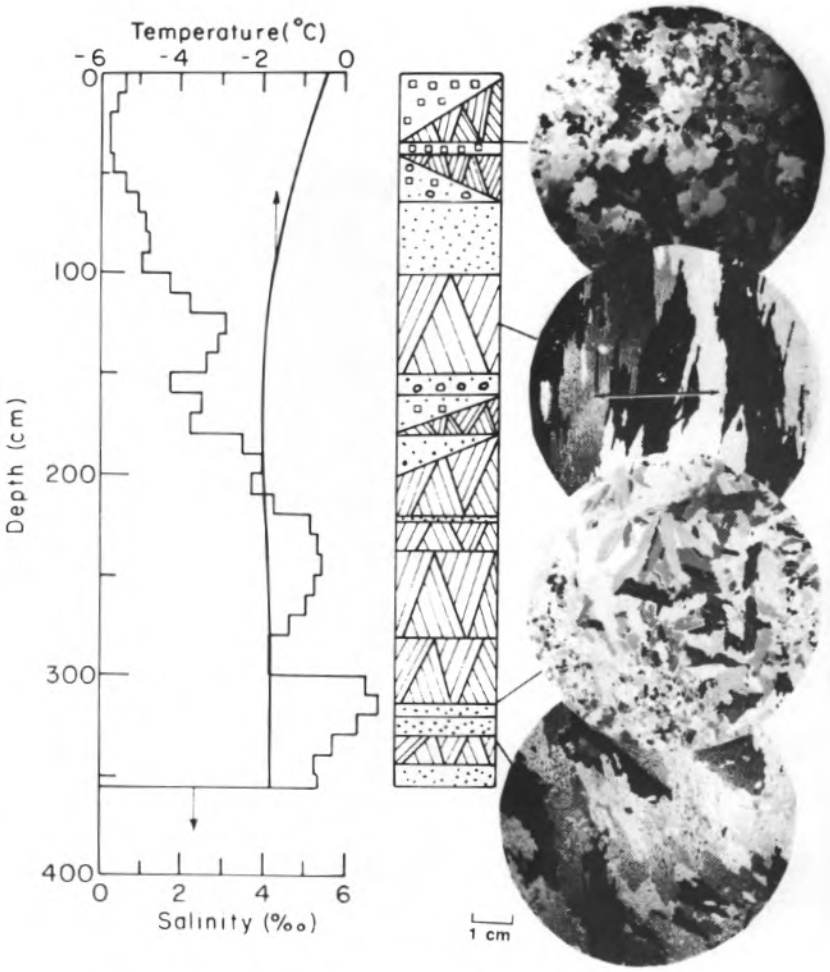

Figure A22. Site 6-27-1.

Core from a large multi-year floe exhibiting several surges in its salinity profile possibly related to three or more years of ice growth. However, the thickness (3.55 m) and high average salinity (3.2‰), together with evidence in the top 2 m of tilted blocks intermingled with frazil ice, indicate that this part of the floe, at least, was originally linked to ridge building. The high percentage of granular ice, 38%, and the occurrence of frazil at the bottom of the core further reinforce such an origin.

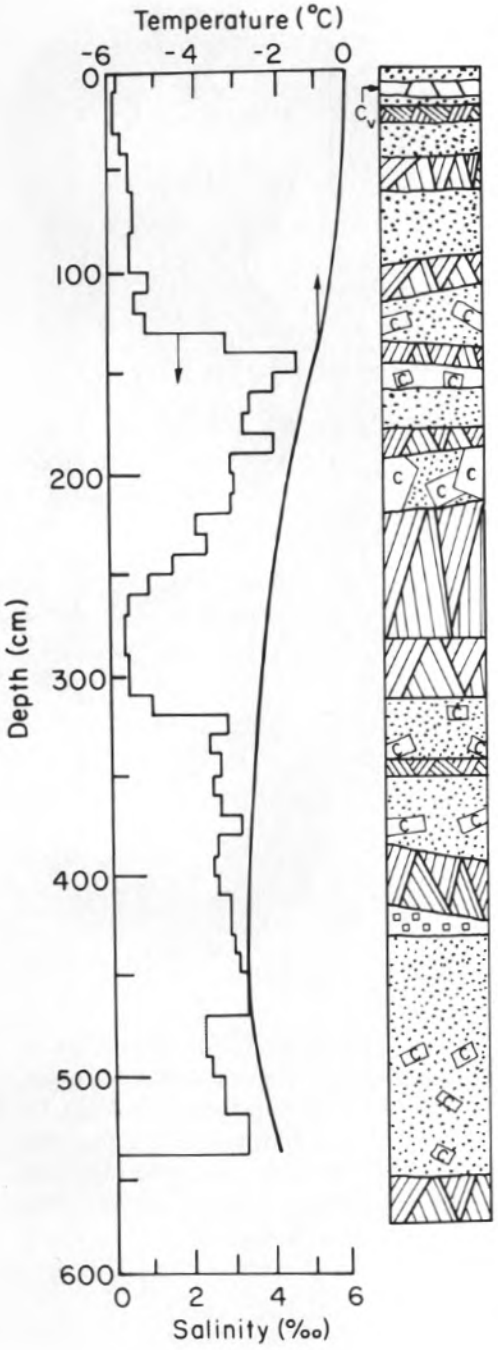

Figure A23. Site 6-27-2.

Core obtained to a depth of 3.74 m from a very large floe although the bottom of the floe was not penetrated. Temperature measurements indicated that several meters of ice remained to be drilled. Salinity and structural characteristics (based solely on examination of vertical slices) clearly demonstrated that the coring site was located on a multi-year ridge, the worn-down surface of which gave no indication of its true identity. The mean salinity measured 1.6‰ and the core contained approximately equal amounts of granular (53%) and congelation ice (47%). Three dirt zones at 1.22 to 1.33, 1.45 to 1.53 and 1.77 to 2.02 m were all associated with frazil ice.

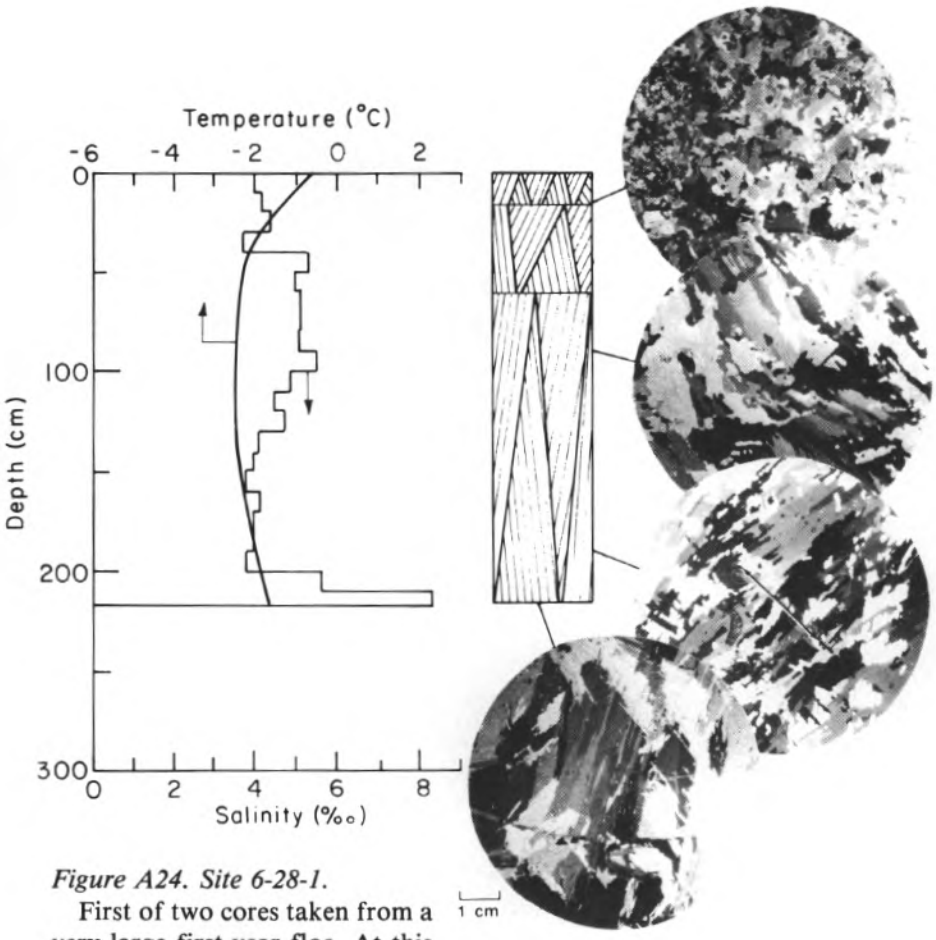

Figure A24. Site 6-28-1.

First of two cores taken from a very large first-year floe. At this particular location the floe was 2.15 m thick and was composed entirely of congelation ice with a mean salinity of 4.7‰. A moderate alignment of c-axes was observed; the cross-cutting, randomly aligned nature of crystals in the bottom ice clearly indicated that it was accreted as the floe was making its way out of the Arctic Basin into Fram Strait. A brown discoloration in the basal ice is attributed to entrainment of algae.

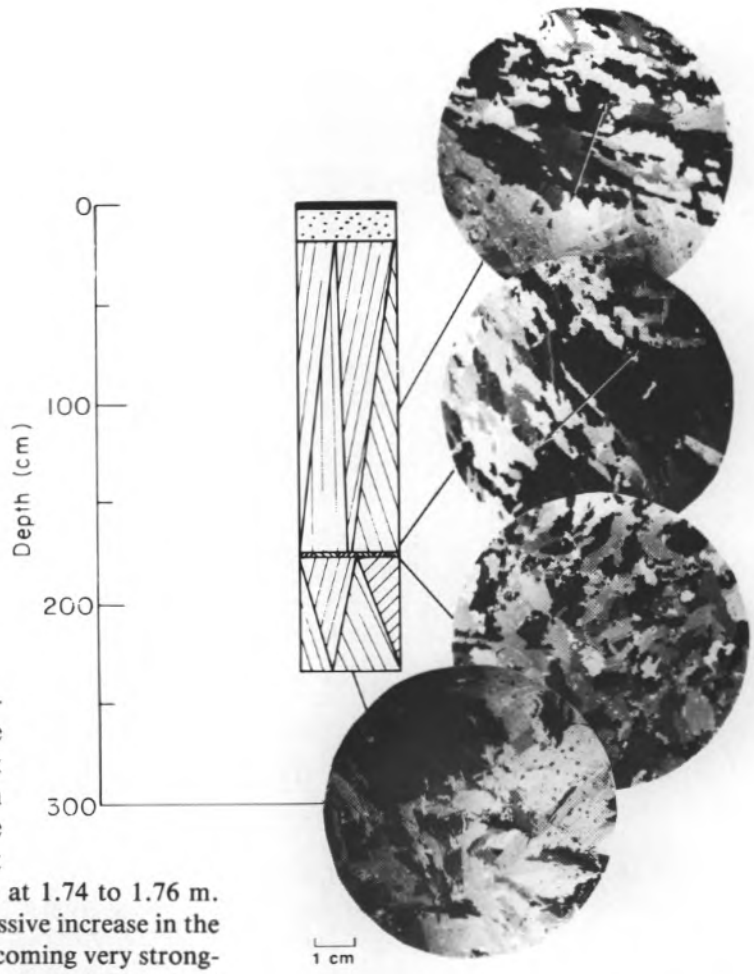

Figure A25. Site 6-28-2.

Core located 60 m from that of site 6-28-1 and consisting of 92% congelation ice overlain by granular ice and a 3-cm-thick layer of freshwater ice. The congelation ice component exhibited two distinctive growth textures separated by a 2-cm-thick layer of very fine-grained congelation ice at 1.74 to 1.76 m. The zone above 1.74 m exhibited a progressive increase in the degree of c-axis alignment, the crystals becoming very strongly aligned directly above the fine-grained layer at 1.74 to 1.76 m. The ice below 1.76 m lacked any significant alignment of its c-axes, indicating that it had accreted during the time the floe was in a freely-drifting state. This zone of ice also exhibited widespread banding, most probably related to fluctuations in ice growth velocity.

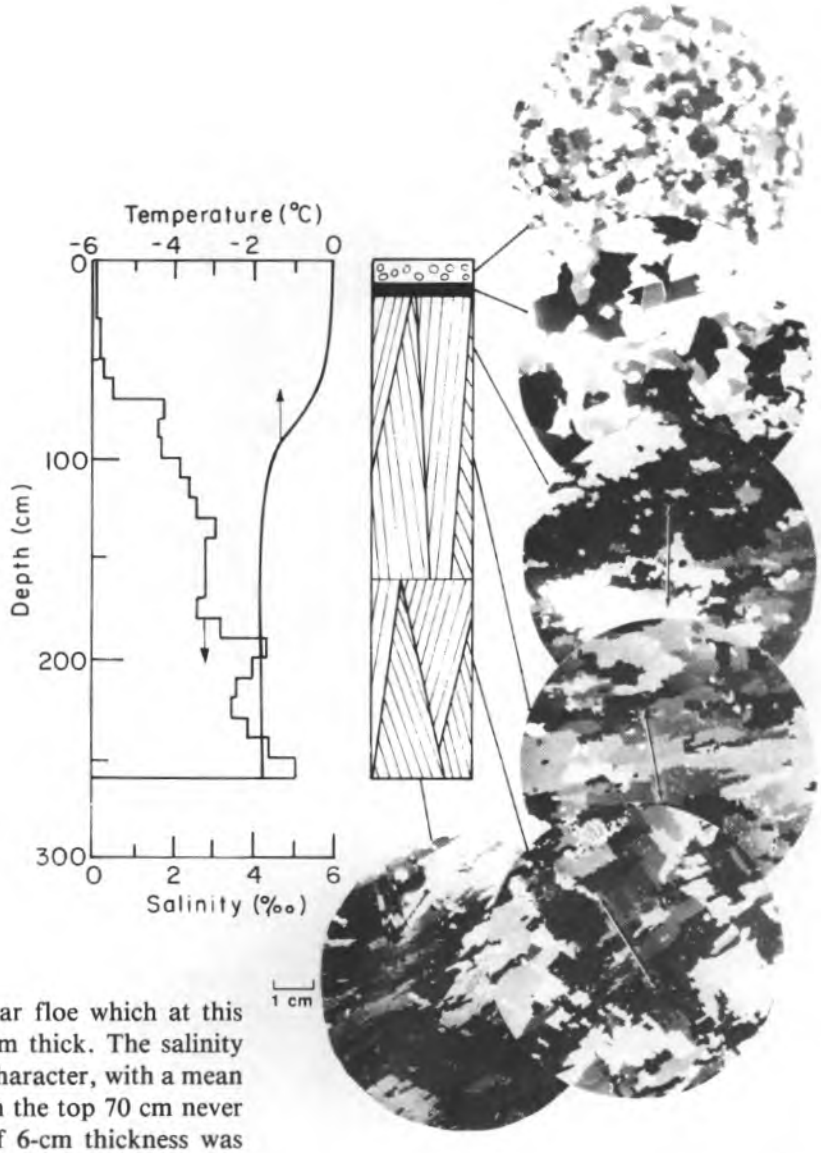

Figure A26. Site 6-28-3.

Core from a very large multi-year floe which at this particular location measured 2.61 m thick. The salinity profile was typically multi-year in character, with a mean salinity of 2.3‰ and with values in the top 70 cm never exceeding 0.5‰. Melt pond ice of 6-cm thickness was overlain by 11 cm of snow-ice at the top of the floe. All ice below the refrozen melt pond consisted of congelation ice representing 92% of the total ice thickness. Salinity and structural properties of the core indicate that this floe is two years old. The horizontal thin section structure at 76 cm displayed the effects of extensive, summertime retexturing consistent with the desalinated and semi-transparent nature of the top 76 cm of core. However, the original strong c-axis alignment of crystals was still preserved in the retextured ice. The direction of this alignment was identical to that in a crystal of ice not subject to retexturing at 99 cm. The onset of the 1983–84 winter's growth corresponded closely with the increase in salinity at around 1.80 m. C-axis alignments in this ice were weakly developed to nonexistent, particularly at the bottom where cross-cutting crystals, typical of growth under free-drift conditions, were much in evidence.

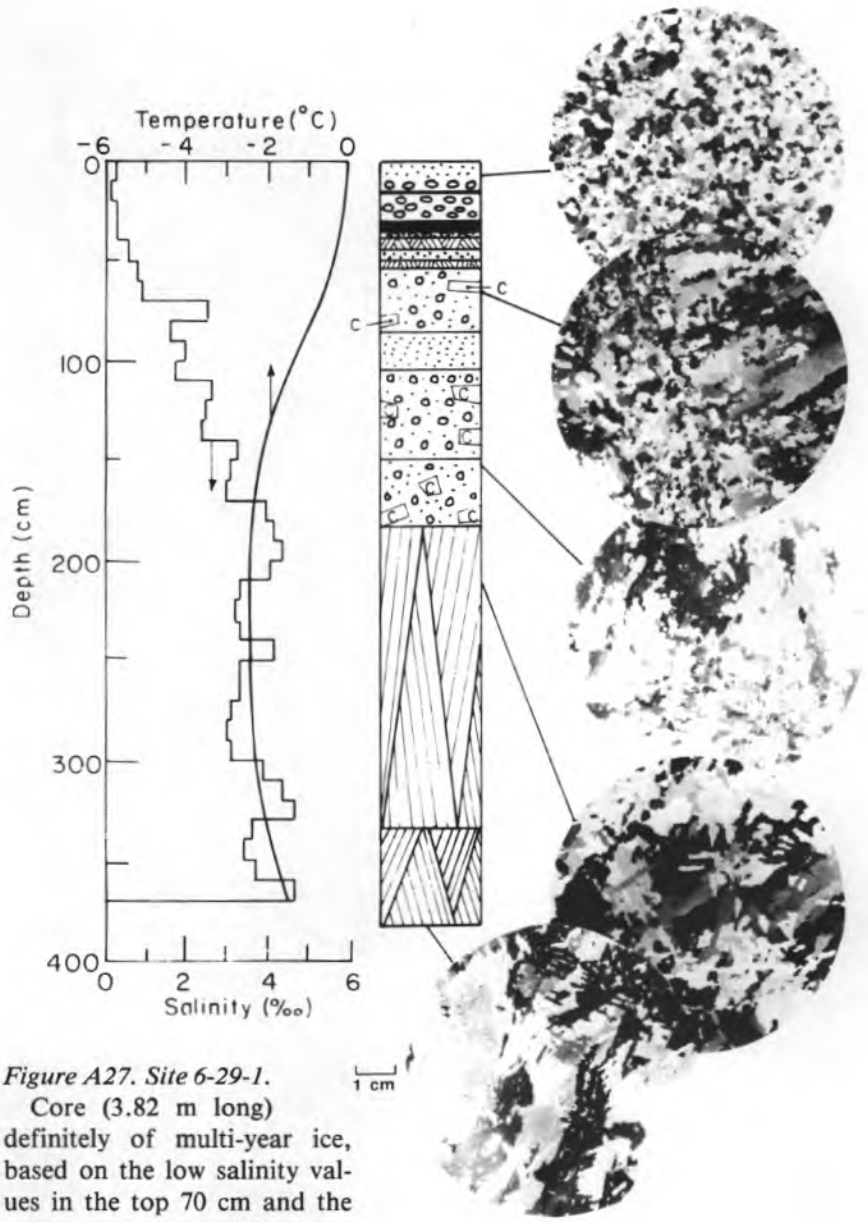

Figure A27. Site 6-29-1.

Core (3.82 m long) definitely of multi-year ice, based on the low salinity values in the top 70 cm and the existence at 30 to 35 cm of melt pond ice containing vertical, tubular air bubbles. Overlying the melt pond ice was an unusually thick layer (28 cm) of bubbly snow ice. However, at this particular location the floe appeared to consist of two structurally dissimilar components, with the top dominated by frazil ice, including three separate zones in which thin slabs of congelation ice were intermixed with frazil ice. Such structure may indicate a multiple rafting event. The lower component consisted entirely of congelation ice with a relatively high average salinity of 3.7‰. Despite its thickness this zone of congelation ice appeared to be devoid of any significant c-axis alignments, indicating its growth occurred under conditions in which the direction of the current at the ice/water interface was constantly disturbed or changing.

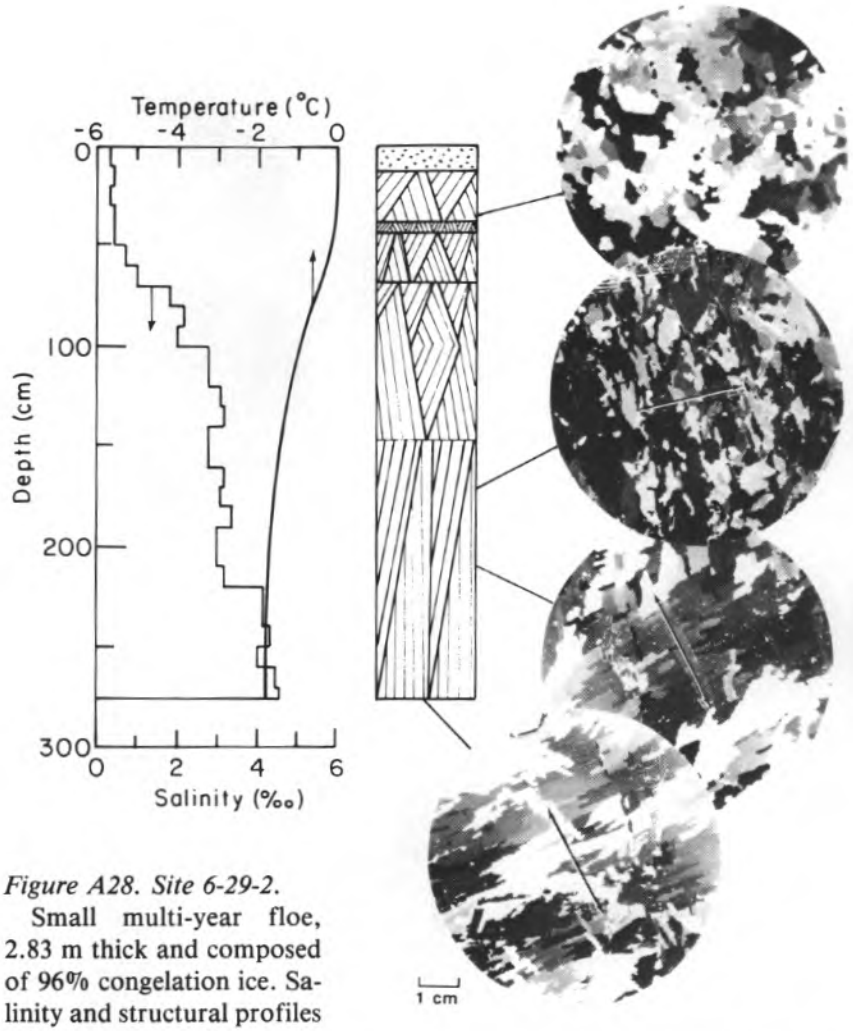

Figure A28. Site 6-29-2.

Small multi-year floe, 2.83 m thick and composed of 96% congelation ice. Salinity and structural profiles of this core were characteristic of multi-year ice, with the salinity averaging 2.7‰. Thermal modification of the upper layers of the floe the previous summer (1983) had produced clear, bubble-poor ice at 12 to 39 cm followed by bubbly semi-transparent ice down to 70 cm. This strong outward change in the appearance of the core was also accompanied by extensive retexturing of the congelation crystals themselves. The lowermost section of this ice displayed moderate to strong c-axis alignments. However, crystals in ice from the bottom of the floe were not significantly oriented, indicating growth while the floe was in a freely drifting state as it transited Fram Strait.

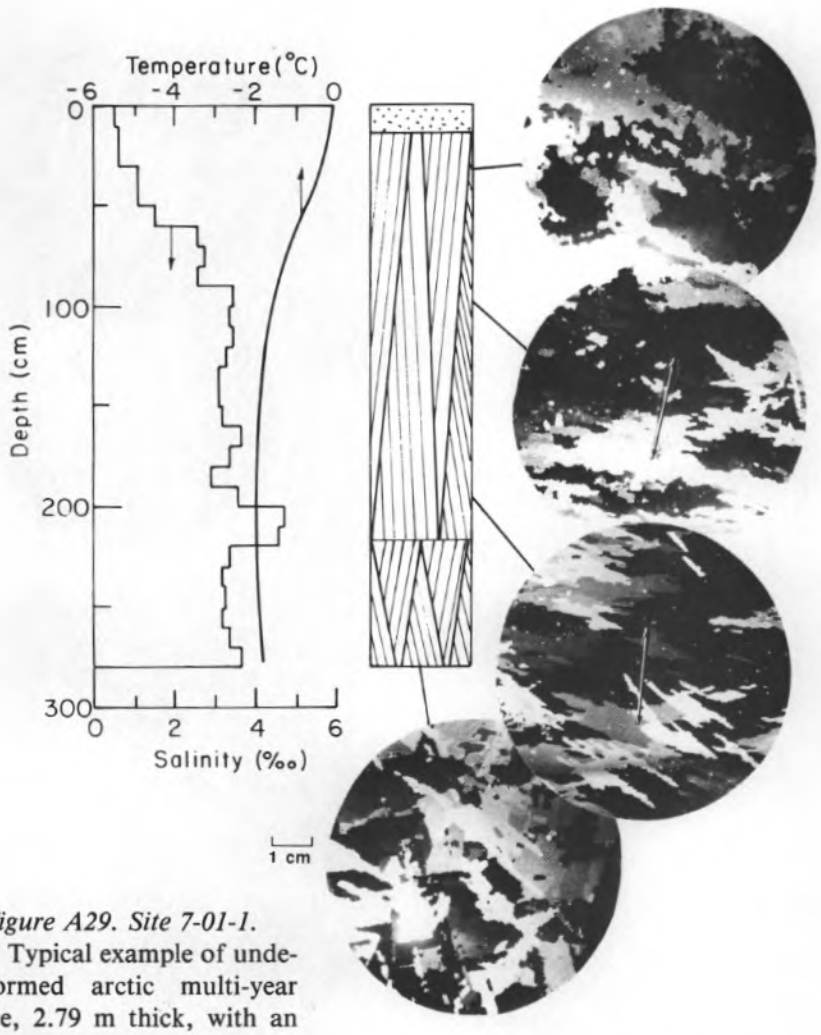

Figure A29. Site 7-01-1.

Typical example of undeformed arctic multi-year ice, 2.79 m thick, with an average salinity of 2.8‰ and composed of 95% congelation ice. Lower salinities in the top 50 cm coincided with the formation of semi-transparent ice in which appreciable retexturing of the crystals had also occurred. Structural evidence indicated two years of ice growth with the transition between the two occurring at around 2.0 m. The first winter's growth and part of the second displayed a moderate degree of c-axis alignment, consistent with freezing under fast ice conditions. Conversely, loss of alignment in the bottom ice is compatible with freezing as the floe was exiting the Arctic Basin.

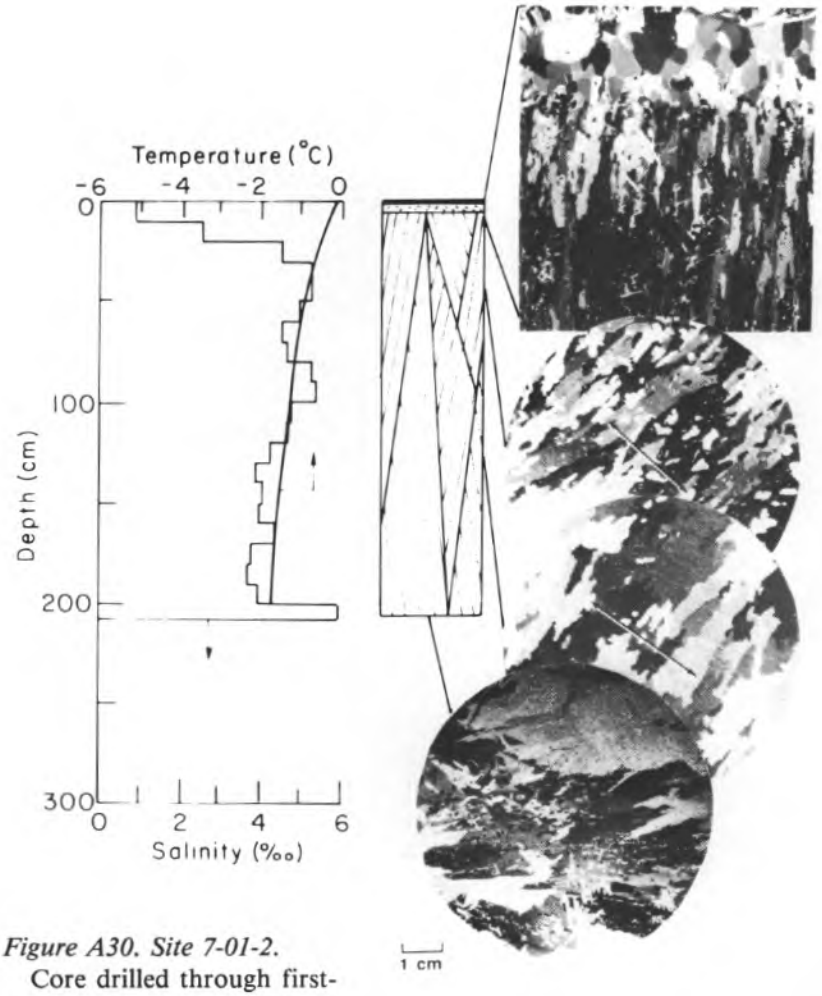

Figure A30. Site 7-01-2.

Core drilled through first-year ice attached to a large multi-year floe, 2.06 m thick, with a bulk salinity of 4.4‰. This ice consisted of 97% congelation ice, overlain by a thin layer of granular ice and a 2-cm-thick ice layer formed either from freezing rain or by refreezing of early spring snowmelt. Structural details of this particular section of core are featured in the vertical thin-section photograph from 0–12 cm. Strong c-axis alignments were developed early and extended to at least 1.35-m depth. Clearly established under fast ice conditions in the winter pack, this section of aligned crystal texture reverted to an essentially random directional orientation near the bottom, consistent with growth of ice during unencumbered drift of the floe as it exited the Arctic Basin. The large piece of multi-year ice to which the above fragment of first-year ice was attached was also core-drilled to confirm its multi-year identity, which was readily established on the basis of the hard, semi-transparent character of the top half-meter of core.

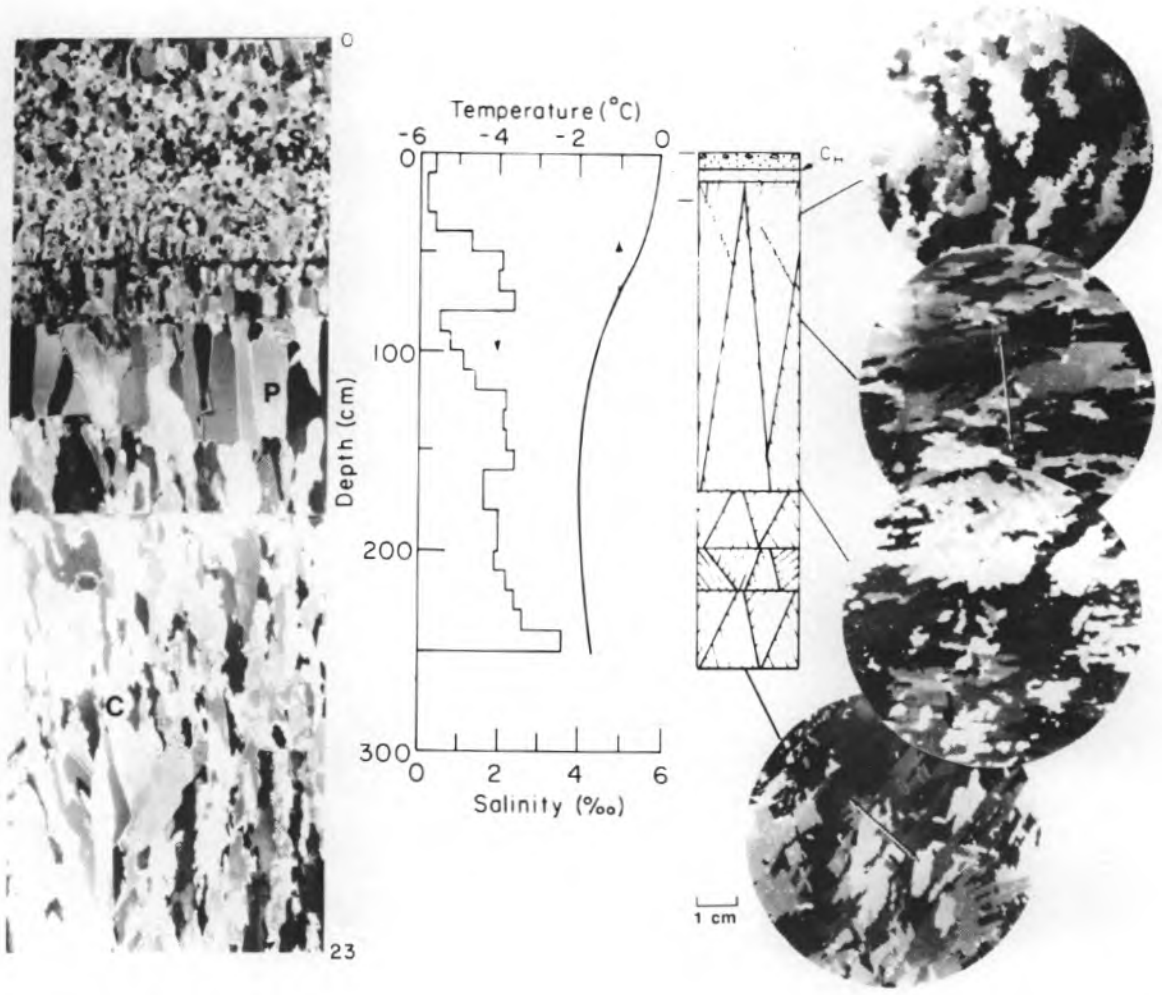

Figure A31. Site 7-01-4.

Small piece of undeformed multi-year ice, 2.58 m thick and composed of 94% congelation ice, including a 6-cm-thick freshwater melt pond layer overlain by 10 cm of snow ice. Details of this tripartite structure are shown in the vertical thin section photograph; segments A, B and C representing snow ice, pond ice and congelation ice, respectively. The salinity profile featured several surges and averaged 1.7‰. Salinities did not exceed 0.4‰ in the top 40 cm of ice, in which significant retexturing of crystals was also observed. Structure and salinity characteristics of this floe indicated three years of growth.

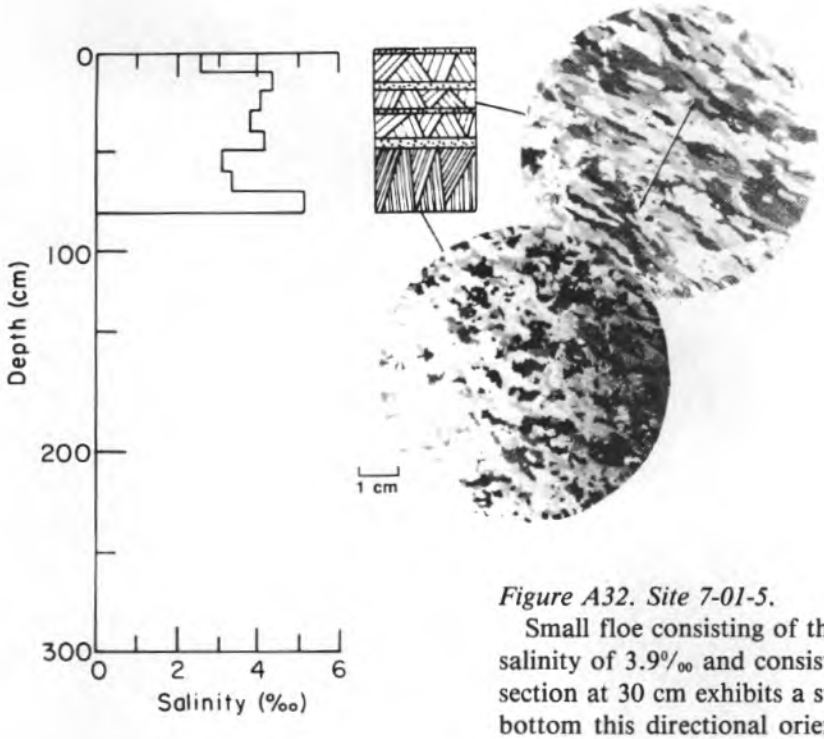

Figure A32. Site 7-01-5.

Small floe consisting of thin (0.81-m) first-year ice with a mean salinity of 3.9‰ and consisting of 86% congelation ice. The thin section at 30 cm exhibits a strong c-axis alignment but toward the bottom this directional orientation weakens and the ice becomes much finer-grained. Widespread occurrence of brine drainage features imbued this particular core with a distinctly corroded appearance.

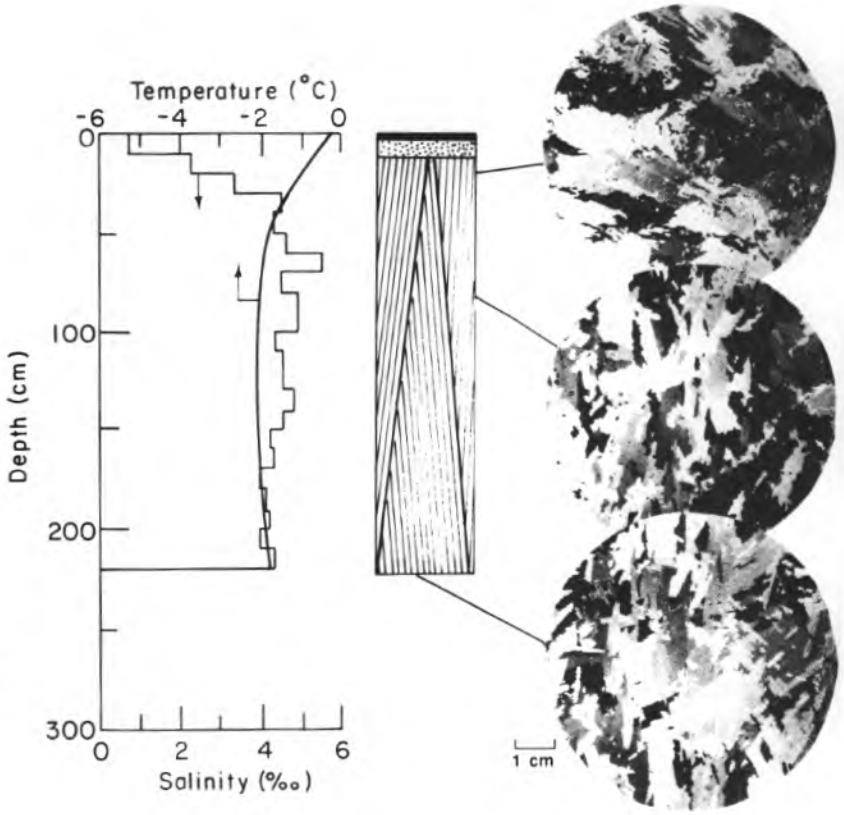

Figure A33. Site 7-01-6.

This core from a relatively thick first-year floe (2.22 m), was composed of 95% congelation ice with a mean salinity of 4.2‰. Ice in this floe was characterized by only moderate directional orientation of the crystal c-axes. Widespread optical banding testified to frequent fluctuations in the growth velocity in this particular floe.

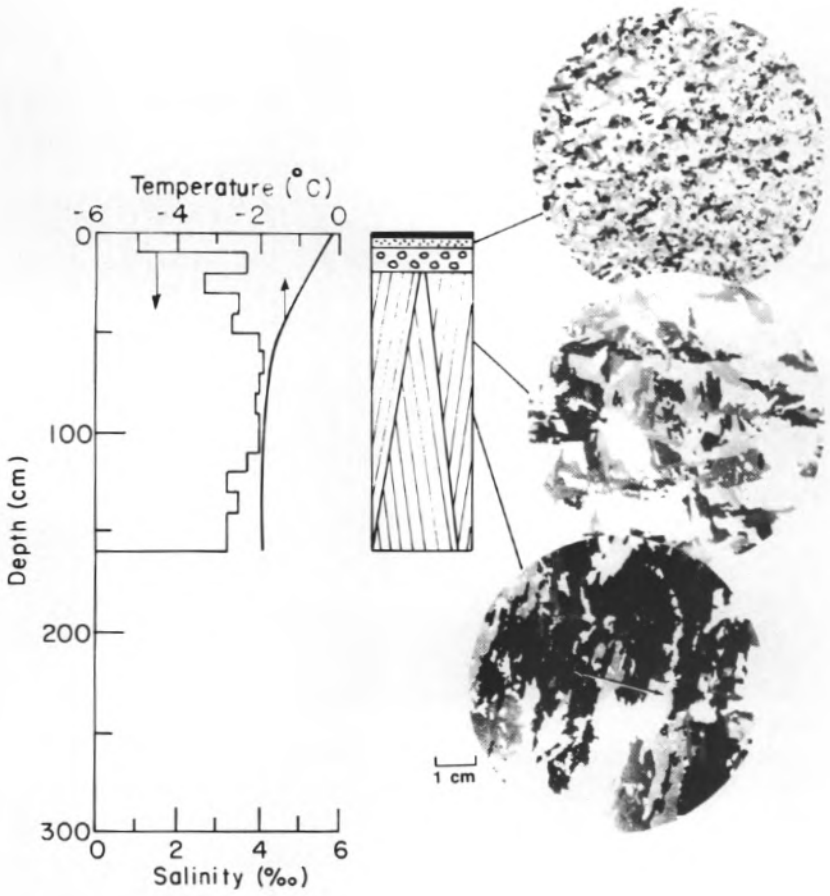

Figure A34. Site 7-03-1.

First of three cores drilled into a large first-year floe. Ice at this location, measuring 1.59 m thick, consisted mainly of congelation crystals (87%) overlain by granular ice topped by a 2-cm-thick ice crust. The bulk salinity measured 3.5‰. Optical banding was prevalent in the bottom 70 cm of ice, crystals of which exhibited moderate to strong c-axis alignments. The bottom ice contained algae incorporated into the dendritic structure of the congelation crystals.

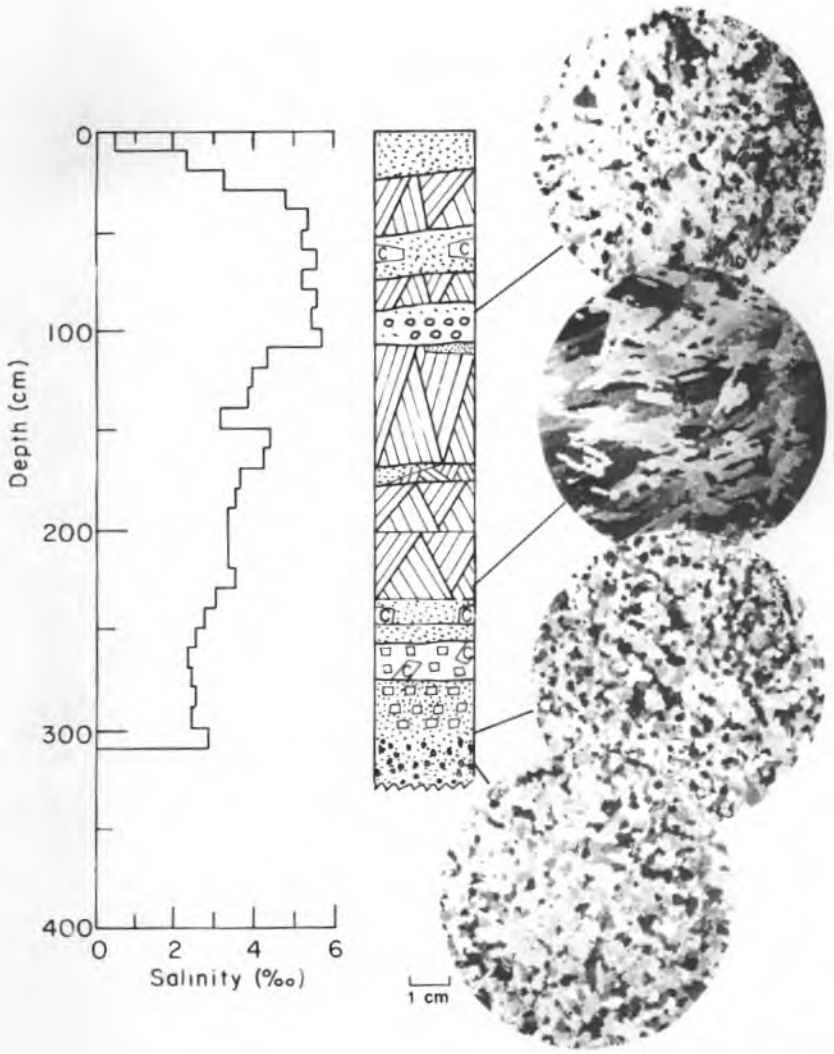

Figure A35. Site 7-03-2.

Core purposely drilled into the flank of a 3.25-m-thick first-year ridge with a bulk salinity of 3.7‰. Vertical sectioning of the core revealed deformed structure throughout the ridge, including blocks inclined up to 30° from the horizontal. The salinity profile was unusual but consistent with seawater infiltration and freezing between ice blocks. Salinities were significantly higher at the top of this ridge. Congelation and frazil ice were present in approximately equal amounts.

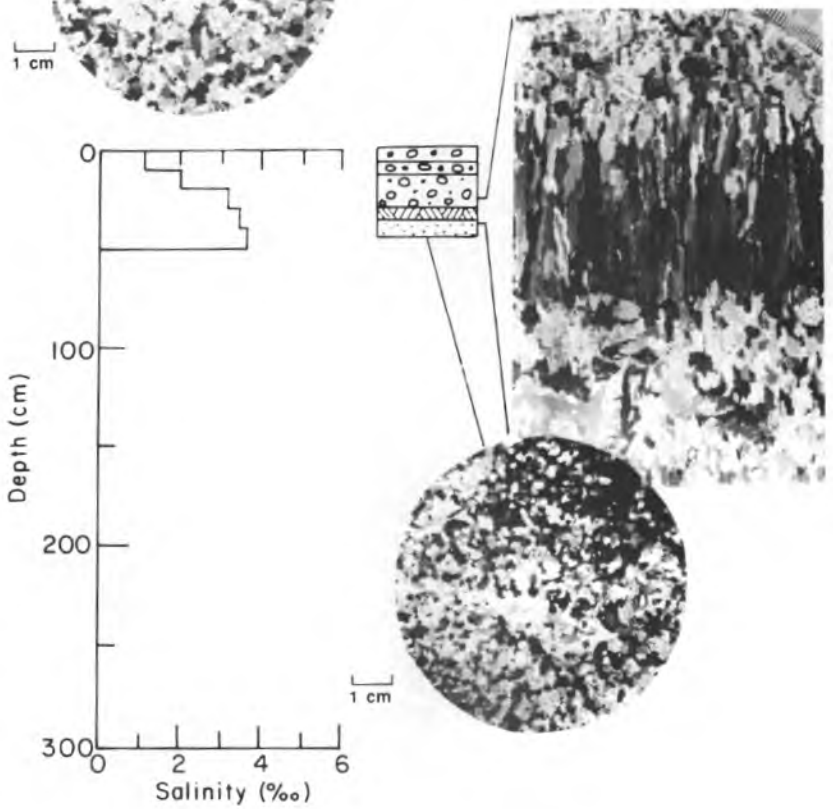

Figure A36. Site 7-03-3.

Lead ice, 44 cm thick and composed mainly of frazil ice (85%). Structure details of a thin layer of congelation ice and its relationship to frazil ice above and below is demonstrated in the vertical thin section at 27 to 39 cm.

Figure A37. Site 7-04-1.

Relatively thin piece of multi-year ice from a very large floe. Though the structure core measured 1.74 m thick, a 1.95-m-thick salinity core was obtained at the same site, indicating that 21 cm of bottom ice was not recovered during drilling of the structure core. The core consisted of 98% congelation ice, including a 10-cm-thick section of pond ice exhibiting both c-axis vertical (c_v) and c-axis horizontal (c_h) textures. Details of the structure and the transition to congelation ice are demonstrated in the vertical thin section from 9 to 20 cm. Salinity profile characteristics, including a low mean value of 2.5% and the semi-transparent, retextured nature of ice in the top half meter of the core, confirm the multi-year identity of this floe.

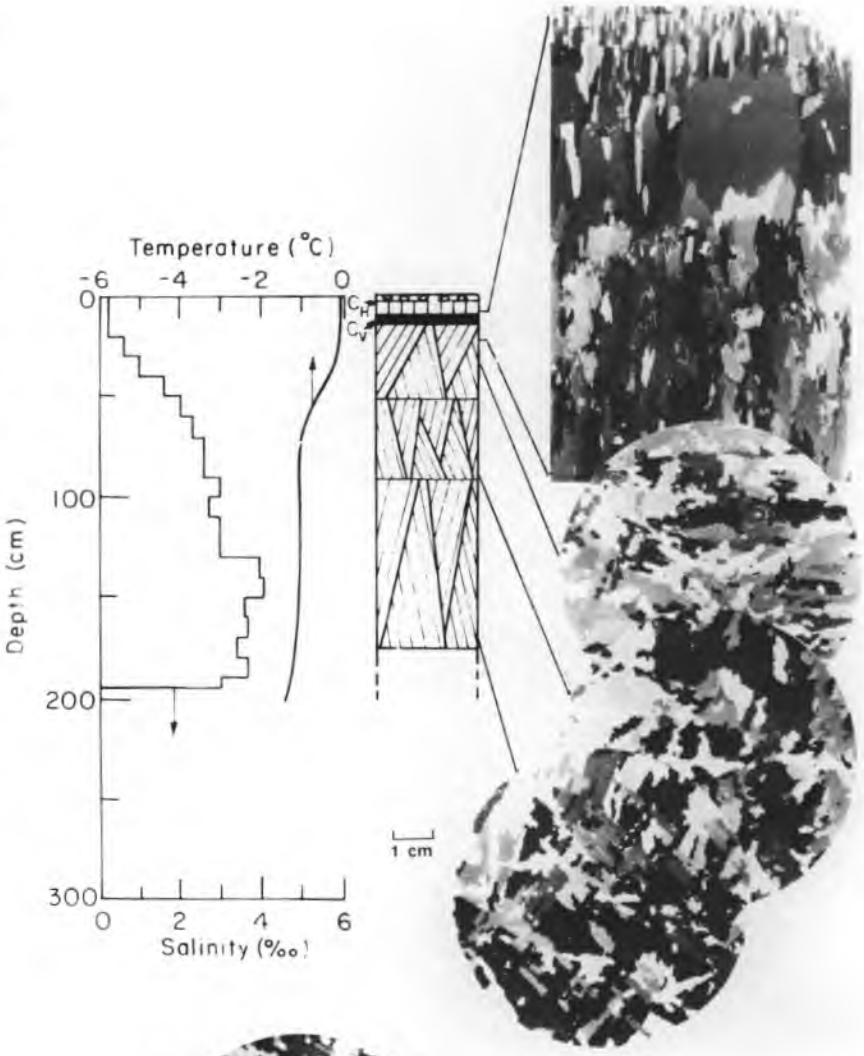

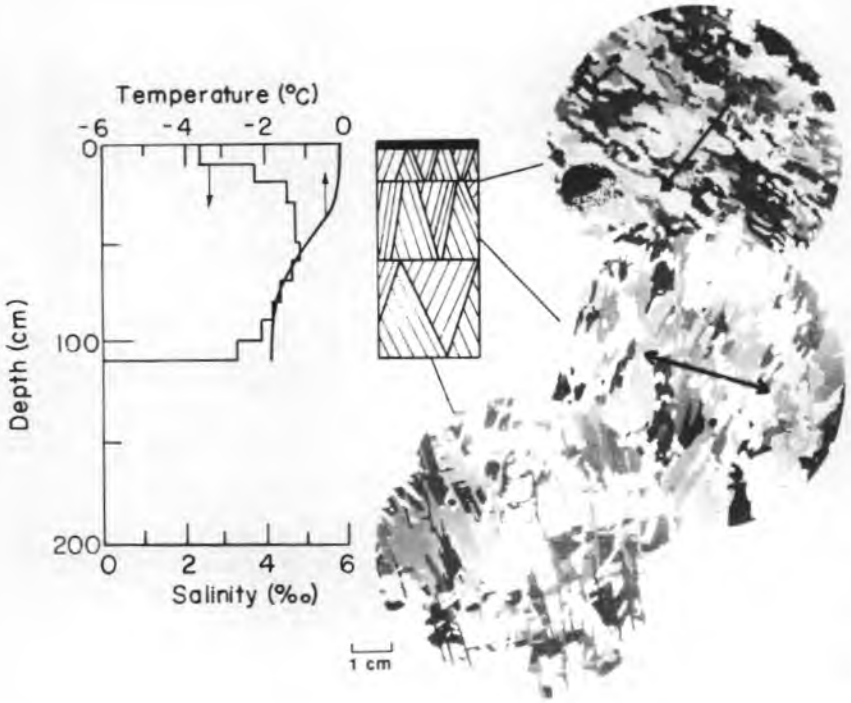

Figure A38. Site 7-05-1.

Undeformed first-year floe, 1.09 m thick, consisting of 95% congelation ice with a bulk salinity of 4.3‰. Optical banding was observed at several levels in the core. An approximate 60° change in c-axis alignment testified to a major change in the direction of the prevailing current at the ice/water interface, linked most probably to repositioning of the winter pack in which this first-year ice was growing.

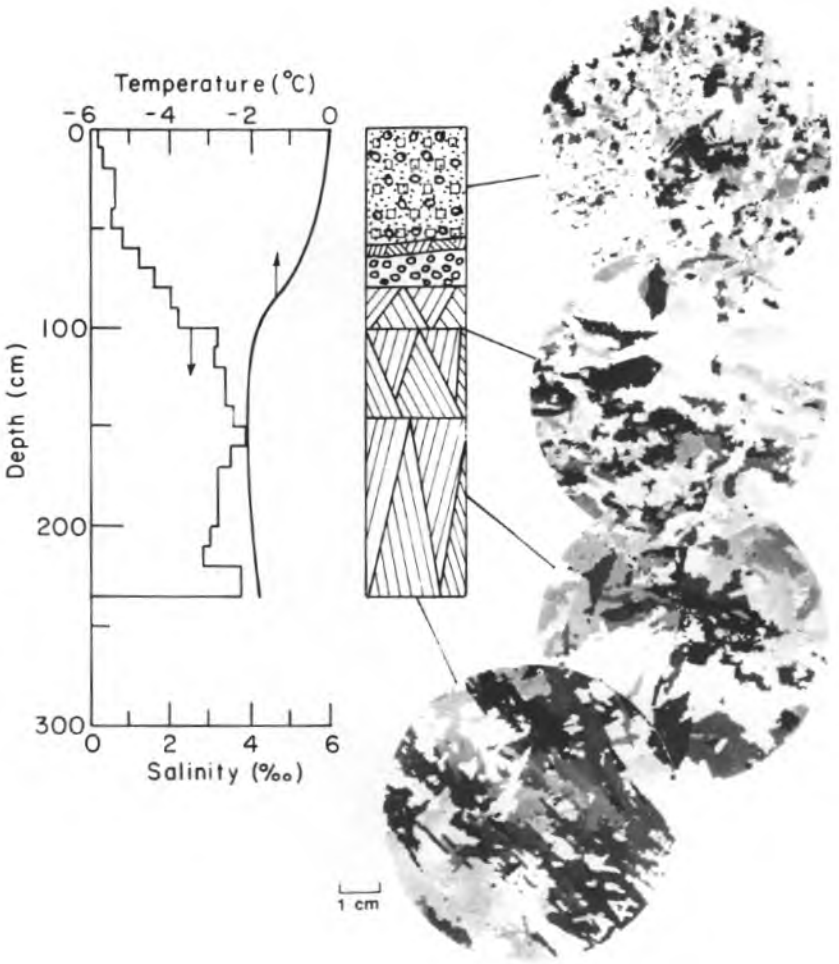

Figure A39. Site 7-05-2.

Piece of undeformed multi-year ice, 2.35 m thick, with a bulk salinity of 2.4‰. Core structure indicated presence of a piece of rafted ice mixed in with granular ice to a depth of 80 cm, underlain by congelation ice in which crystal c-axes are only weakly aligned. Diminished salinities in the top 50 cm of core, together with evidence of the retextured condition of ice in the thin section from 1.01 m, confirm the multi-year nature of the floe. Surface of this floe showed onset of puddling.

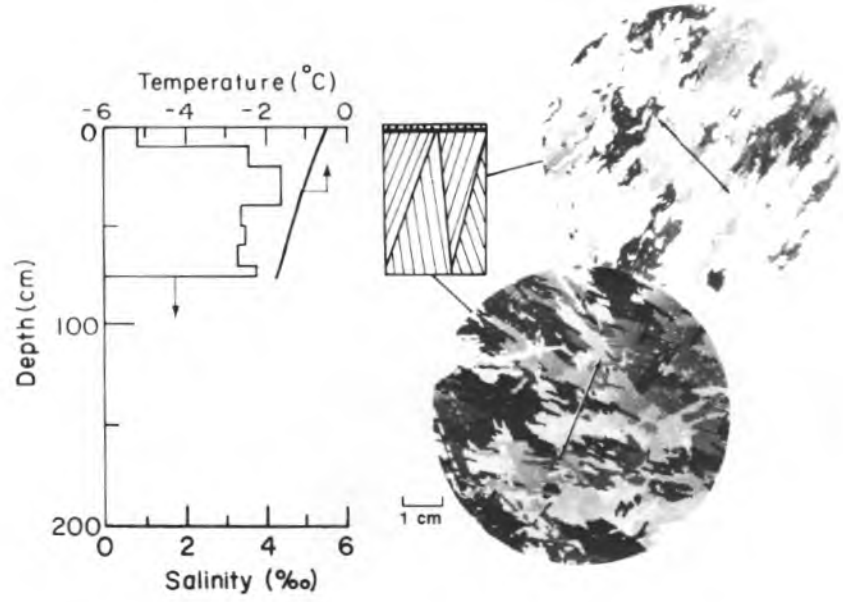

Figure A40. Site 7-05-3.

Small piece of first-year ice, 75 cm thick, attached to multi-year ice (site 7-5-4). Core was composed of 95% congelation ice with an average salinity of 3.4‰. The upper part of the core contained numerous brine drainage cavities. Aligned c-axes were in evidence by 25 cm, but crystals were only weakly to moderately oriented at the bottom and offset by nearly 90° from the alignment direction at 25 cm.

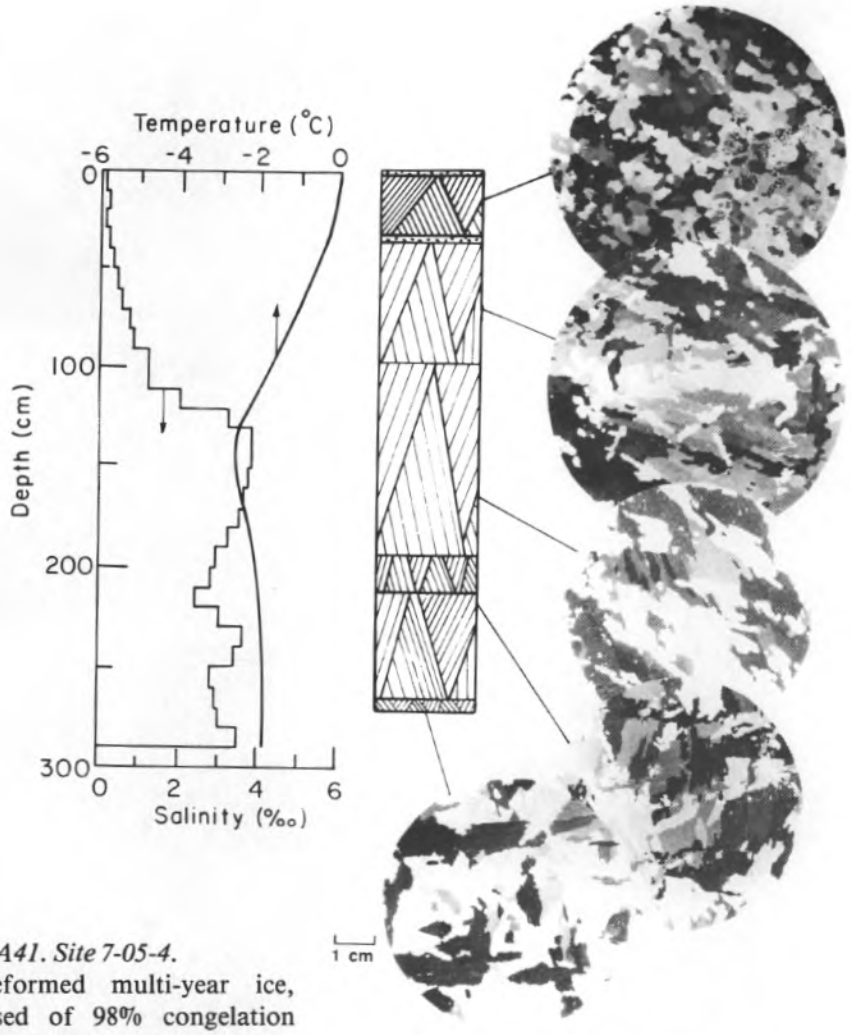

Figure A41. Site 7-05-4.

Undeformed multi-year ice, composed of 98% congelation ice. Salinity averaged 2.2‰ but did not exceed 1‰ in the top 90 cm. This and the semi-transparent, retextured condition of ice in the top meter confirmed the multi-year nature of this floe to which was attached the small piece of first-year ice cored at site 7-05-3. Only the thin section from 1.64 m showed any sign of significant alignment of c-axes. Two salinity surges, the second corresponding closely with a change in the size of congelation crystals, were interpreted as indicating a second and third winters' growth. The structure core measured 2.71 m thick, 16 cm less than the salinity core.

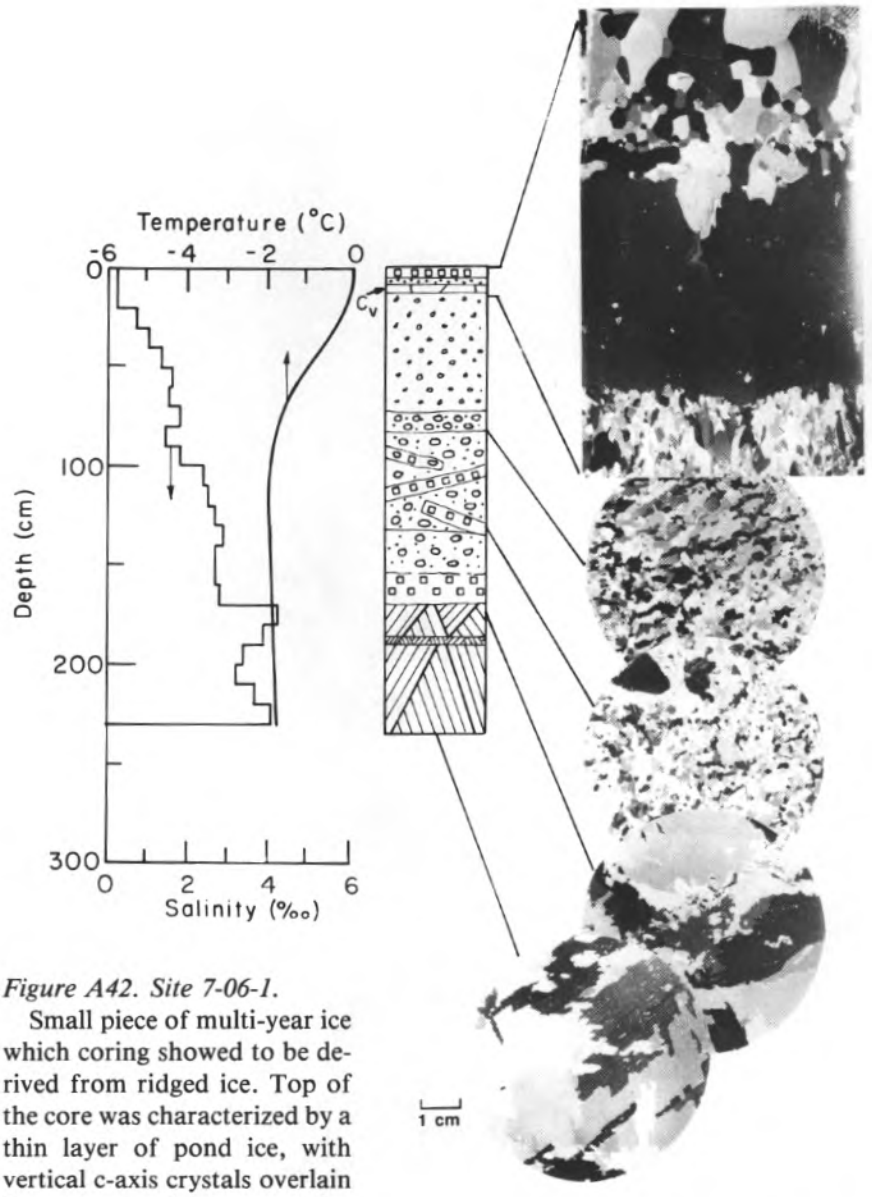

Figure A42. Site 7-06-1.

Small piece of multi-year ice which coring showed to be derived from ridged ice. Top of the core was characterized by a thin layer of pond ice, with vertical c-axis crystals overlain by coarse-grained snow ice and underlain by granular ice as demonstrated in the vertical sections from 0–15 cm. The mid-section of the core contained tilted blocks of both congelation and granular ice underlain by congelation ice representing only 29% of the total thickness of ice at this particular coring site. Salinity of the core averaged 2.3‰.

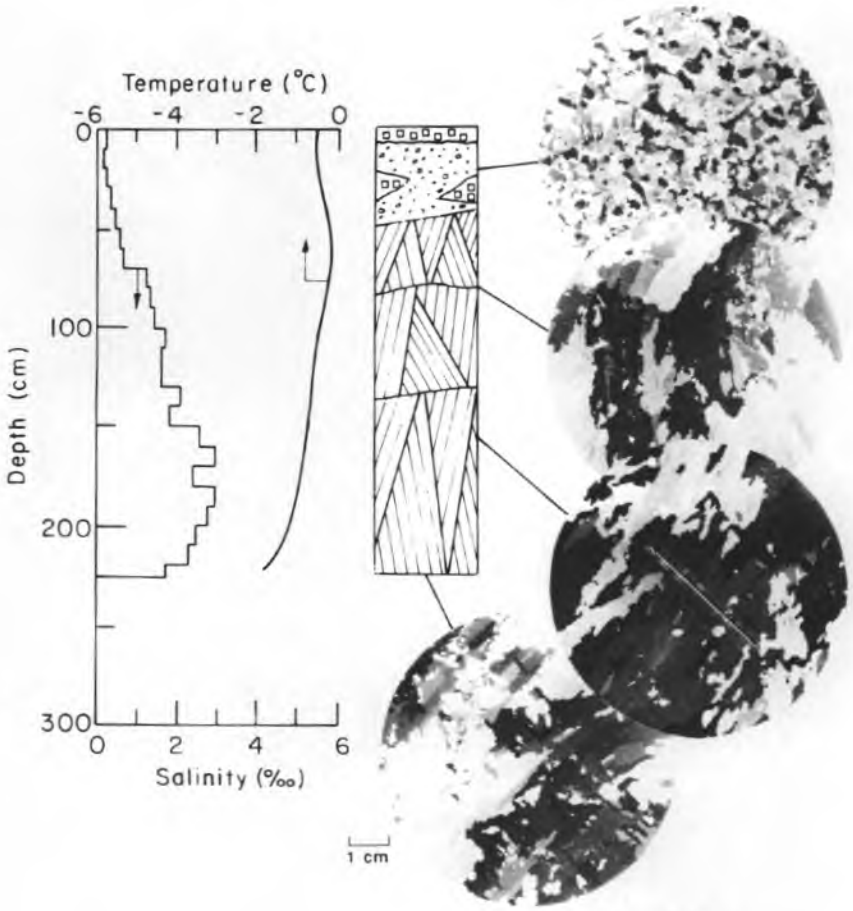

Figure A43. Site 7-07-1.

Core from a very large multi-year floe measuring several kilometers in diameter. The coring site was located close to a multi-year ridge and the nature of structure in the top meter of the core showed that this part of the core was also associated with a ridging event. The floe at this location consisted of 80% congelation ice and its salinity averaged 1.5‰. Floe was fringed by pieces of first-year ice and intersected by ridges and refrozen leads.

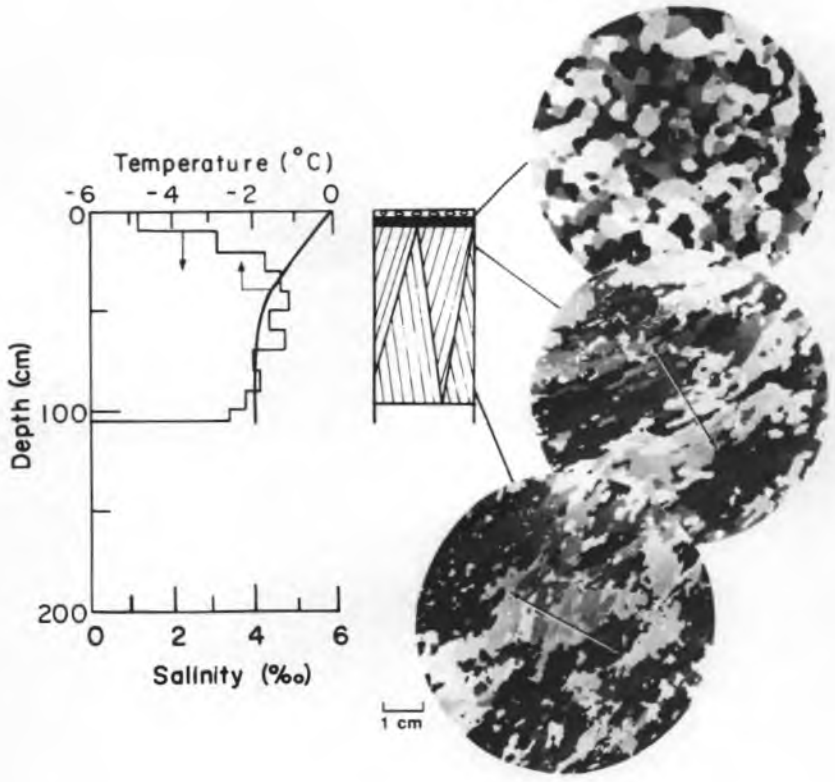

Figure A44. Site 7-07-2.

Core from a 97-cm-thick refrozen lead located on the same multi-year floe from which the core at site 7-7-1 was obtained. The top of the lead contained a 4-cm-thick ice layer overlain by snow-ice and underlain by congelation ice representing 92% of the total ice thickness. Congelation ice, in which crystals were strongly aligned throughout, exhibited much banding related to growth rate fluctuations. The salinity averaged 3.9‰.

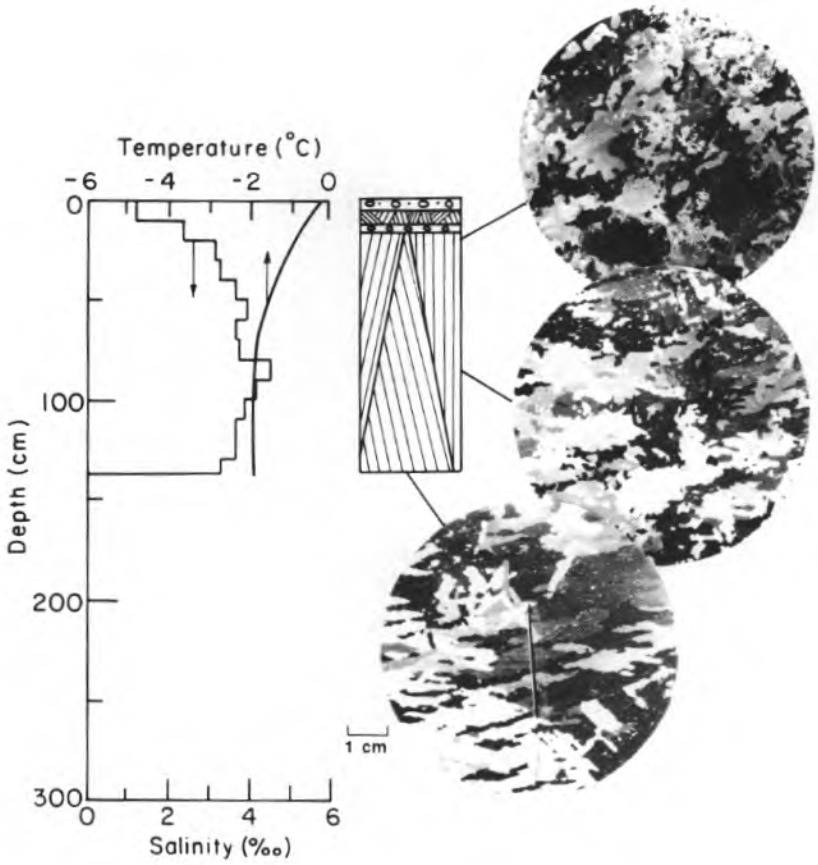

Figure A45. Site 7-07-3.

Core from a fragment of first-year ice attached to the edge of the multi-year floe sampled previously at site 7-7-1. Core was 1.36 m thick and consisted of 93% congelation ice with an average salinity of 3.5‰. The congelation component was characterized by widespread growth banding and the development of a moderate c-axis alignment.

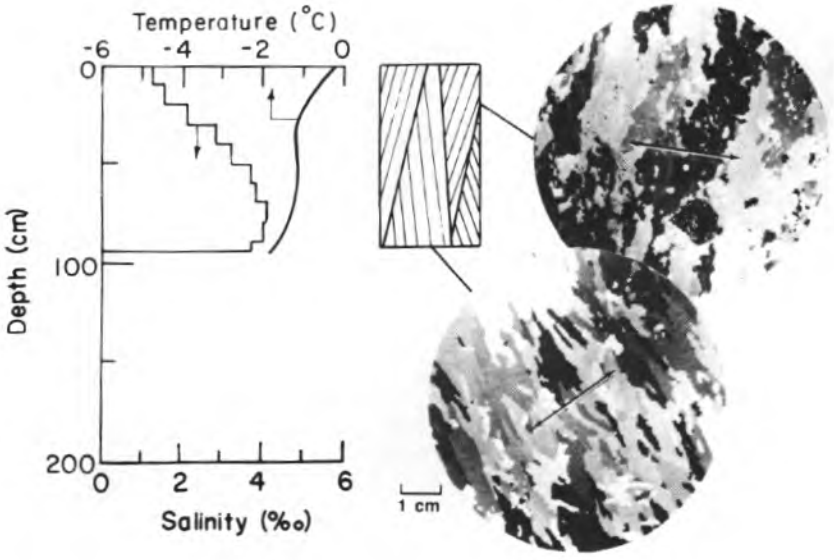

Figure A46. Site 7-07-4.

Small piece of first-year ice, 92 cm thick, consisting entirely of congelation ice with an average salinity of 3.0‰. A strong c-axis alignment was observed at the bottom of the floe; c-axes were less strongly aligned near the top and offset by nearly 90° from the alignment direction at the bottom, a situation indicative of two separate periods of fast ice growth with a period of rotation in between.

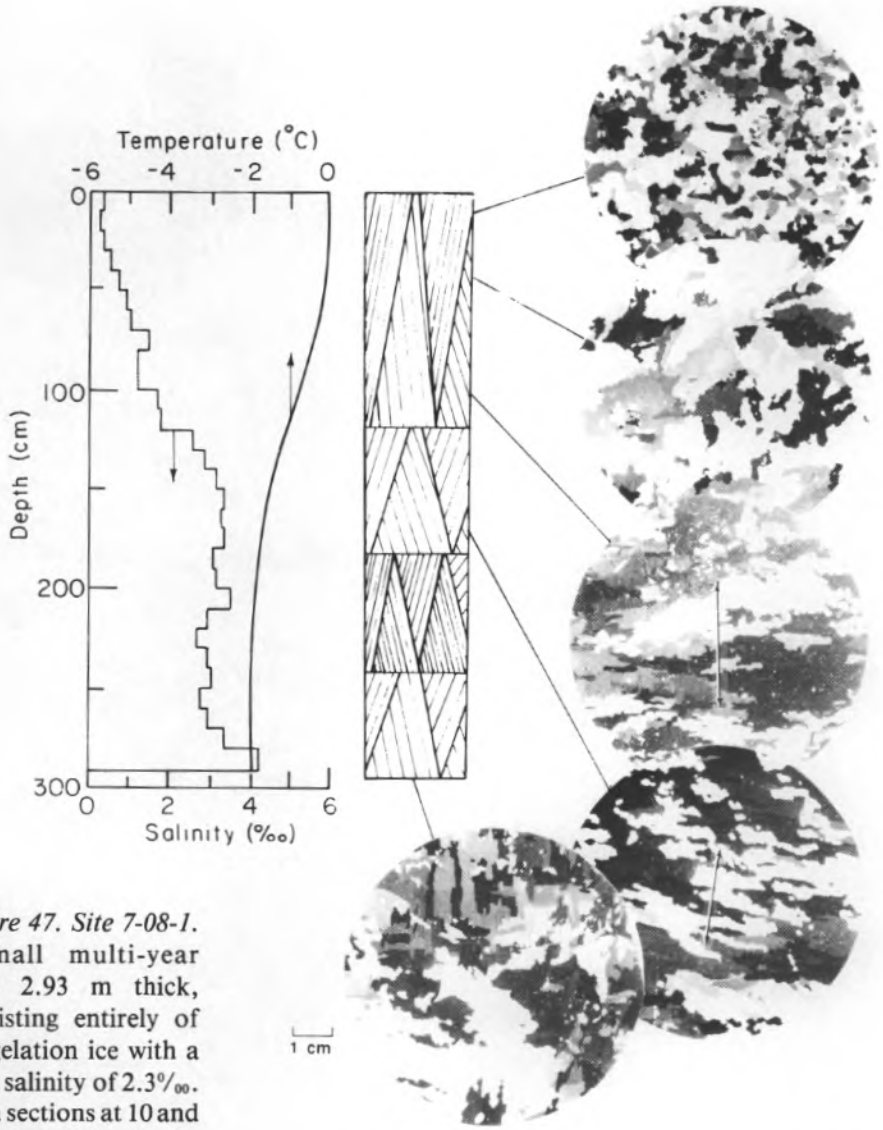

Figure 47. Site 7-08-1.

Small multi-year floe, 2.93 m thick, consisting entirely of congelation ice with a bulk salinity of 2.3‰. Thin sections at 10 and 40 cm show the effects of substantial retexturing, consistent with the hard, semi-transparent condition of the ice over the top 50 cm of core. Crystals in ice at 1.70 m were moderately aligned, less so at 1.00 m. If significant discontinuities in the size of crystals at 1.17, 1.80 and 2.40 m signify annual growth increments, then the floe would be four years old.

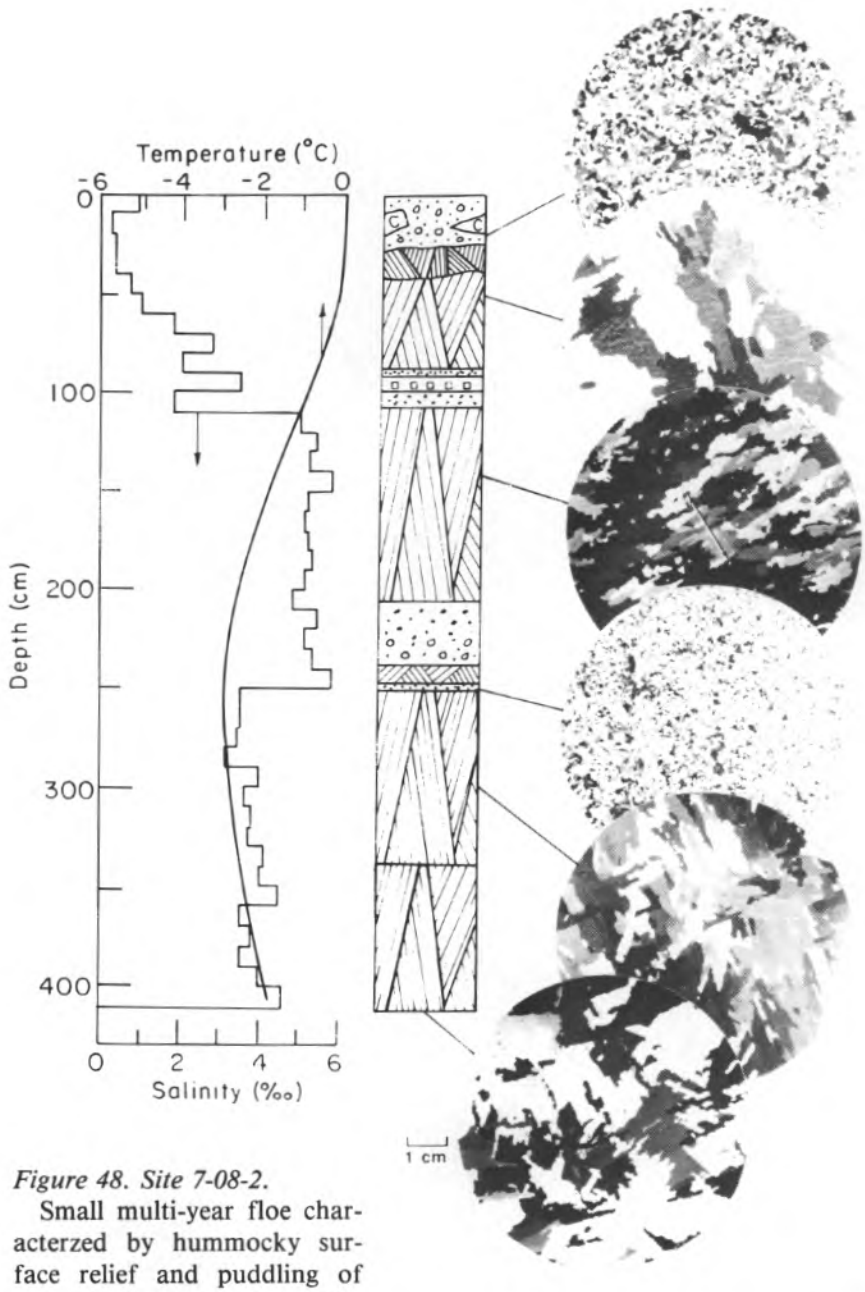

Figure 48. Site 7-08-2.

Small multi-year floe characterzed by hummocky surface relief and puddling of water in the depressions. The structure indicates rafting of ice in the top 5 cm of the core. Floe was 4.11 m thick with an average salinity of 3.6‰, rather high for multi-year ice and due largely to a zone of enhanced salinity, averaging 5.0‰ at 1.10 to 2.50 m. This and the existence of granular ice layers at several different levels in the floe, together with the thickness of the floe, all suggest that it is a multi-year ridge remnant.

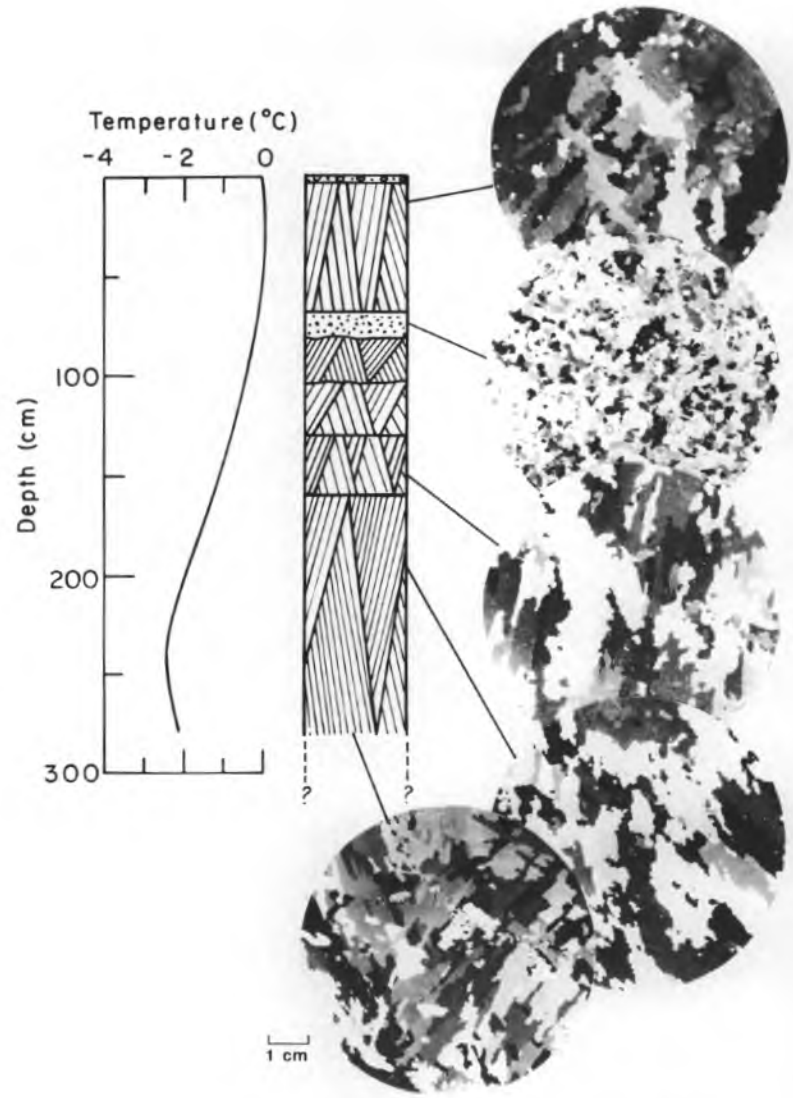

Figure A49. Site 7-09-1.

Core from near the edge of a very large multi-year floe composed of 95% congelation ice. The bottom of the floe was not penetrated and no salinity profile was obtained; however, the retextured condition of the ice at 15 cm confirmed the multi-year nature of this floe. Extrapolation of the temperature profile indicated a probable thickness of ≈ 3.0 m. Thin sections at 1.50 and 1.96 m exhibit moderately strong c-axis alignments.

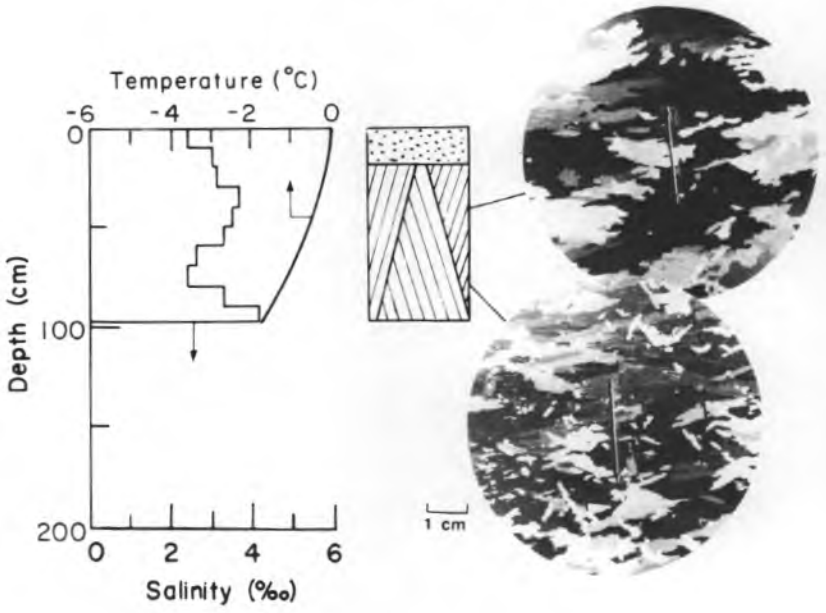

Figure A50. Site 7-09-2.

Small section of thin first-year ice (0.97 m) near the center of the same vast multi-year floe from which the core at site 7-9-1 was obtained. Ice is of probable lead origin, composed of 81% congelation ice with a mean salinity of 3.2‰. Granular ice at the top of the core was quite soft and beginning to show obvious signs of candling. The congelation ice component exhibited moderately strong c-axis alignments.

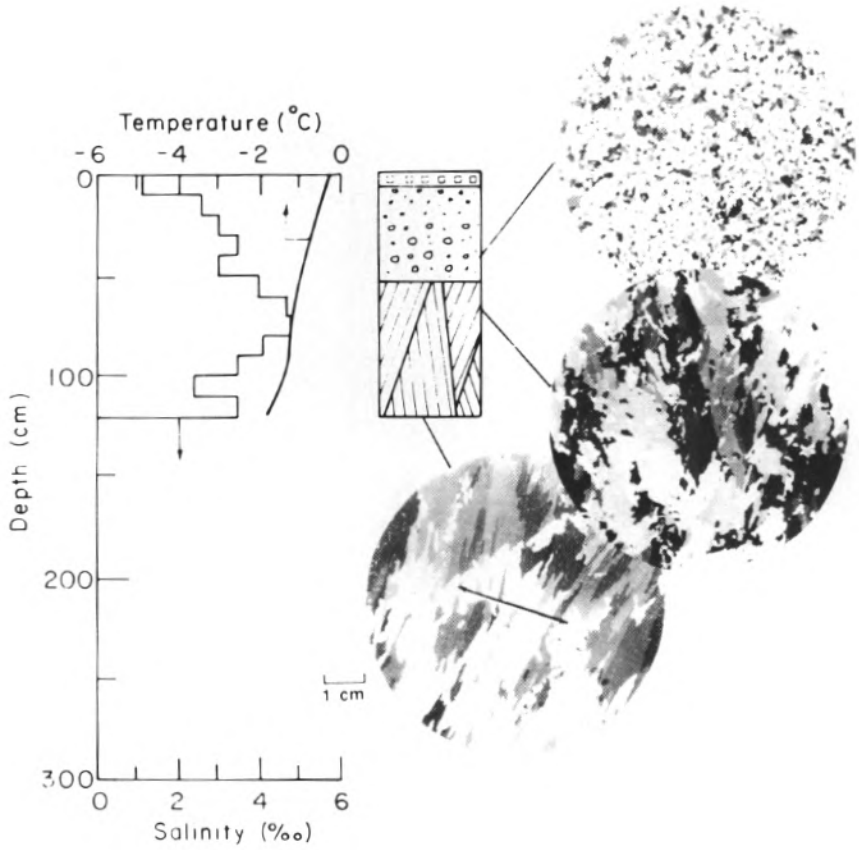

Figure A51. Site 7-09-3.

Another piece of lead ice from near the edge of the same floe from which cores at sites 7-9-1 and 7-9-2 were obtained. Structurally, this core was composed of granular ice (45% of total ice thickness) overlying congelation ice, the bottom of which consisted of crystals displaying moderate c-axis alignments. The ice was 1.20 m thick with an average salinity of 3.4‰.

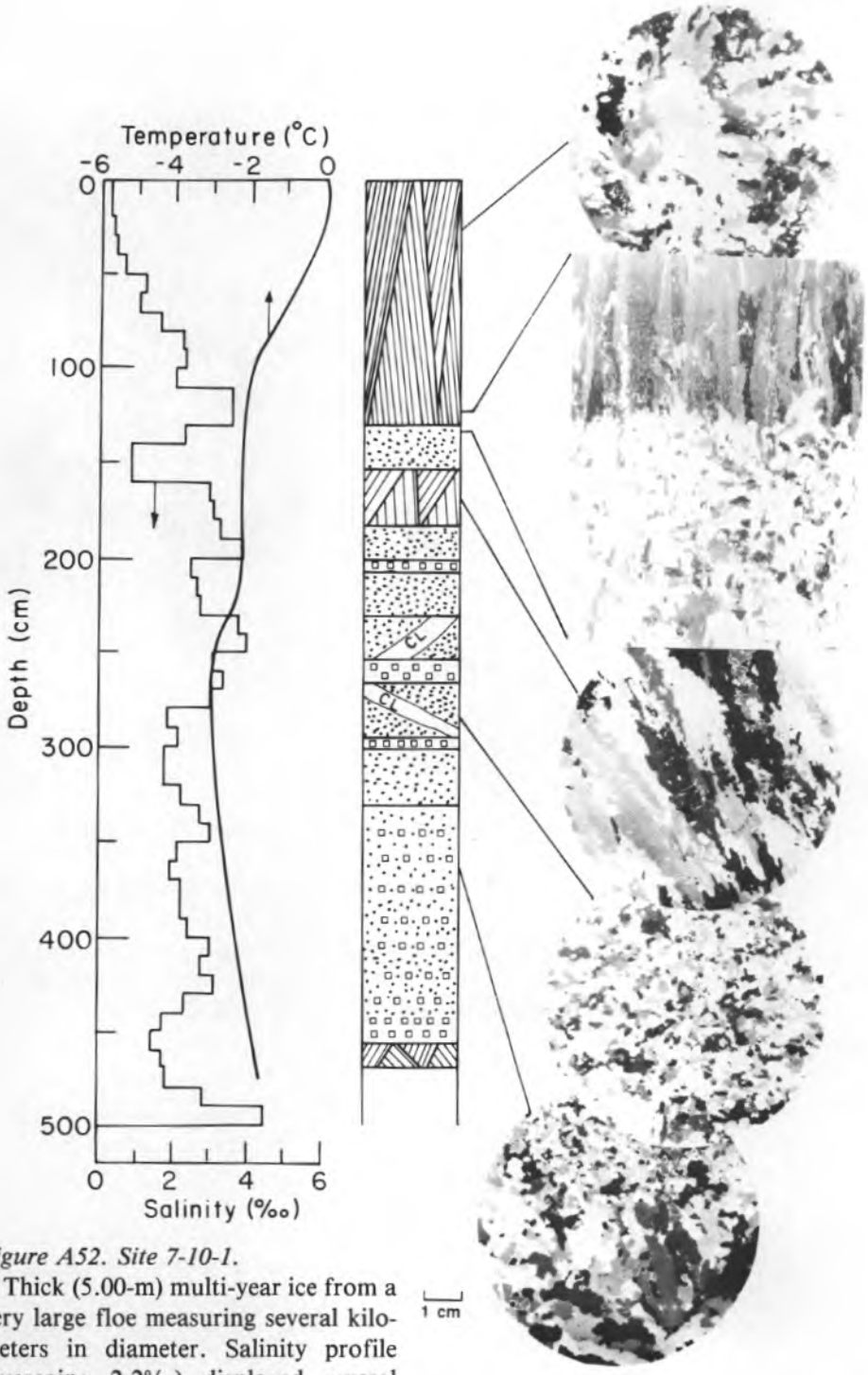

Figure A52. Site 7-10-1.

Thick (5.00-m) multi-year ice from a very large floe measuring several kilometers in diameter. Salinity profile (averaging 2.2‰) displayed several surges and this, together with evidence of tilted blocks in the middle of the core and the abundance of frazil, indicates that this part of the floe was an old ridge remnant. Structurally, the core consisted of retextured congelation ice at the top of the floe underlain by granular ice (see vertical section from 123–134 cm), principally frazil representing 58% of the total ice thickness, and a thin layer of congelation near the bottom (structure core only recovered to a depth of 4.67 m).

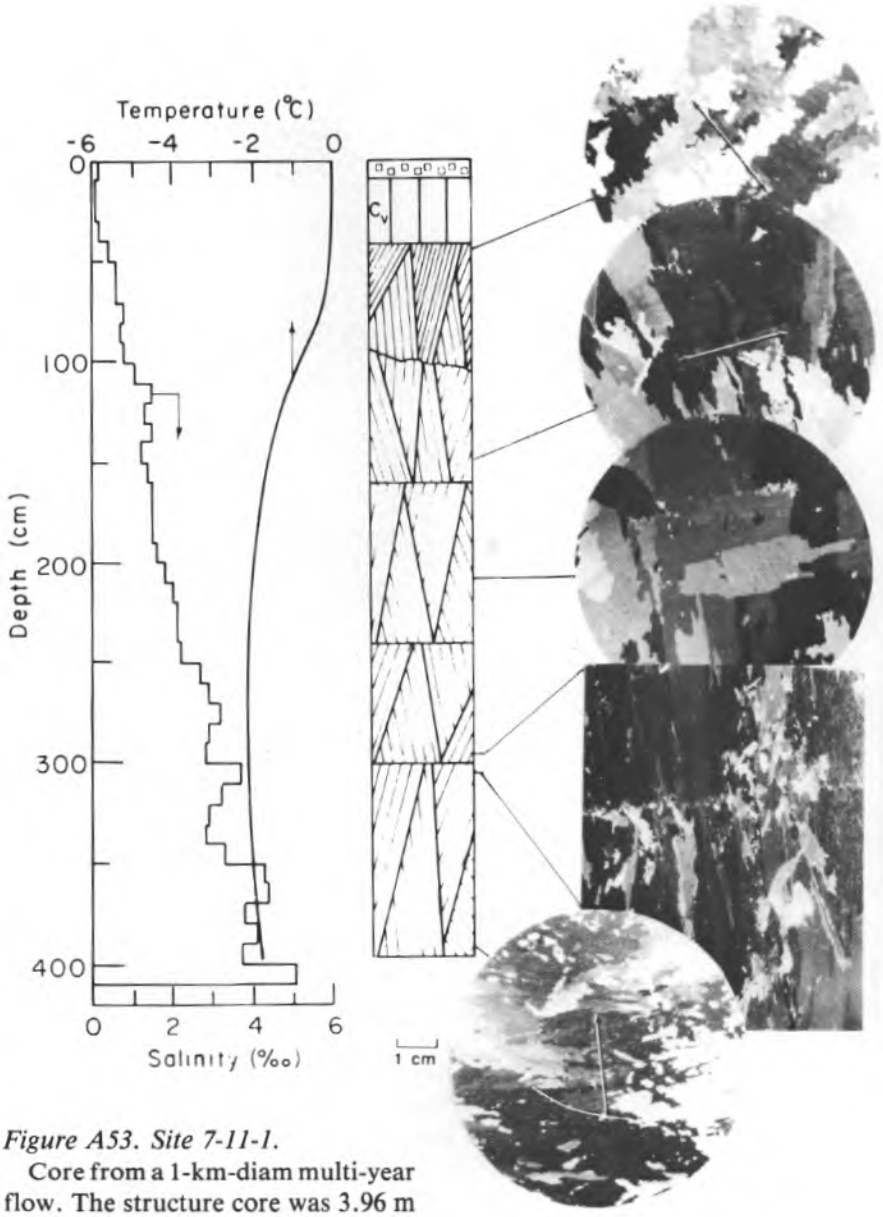

Figure A53. Site 7-11-1.

Core from a 1-km-diam multi-year flow. The structure core was 3.96 m long, 15 cm shorter than the salinity core, and consisted of 91% congelation sea ice overlain by 26 cm (7%) of melt pond ice with vertical c-axes and 8 cm (2%) of coarse-grained snow ice. Salinity increased progressively with depth, never exceeding 1‰ in the top meter, but reaching a maximum value of 4.5‰) at the bottom and averaging 2.1‰. Pond ice was directly underlain by transparent, bubble ice extending to a depth of one meter that also exhibited substantial retexturing, crystals of which still retained their original c-axis alignments. Based on structure transitions (an example of which is shown in the vertical thin section at 2.94 to 3.05 m) and the salinity and variable crystal alignment characteristics, this floe could represent five years of growth unaffected by deformation. Much of the surface of this floe was characterized by formation of slush and puddled areas, as demonstrated in Figure 3e.

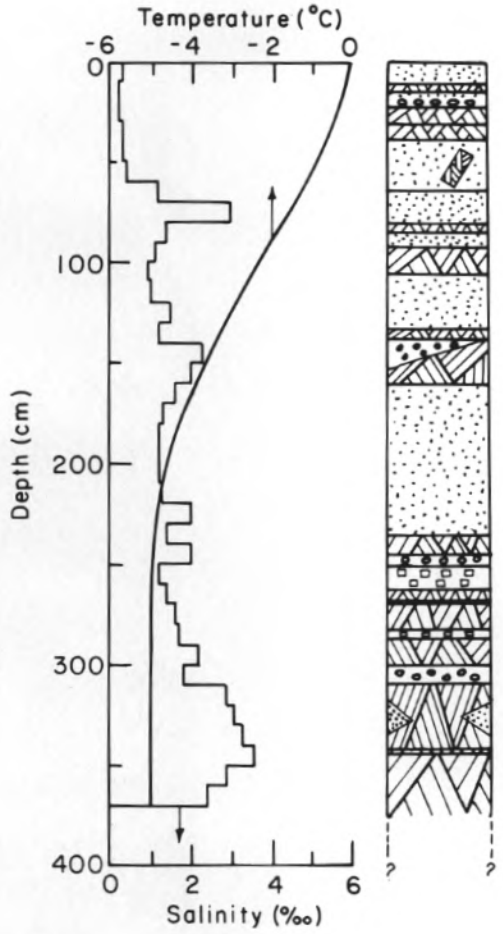

Figure A54. Site 7-13-1.

Core (5.74 m long) from a multi-year floe, which vertical structure profile studies indicated was intimately associated with ridge building. The core's thickness, the desalinated condition of ice in the top 1.3 m, the pulsed nature of the salinity profile, and the widespread occurrence of inclined blocks and fragments of congelation ice interspersed with granular ice representing 59% of the total floe thickness all confirm that this core was taken from an old multi-year ridge. The surface of the floe was characterized by "hummock and swale" topography.

APPENDIX B: CRYSTAL RETEXTURING IN MULTI-YEAR ICE

45 cm

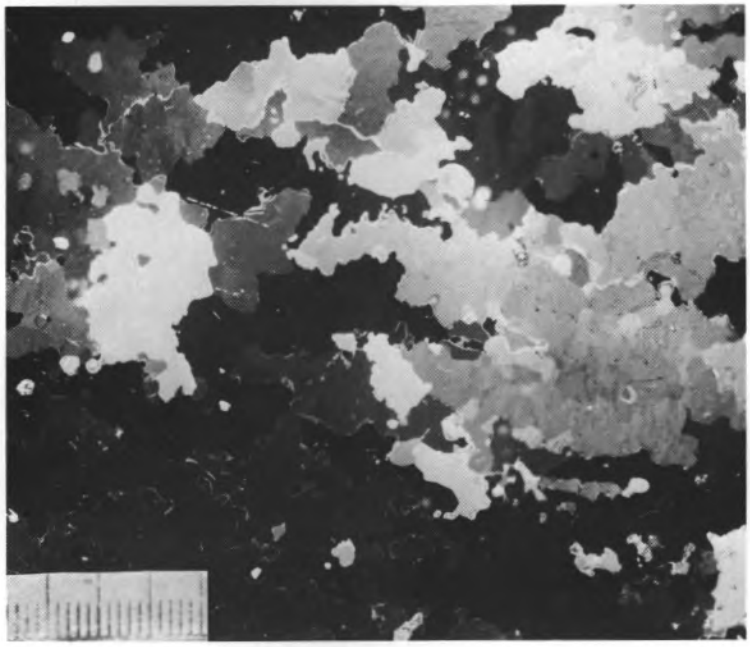

90 cm

Figure B1. Horizontal thin sections demonstrating retexturing in the upper levels of a multi-year ice floe (site 6-15-1). Note in section from 90 cm that original c-axis alignment (arrow) is maintained despite nearly complete loss of brine pocket substructure. Smallest scale subdivision measures 1 mm. Same scale applies to all four sections.

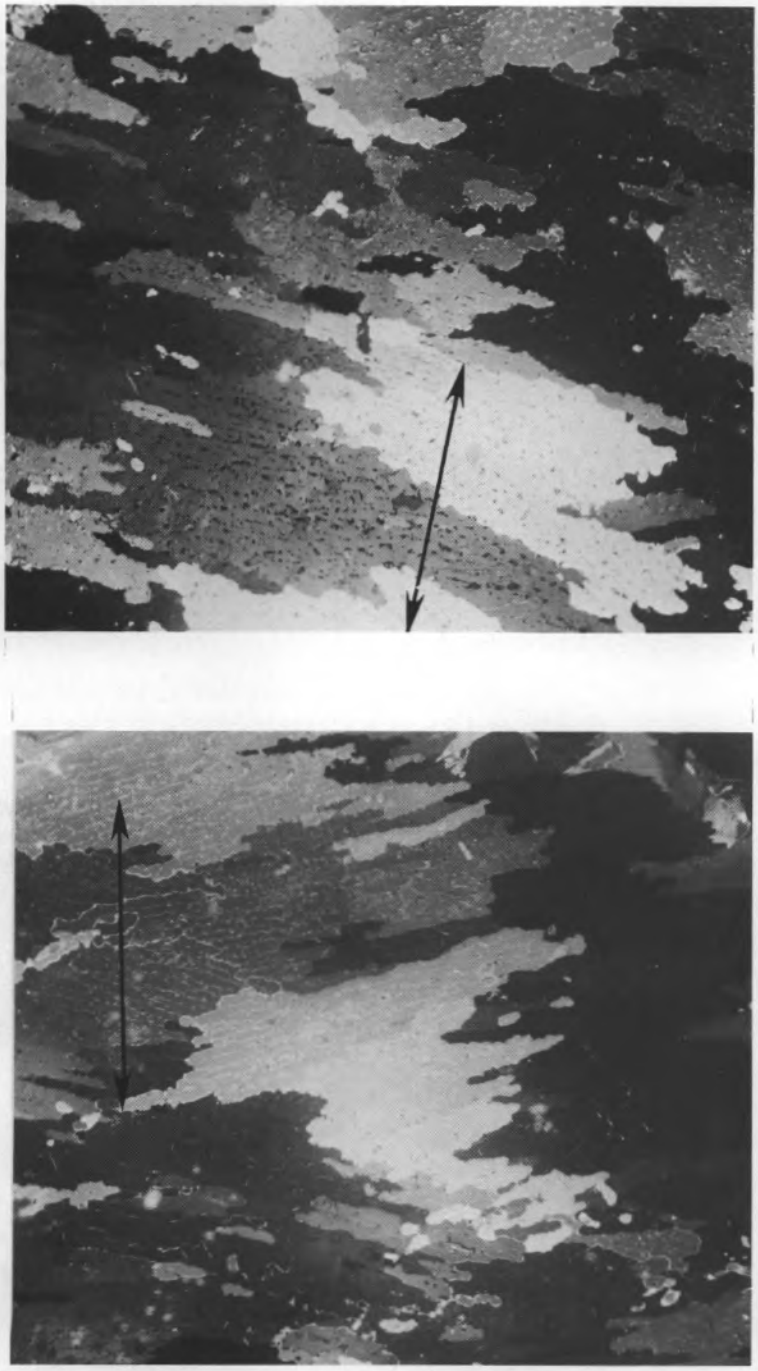

Figure B1 (cont'd). Horizontal thin sections demonstrating retexturing in the upper levels of a multi-year ice floe (site 6-15-1). Note in section from 90 cm that original c-axis alignment (arrow) is maintained despite nearly complete loss of brine pocket substructure. Smallest scale subdivision measures 1 mm. Same scale applies to all four sections.

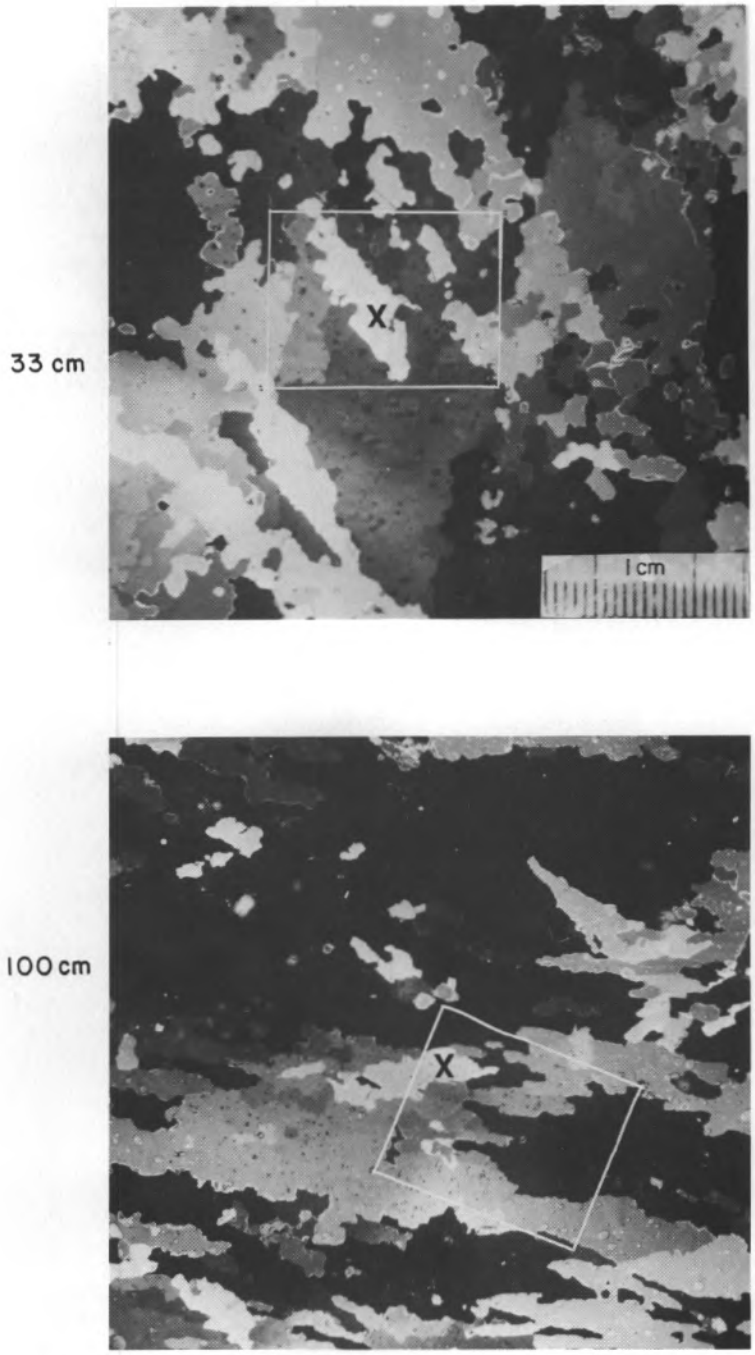

Figure B2. Thin section of retextured ice from site 7-07-1 photographed at two different magnifications. Areas of ice photographed at the higher magnification are indicated. Note remnant brine layer structure in the more highly magnified section from 100-cm depth. Inclusions marked B *are artifacts of the thin sectioning process.*

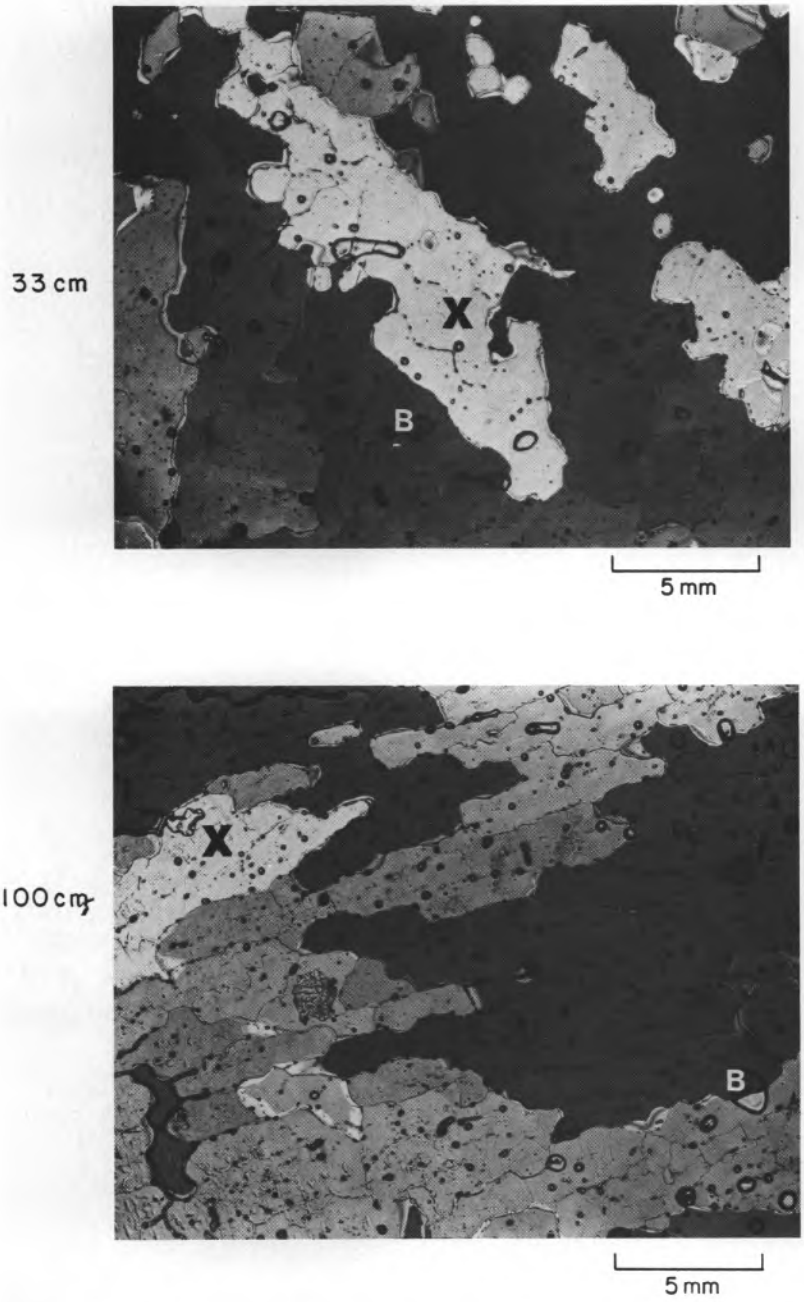

Figure B2 (cont'd). Thin section of retextured ice from site 7-07-1 photographed at two different magnifications. Areas of ice photographed at the higher magnification are indicated. Note remnant brine layer structure in the more highly magnified section from 100-cm depth. Inclusions marked B *are artifacts of the thin sectioning process.*

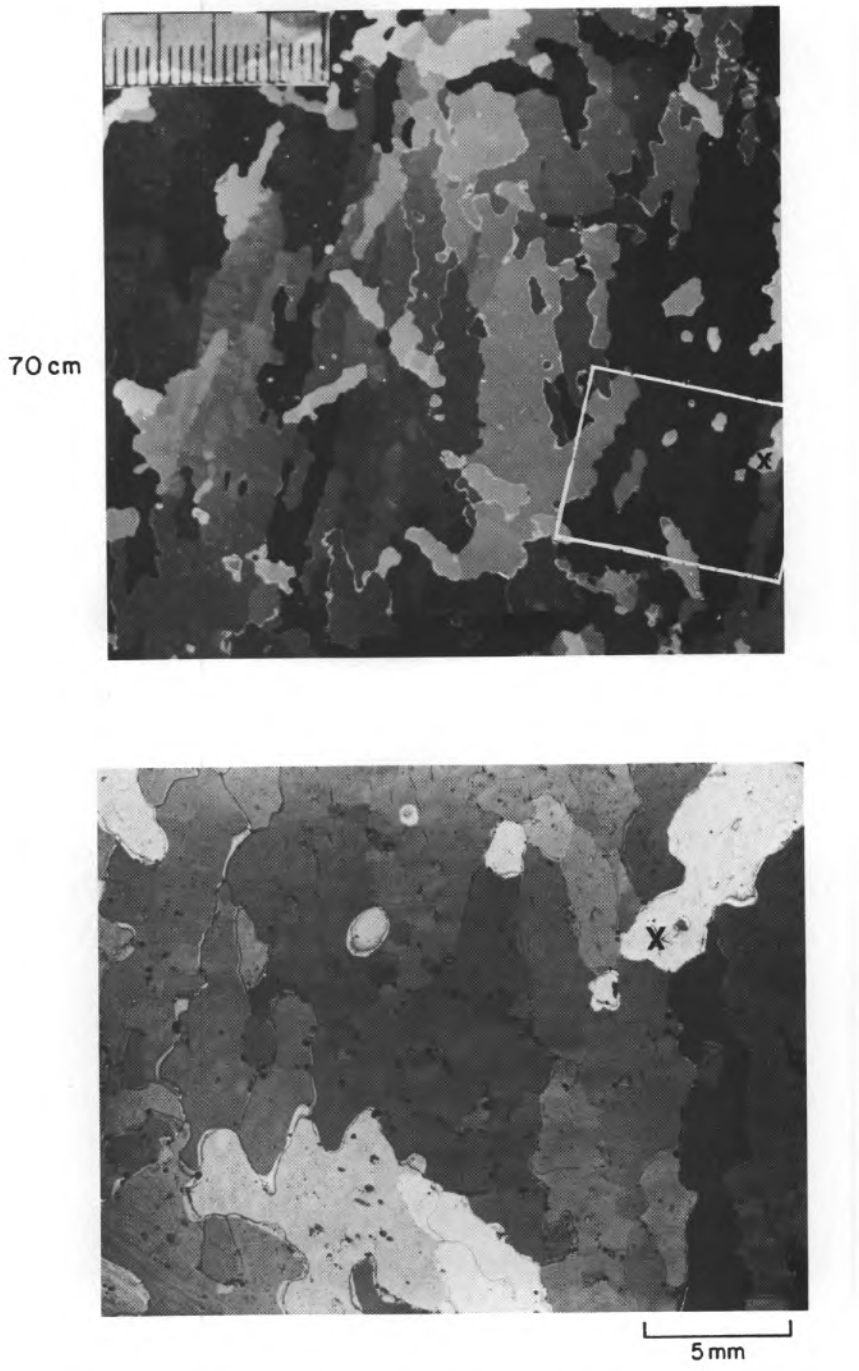

Figure B3. Retextured ice from 70-cm depth at site 7-05-4 photographed at two different magnifications. A few small inclusions are all that remain of the original brine layer/ice plate substructure.